FORECASTERS' REFERENCE BOOK

Met.O.1023

Meteorological Office College

February 1997

ISBN 0 86180 325 6

Published by The Met. Office
London Rd
Bracknell
Berkshire
RG12 2SZ

PREFACE

This latest edition of the *Forecasters' Reference Book* (*FRB*) builds on the strengths of the previous editions and handbooks, incorporating the latest science, where this is available in 'forecaster-friendly' form. From the outset, in designing the contents and format, every regard has been paid to forecasters' suggestions; the draft chapters have been thoroughly reviewed by a panel of forecasters and specialists. In this review process it became apparent that, to do justice to the copious literature on forecasting techniques, it was sensible to present not only a *FRB* of selected forecasting techniques but also a more erudite account of techniques, alternatives and limitations in a *Source Book*. The Chapters of the *FRB* and the *Source Book* should be seen as complementing many of those in *Images in Weather Forecasting*, 1995 (Ed. M. Bader et al.).

Remote Sensing, and Numerical Weather Prediction, now integral parts of the the forecasters' armoury are constantly referred to in the text but, with many guides available (e.g. *Images in Weather Forecasting*), they are only touched upon in the *Source Book* and *FRB*. Other chapters reflect the increasing concern over Air Pollution (*Source Book* Chapter 12), as well as the customer demand for Probability Forecasting (*FRB* and *Source Book* Chapter 11). I am grateful to Eddie Carroll for contributing Chapter 8, reflecting his insight on the use of dynamical concepts in assessing development. Chapter 11, Probability Forecasts, is based on a lecture course prepared by Bob Riddaway.

Where appropriate, Sections have references to key published papers as well as useful general reading articles/books. Reference is often made to the *Handbook of Weather Forecasting*, 1975 (HWF), which contains detailed accounts of forecasting techniques, accompanied by copious references.

There are some topics, such as fog, stratocumulus, and airflow over hills, where a more-detailed physical and dynamical picture has been included in the *Source Book* to enable the forecaster to make more considered judgements in forecasting elements whose behaviour is at best capricious.

As with previous editions it should be noted that this *Forecasters' Reference Book* has been produced specifically for the UK Meteorological Office forecaster; thus, forecasting techniques and rules apply mainly to the British Isles and north-west Europe and will not necessarily be applicable in other areas.

John R. Starr
Meteorological Office College
Shinfield Park
February 1997

FORECASTERS' REFERENCE BOOK

* To be found in the *Source Book*

FORECASTERS' REFERENCE BOOK

CONTENTS

CHAPTER 1 — WIND

1.1 Winds in the free atmosphere

1.1.1 Geostrophic wind (V_g)

V_g is defined as the steady (unaccelerating), horizontal wind which results from the balance of two forces only — namely the pressure gradient force and the Coriolis force, *f*. It follows that geostrophic wind is a good approximation to the actual wind only with isobars (or contours) which are straight, parallel and not changing with time. There are significant differences from V_g in strongly curved flow and flow near surfaces (**SB**).

1.1.1.1 Tables for geostrophic winds

Table 1.1 may be used to derive V_g for charts on which no geostrophic wind scale is provided. It gives 'multipliers' corresponding to a pressure (contour height) change over a distance of 300 n mile (or 5° latitude) of 1 hPa (1 dam).

Examples:

(i) A gradient of 5 hPa per 300 n mile at 55° N corresponds to $V_g = 5 \times 2.4 = 12$ kn (approx.).

(ii) A gradient of 12 dam per 300 n mile at 50° N corresponds to $V_g = 12 \times 3.1 = 37$ kn (approx.).

Table 1.1. To derive V_g for charts with no geostrophic scale

	Pressure/height change over 300 n mile	
	Isobars (hPa)	Contours (dam)
Latitude (°)	multipliers	
70	2.1	2.5
60	2.3	2.7
55	2.4	2.9
50	2.6	3.1
45	2.8	3.3
40	3.1	3.7
35	3.4	4.1
30	3.9	4.7

If gradients are measured over shorter distances, the factors should be altered in proportion, i.e. for 150 n mile (2.5° latitude span) the factors are doubled. Correction factors for density variations may be applied to geostrophic wind values measured by scales based on the Standard Atmosphere (1013.2 hPa, 15 °C) and era tabulated in **SB Table 1.2**.

1.1.2 Gradient wind

When its trajectory is curved, air must be subjected to a local centripetal acceleration (**SB**).

1.1.2.1 Estimation of gradient wind (tabular method)

Corrections to be applied to the geostrophic wind to obtain the gradient wind are given in **SB**, **Table 1.3**. The top section of the table (a) shows how changes in the Coriolis parameter affect the results. Thus a radius of **600** n mile at latitude 50° is equivalent to a radius of **489** n mile at latitude 70° or **919** n mile at latitude 30°.

1.1.2.2 Estimation of gradient wind (graphical method)

Fig. 1.1 is a graph for obtaining the gradient wind speed from the speed of the geostrophic wind and the radius of curvature. The graph is drawn for use at latitude 50°. For use at other latitudes the radius of curvature must be multiplied by a correction factor to obtain the equivalent value at latitude 50°.

To use the graph:

(i) Use the right-hand inset to find the equivalent radius of curvature for latitudes other than 50°. Multiply the actual radius by the factor shown against the value for latitude. If, for example, the radius at latitude 39.5° N is 1200 n mile, the correction factor is 0.83 and the equivalent radius at latitude 50° is about 1000 n mile.

(ii) Find the point of intersection of the geostrophic wind speed (shown along the left-hand axis) with the curve showing the radius of curvature. The cyclonic curves lie to the left and the anticyclonic curves lie to the right of the straight line denoting infinite radius. The gradient wind speed is shown along the bottom of the diagram. Thus with a radius of curvature of 1000 n mile and V_g = 90 kn, the gradient wind is 76 kn for cyclonic curvature and 136 kn for anticyclonic curvature.

The theoretical maximum gradient wind speed for anticyclonic curvature is twice the geostrophic wind. The graphs show that as the gradient wind approaches this value, small increases in the geostrophic wind can produce very large increases in the gradient wind.

1.1.2.3 Curvature of trajectories for systems in motion

Significant differences occur between the curvature of trajectories and the curvature of isobars or contours when the systems are in motion (**SB**, **Fig. 1.2**).

Holton (1992)

1.1.3 Variations in the mean wind

1.1.3.1 Ageostrophic winds (see Chapter 8)

An actual wind may be considered to have two components, one of which is geostrophic and the other ageostrophic (non-geostrophic).

1.1.3.2 Thermal winds

(i) The *thermal wind* in the layer between two pressure levels is the vector difference between the geostrophic winds at two levels B (upper level) and A (lower level). Thus in **Fig. 1.3**: $V_{thermal} = V_A - V_B$.

(ii) A geostrophic wind is proportional to the contour height gradient at a pressure level; a thermal wind, $V_{thermal}$, measures the difference in the contour gradient between two pressure levels. $V_{thermal}$ is proportional to the horizontal temperature gradient in the layer. It may be regarded as a steering wind for surface features.

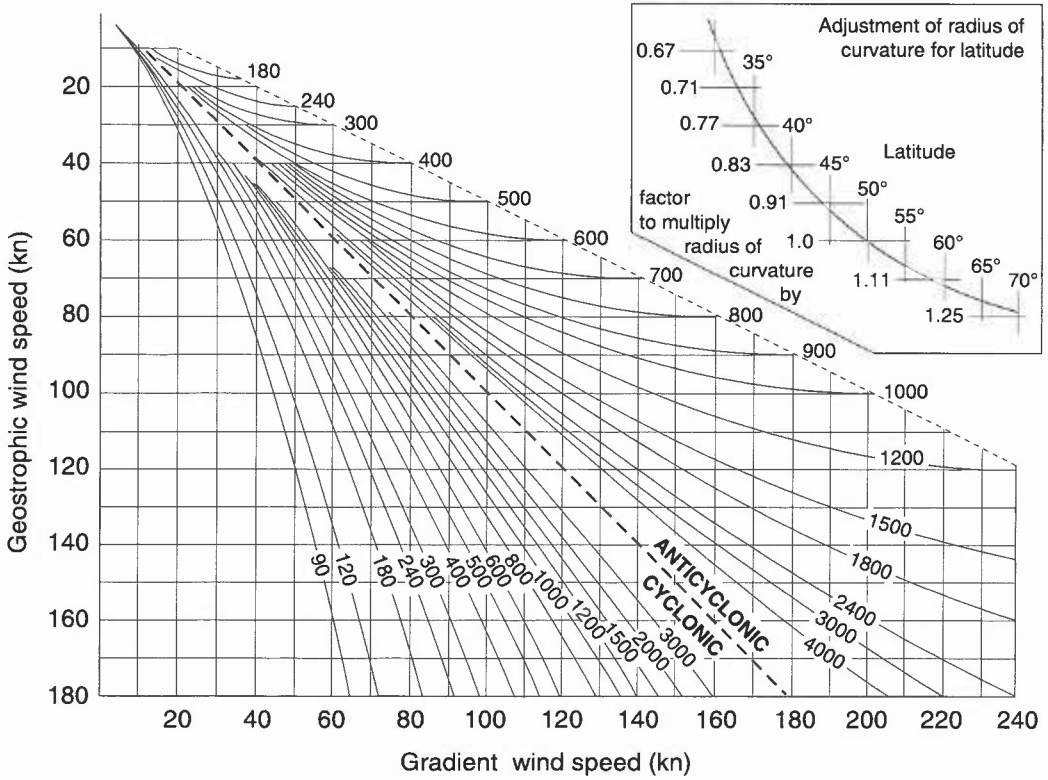

Figure 1.1. A graph to obtain the gradient wind speed from the speed of the geostrophic wind and the radius of curvature.

(iii) A strong north–south temperature gradient implies a strong westerly thermal wind with a westerly wind component increasing with height in the layer. A reversed temperature pattern gives easterly thermal winds, and a westerly wind component decreasing with height.

(iv) Although the thermal wind is geostrophic, practical computations use the difference between the actual winds at two levels. This is normally acceptably accurate.

Holton (1992)

1.1.4 Use of the hodograph

Plotting

Wind vectors are plotted on a hodograph so that they end at the centre of the diagram. **Fig. 1.3** shows a 900 hPa wind of 240° 20 kn and an 800 hPa wind of 300° 30 kn. The thermal wind in this layer is the vector from B to A. A normal hodograph plot only shows the points at each pressure level, joined to show the thermal winds in each layer.

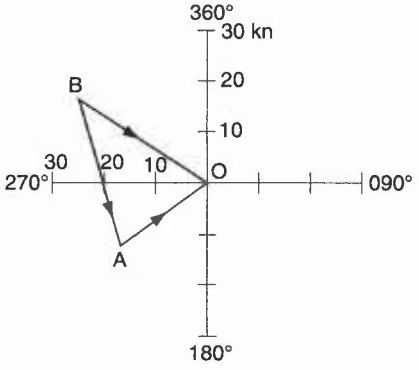

Figure 1.3. Plotting wind vectors on a hodograph. AO is the lower-level wind vector (say, 900 hPa). BO is the upper-level wind vector (say, 800 hPa). BA is the thermal wind vector (directed from the upper to the lower wind vectors).

Identifying the direction of warm and cold air

In **Fig. 1.4** the colder air is shown by light stippling and the warmer air by heavy stippling. Arrows show the direction of the thermal winds in the different layers. Thus between 850 and 500 hPa the thermal wind direction is 240° which shows that the colder air lies towards the north-west. Between 500 and 400 hPa the thermal wind direction is 005° indicating that in that layer the colder air is towards the east.

Warm and cold advection

Between 900 and 850 hPa in **Fig. 1.4** the thermal wind direction is 315°, indicating colder air to the north-east. Since the mean wind direction between these levels is from the north-east, colder air is being advected towards the station. This cold advection is in fact taking place at all levels up to 500 hPa. (i.e. wind is backing with height). Between 500 and 400 hPa the thermal wind is from 005° while the mean wind is about 345° indicating weak warm advection (wind is veering with height).

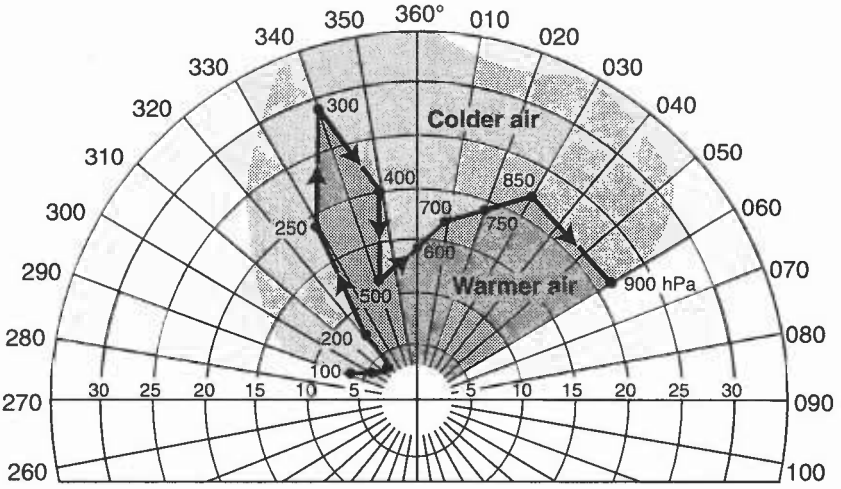

hPa	deg	kn
900	060	22
850	030	22
750	020	19
700	010	17

hPa	deg	kn
600	360	14
500	340	12
400	350	20
300	340	29

hPa	deg	kn
250	330	18
200	320	7
150	320	4
100	300	6

Figure 1.4. Hodograph example: Stornoway, 0600 UTC on 9 June 1961.

1.1.4.1 Fronts and vertical motion

Fig. 1.5 shows a construction which can be useful when a frontal surface lies over the station at some level.

(i) Mark the surface front through the centre of the hodograph, its orientation being as shown on a surface chart.

(ii) Determine the upper and lower levels of the frontal zone from a tephigram (i.e. noting change of θ_w), and mark them on the hodograph. The thermal wind direction in the frontal zone is often roughly parallel to the front.

(iii) Measure the wind component normal to the front at each level in the frontal zone and in the warm air mass above.

(iv) The frontal speed at the surface approximates to the speed of the cold air normal to the front at the base of the frontal zone (although adiabatic effects often lead to this being an overestimate).

(v) If the wind component normal to the front increases with height in the warm air, then: a warm front is an anafront, and a cold front is a katafront.

(vi) If the wind component normal to the front decreases with height in the warm air, then: a warm front is a katafront, and a cold front is an anafront.

HWF (1975), Chapter 3.4.3

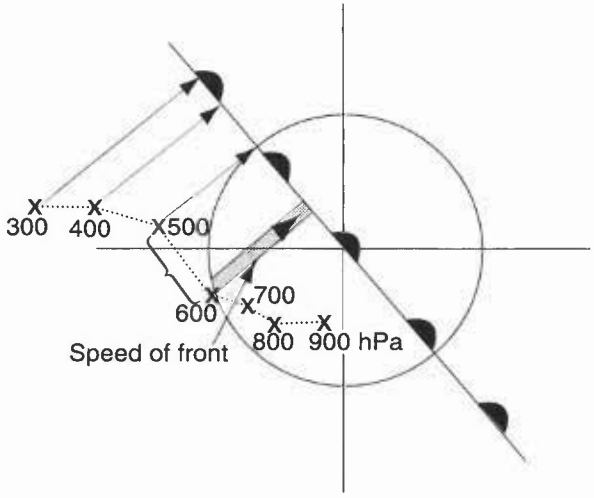

Figure 1.5. Assessment of ana- and kata-frontal characteristics from a hodograph.

1.1.5 Jet streams

1.1.5.1 The polar-front jet (SB, Figs 1.6 and 1.7)

Height
Direction
Speeds (**SB, Fig. 1.8**)
Vertical shear
This varies in relation to the strength of the jet (**Table 1.4**):

Table 1.4. Vertical shear associated with jet streams

Typical values:	
Normal	3–6 kn per 1000 ft
Large	10–15 kn per 1000 ft
Extreme	more than 20 kn per 1000 ft

(i) The maximum horizontal shear is generally on the cold side of the jet at about the core level, or slightly below.
(ii) On the warm side of the jet the maximum anticyclonic shear is slightly above the core level.
(iii) Theoretically the anticyclonic shear cannot exceed the Coriolis parameter which has values as follows (**Table 1.5**).

Table 1.5. Coriolis parameters

Latitude (°)	30	35	40	45	50	55	60	65	70
Coriolis parameter (kn/100 n mile)	26	30	34	37	40	43	45	47	49

When the warm-side maximum shear values are attained, or exceeded, the flow becomes turbulent.

1.1.5.2 The subtropical jet (SB)

1.1.5 3 Overlapping of jets (SB)

Satellite pictures show that a cyclonically curved polar-front jet may cross underneath the anticyclonically curved subtropical jet.

HAM (1994)

1.2 Winds near the surface

Forecasts required will depend on what is at risk and the nature of the wind/gust hazard (see Chapter 6: Turbulence and gusts).

Hunt (1995)

1.2.1 Surface wind and gradient wind

(i) The surface wind is usually reduced in speed and backed in direction from the gradient wind **(Fig. 1.9)**.

(ii) The magnitude of the change depends on the stability of the air and the roughness of the surface. Rough surfaces increase the frictional effect; greater stability reduces the turbulent exchange of energy between the flow aloft and that at the surface. An increase in stability near the surface implies a change in the vertical wind profile.

1.2.1.1 Surface wind and 900 m wind (statistical relations)

Table 1.6 shows some observed relationships between the speed of the surface wind (V_0) and the 900 m wind (V_9), together with the angle (α) between them.

Lapse-rates are classified as:

1. Superadiabatic.
2. Conditionally unstable.
3. Conditionally stable.
4. Stable.
5. Isothermal/Inversion*.

*Important from the aviation point of view is the breaking up of the surface inversion with the consequent increase in mean surface wind

(The above lapse rate classes are based on the difference between surface and 900 hPa temperatures, differences which may not reflect the boundary-layer stability all that well.)

Table 1.6. Observed relationships between the speed of the surface wind (V_0) and the 900 m wind (V_9) together with the angle (α) between them

(a) Over the sea: at 59° N, 19° W and 52° N, 20° W

Lapse class	900 m wind speed (kn) 10–19		20–29		30–39		40–49		>50	
	V_0/V_9	α	V_0/V_9	α	V_0/V_9	α	V_0/V_9	α	V_0/V_9	α
1	0.95	0	0.90	0	0.85	0	0.80	0	0.80	0
2	0.90	5	0.85	5	0.80	5	0.75	5	0.75	5
3	0.85	10	0.75	10	0.70	10	0.65	10	0.65	10
4	0.80	15	0.70	20	0.65	20	0.60	20	0.60	20
5	0.75	15	0.70	20	0.65	20	0.60	20	0.55	25

(b) Over land: at London (Heathrow) Airport

Lapse class	900 m wind speed (kn) 10–19		20–29		30–39		40–49		>50	
	V_0/V_9	α	V_0/V_9	α	V_0/V_9	α	V_0/V_9	α	V_0/V_9	α
Daytime										
1, 2	0.65	5	0.55	5	0.50	10	0.50	10	0.35	15
3	0.50	20	0.45	20	0.45	20	0.45	20	0.45	15
4	0.45	35	0.45	30	0.40	25	0.30	20	0.40	25
5	0.35	45	0.40	35	0.35	35	0.40	30	0.40	30
Night-time										
1, 2	0.25	20	0.35	25	0.30	35	0.40	15	0.40	25
3	0.35	25	0.35	30	0.35	25	0.35	20	0.35	15
4	0.30	35	0.30	35	0.30	30	0.35	30	0.35	15
5	0.30	45	0.25	40	0.25	35	0.30	30	No obs	

(Some results based on less than 10 observations.)

Fig. 1.9 is a useful first-guide summary based on these figures.

Findlater et al. (1966)

1.2.2 Vertical wind shear

1.2.2.1 Vertical wind shear over surfaces with different roughness

(i) **Fig. 1.10** shows the calculated ratio V_z/V_{10} (the winds at z and 10 metres) for different surfaces.

(ii) The curves show that over wooded country: if the 200 m wind is 18 kn, then the 100 m wind should be just under 16 kn and the 10 m wind should be 10 kn.

Table 1.7 gives the variation with height of the mean hourly wind and corresponding gusts, based on statistical data, and likely to be particularly applicable to open areas under neutral conditions.

Local Weather Manuals (1994)

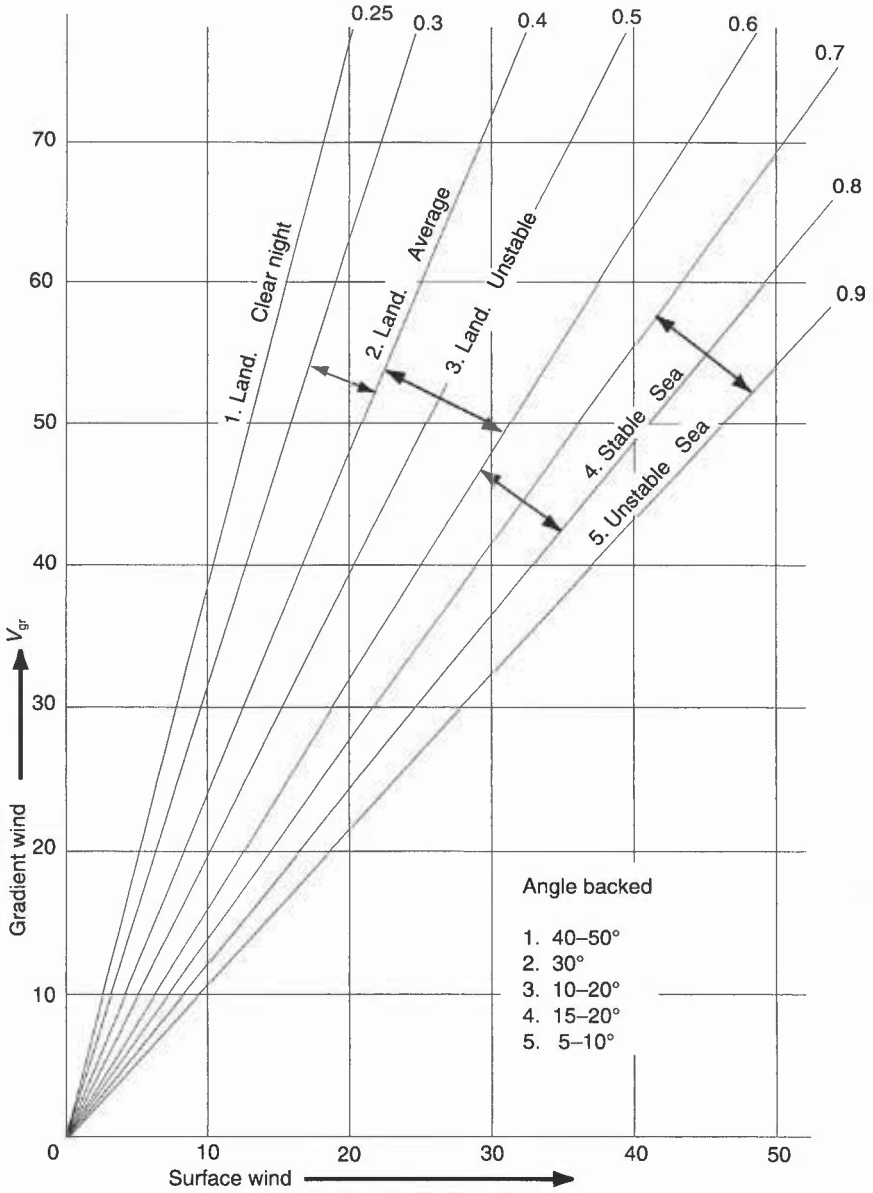

Figure 1.9. Relationship between geostrophic and surface winds over land and sea (units — knots).

1.2.2.2 Vertical wind shear in different stability conditions (SB)

Fig. 1.11 shows how the ratio V_z/V_{10} alters with changes of stability based on observations of wind changes between the surface and 400 ft with lapse rates ranging from +2 °C to −6 °C through that layer (lapse rate of −6 °C means a rise of 6 °C within the layer).

HWF (1975), Chapter 16.5.2
WMO (1969)

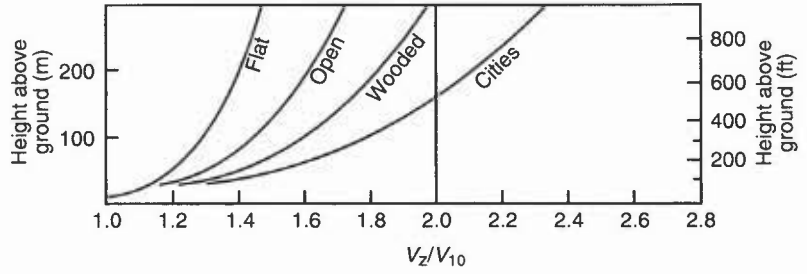

Figure 1.10. Calculated ratio of V_z/V_{10} over different surfaces in neutral stability conditions.

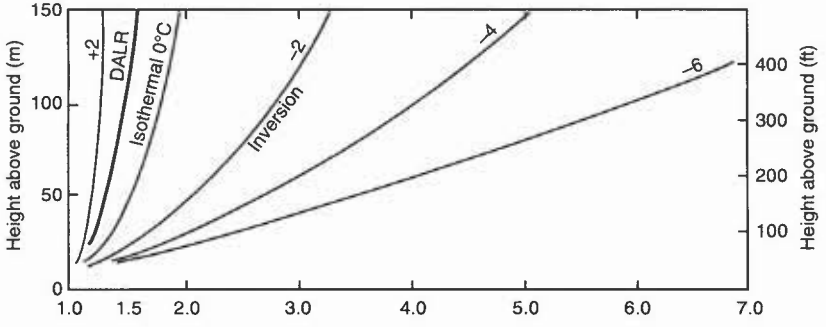

Figure 1.11. Observed ratio of V_z/V_{10} for different lapse-rates, measured at Cardington.

1.2.2.4 The nocturnal jet and diurnal variations of vertical wind shear (SB, Fig. 1.12)

Nocturnal jets can be an embarrassment to light aircraft when landing and will influence pollution transport; they can occur over land when radiation cooling over a sufficient period of time (particularly during spring and autumn) stabilizes the near-surface flow

Downward momentum transfer is an important consideration for night aviation forecasts; it can maintain light surface winds over airfields on ridges and small hills, keeping them from visibility deterioration that might occur in the valley. Conversely, diurnal reversal after sunrise may result in deteriorating conditions of fog/low stratus.

Stull (1988)
Thorpe & Guymer (1977)

1.2.3 Low-level jets

(i) These are bands of strong winds in the lower troposphere (**SB, Fig. 1.13**).
(ii) Unlike high-level jets there is no specified minimum speed and many do not exceed 60 kn.
(iii) These jets are often associated with large vertical and horizontal wind shears.
(iv) Low-level jets occur in the warm conveyor belt just ahead of a surface cold front.
(v) There may be more than one core, each about 100 km wide.
(vi) Maximum speeds are in the range 50–60 kn and at a height of about 1 km.

1.3 Local winds

1.3.1 Sea and land breezes

Sea (and land) breezes are driven by the unequal diurnal heating and cooling of adjacent land and sea surfaces.

1.3.1.1 Sea breezes (SB)

Criteria for sea breezes:

(i) inland temperatures greater than temperature of coastal waters;
(ii) a moderate depth of dry convection to, say, between 750 and 900 m (2500 to 3000 ft) is required before the sea breeze can become established;
(iii) if the air is so stable that the convection is confined to a very shallow layer there will be little or no penetration of the sea-breeze regardless of the temperature difference between land and sea;
(iv) only a weak offshore wind component of <14 kn at 3000 ft initially;
(v) convection to 1500 m (4000 ft) favours deep inland penetration (deep convection, leading to shower or thundery activity, tends to halt the sea-breeze);
(vi) significant inland penetration is only likely if offshore 3000 ft wind is <10 kn. This is typified by the following observations **(Table 1.8)** for the onset of sea breezes as a function of land/sea temperature contrast for the Lincolnshire coast.

Table 1.8.

Off-shore component (kn)	2	4	6	8	10	12	14	16
Temperature contrast (°C)	3.5	5.0	6.0	7.3	9.0	11	14	—

(sea surface temperature measured at light vessel in 19 m of water, 30 miles (48 km) offshore).

Providing these criteria are met the approximate time for a sea breeze to start to move inland is given by **Table 1.9**.

Table 1.9.

Off-shore wind component (kn) at 3000 ft	Time sea-breeze front crosses coast (UTC)
≥15	sea-breeze front unlikely
14	1600
10	1100–1200
5	0900 (or when convection penetrates 3000 ft)

Sea-breeze front
Penetration inland **(SB, Fig. 1.14)**
Speed of movement
The average in the United Kingdom is 4–8 km h^{-1} (2.2–4.4 kn).

Seasonal variation
Depth of sea air

Coastal convergence/divergence effects
SB, Figs 1.15 and 1.16 show typical cloud patterns generated by land and sea breezes along peninsulas and inlets; coastal convergence/divergence zones with associated cloudiness.

Bader et al. (1995), Chapter 6
Bradbury (1989)
Brittain (1970)
Findlater (1964)
HWF (1975), Chap 16
MG (1991)
Pielke (1984)
Simpson (1994)

1.3.1.2 The (nocturnal) land breeze
Occurrence
(i) usually sets in about midnight or later;
(ii) it is usually shallower and less well-developed than the sea breeze;
(iii) it is much influenced by topography and tends to increase during the night near flat coasts; a katabatic flow from hills parallel to the coast may reinforce it;
(iv) the strength and frequency depend, theoretically, on the land-sea temperature contrast, and thus might be expected to be greater in anticyclonic conditions in early autumn;
(v) snow-covered ground encourages persistent flow.

Moffitt (1956)

1.3.2 Airflow over hills **(SB, Fig. 1.17)**

Fig. 1.17 shows the variety of flows possible for different stabilities for the case of an isolated hill.

1.3.2.1 Mountain waves **(SB)**
Summary of guidance on forecasting.
(i) Two types of lee waves can form with different characteristics:
  (a) *Trapped waves* form when wind speeds increase with height and/or a less stable layer overlies a stable layer (wave energy is trapped and propagates downwind, confined to low levels).
  (b) *Untrapped waves* form if stability is high and/or wind speed low, or the hill width large. The wave energy is propagated upwards so that these waves are routinely observed in the stratosphere, having a characteristic orographic cirrus signature with a well defined boundary (**SB, Fig. 6.1**).
(ii) The length scale of the hills is important — there will be a favoured width of hills depending on the wind and stability conditions.
(iii) An idea of the flow strength may be gained from the distance apart of wave elements on a satellite image. (Flight along the wave, i.e. against and across the flow, can result in experiencing prolonged ascent or descent.)

(iv) Beware of strong-wind situations over the hill top and to its lee where there is an inversion or stable layer not far above the hill or ridge top — this is most likely around the periphery of an anticyclone or ahead of an approaching warm front. Winds can be stronger than expected and quite gusty over the hill top and to its lee. Marked turbulence can be encountered, with perhaps a rotor where the wave flow leaves the ground downwind of the hill.

(v) Both wave types are accompanied by pronounced lee troughing in the surface isobaric field.

(vi) Even in the absence of a stable layer, there will tend to be a flow speed-up effect which may cause the winds over a hill or ridge crest to be as much as double or more the upwind values on occasion, depending on hill height and width.

These two wave types can generate *severe downslope winds*.

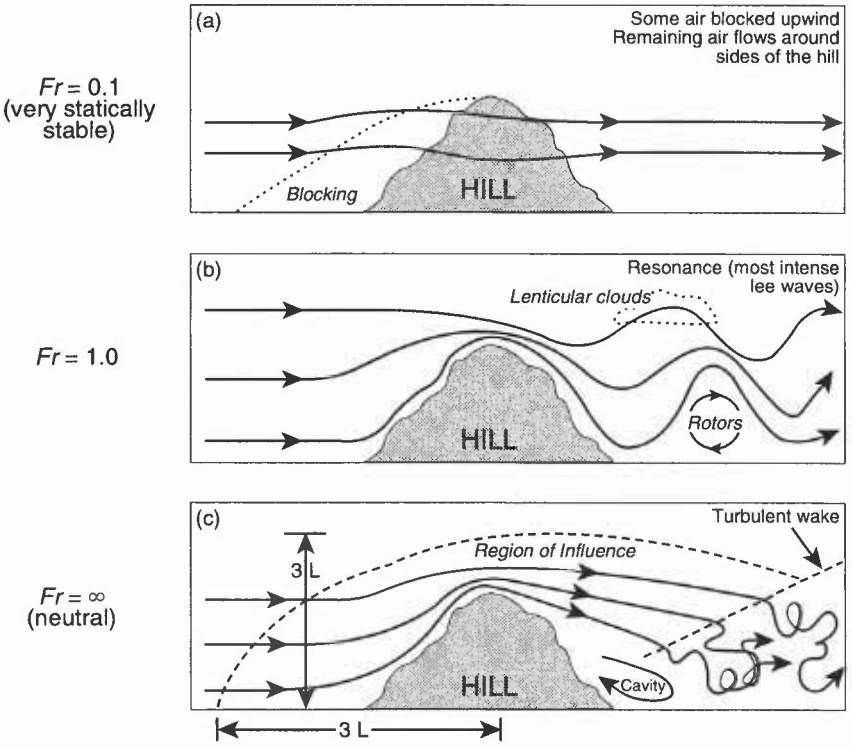

Figure 1.17. Idealized flow over an isolated hill. The Froude number (Fr) compares the natural wavelength of the air to the width of the hill (L). (a) $Fr = 0.1$ (very statically stable), (b) $Fr = 1.0$, and (c) $Fr = \infty$ (neutral).

Bader et al. (1995)
Barry (1981)
Bradbury (1989)
Bradbury et al. (1994)
Corby (1954)
Foldvick (1962)
Hunt (1980)
Scorer (1949)
Shutts & Broad. (1993)
Starr & Browning (1972)
WMO (1973)

1.3.2.2 Casswell's method for predicting mountain wave characteristics (SB, Fig. 1.18)

This graphical method for estimating the likely occurrence and properties of Mountain (lee) waves has little credibility with specialists in the subject. Lee waves are generally found when winds are fairly unidirectional, increase in strength with height and when the lowest 3 km has a higher static stability than normal. However, there are numerous cases reported which do not conform to these or other (e.g. HWF) simplified conditions but which are handled well by Shutts' method.

Casswell (1966)

1.3.2.3 Shutts' method for predicting mountain wave characteristics

(i) Shutts' model looks for trapped lee wave modes in a range of directions centred on the near-surface wind direction; it is available as a PC model.

(ii) In the simplified example in **Fig. 1.19** a wind profile that is linear with height is assumed (governed only by values specified at the surface and at a fixed tropopause height of 10 km). The temperature profile is fixed by three values at the surface (12 °C), at 3.5 km (−3 °C) and at the tropopause (−60 °C), the stratosphere being isothermal at that temperature.

(iii) **Fig. 1.19** shows (a) the resonant wavelength, and (b) the maximum vertical velocity and height for a range of surface and tropopause wind speeds. The figure confirms the tendency of the resonant wavelength to increase with wind speed; beyond a certain surface wind they are non-existent. At low wind speeds plots are complicated by the presence of multiple solutions. Between mode regimes, there appear to be regions with no trapped modes. Strong lower tropospheric stability leads to gigantic waves for strong height-independent flows.

The Sheffield storm of 1962 is well handled by Shutts' method.

Aanensen (1965)
Shutts (1992)
Shutts & Broad (1993)

1.3.2.4 Convection and cloud street waves (SB)

Thermals can act as temporary hills and set off gravity waves in a stable layer, propagating to an altitude of >9 km.

Booth (1980)
Bradbury (1990)

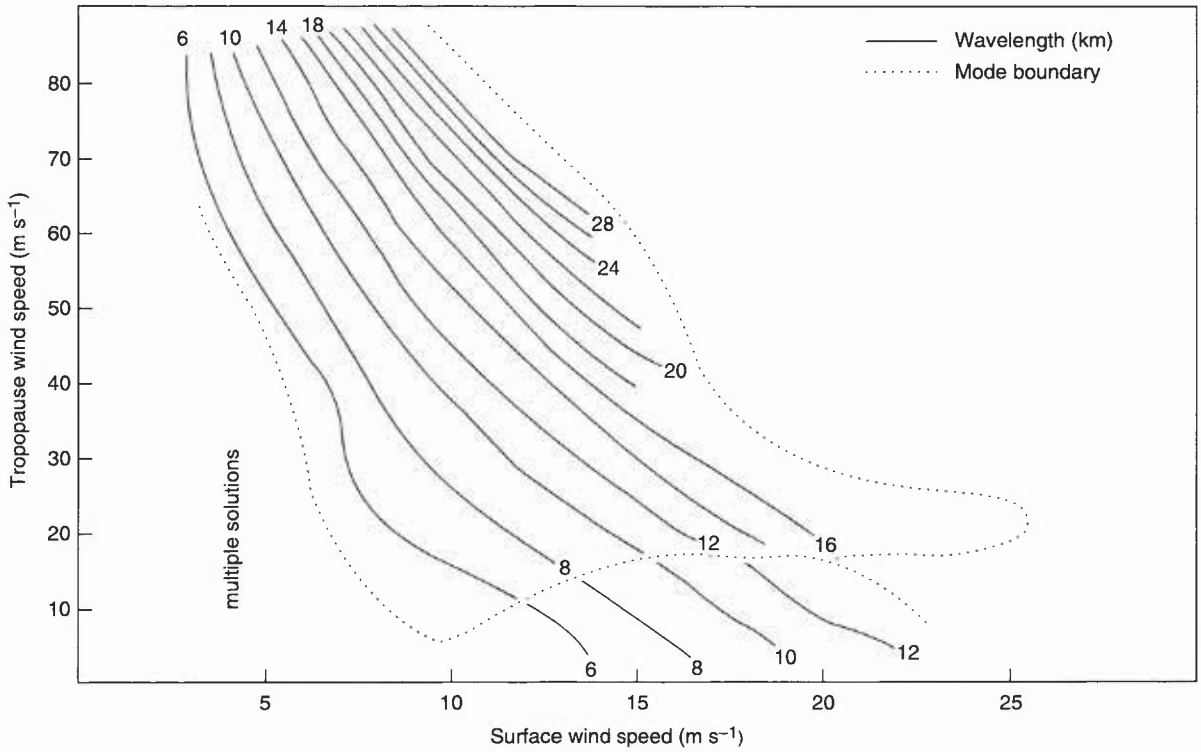

Figure 1.19. (a) Resonant wavelength for a range of surface and tropopause wind speeds.

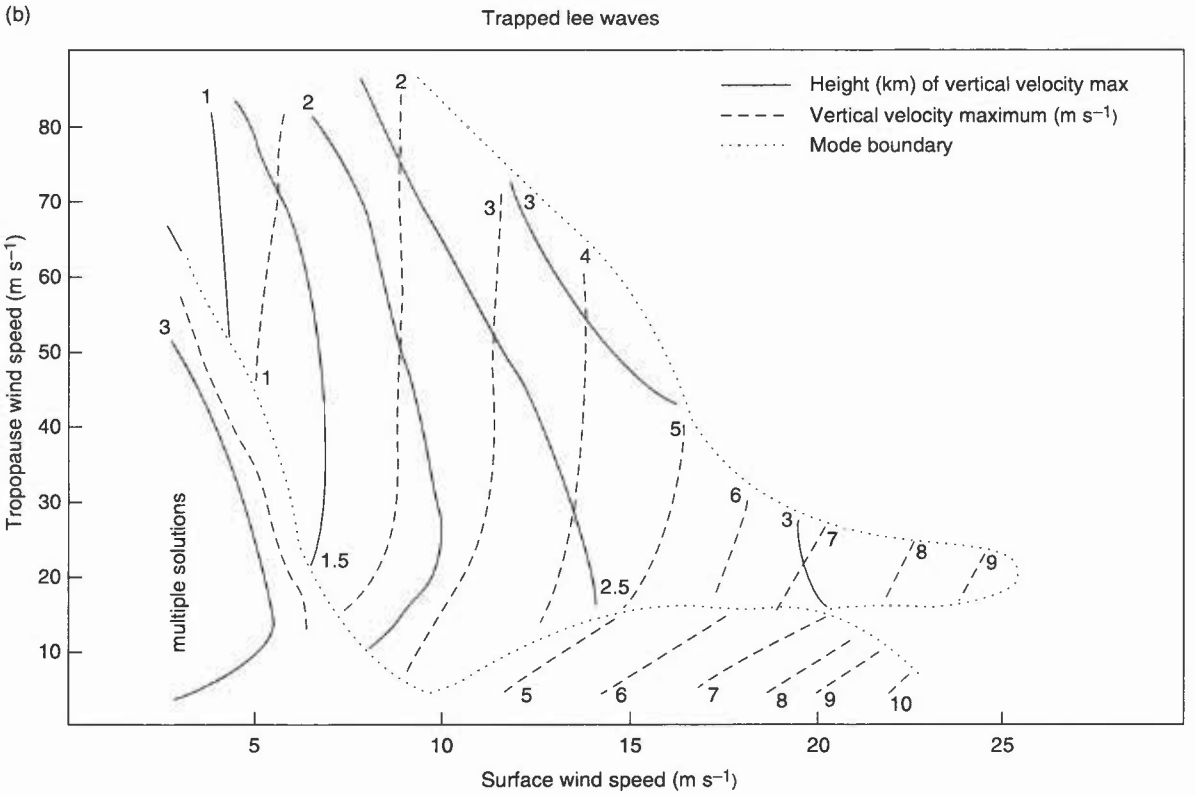

Figure 1.19. (a) Resonant wavelength, and (b) maximum vertical velocity for a range of surface and tropopause wind speeds.

1.3.2.5 Speed-up at the crest of an isolated hill

(i) The fractional speed-up ratio, valid for small slopes (<20°), neutral stability and low hills, is defined as: $\Delta V_{hill} = [V_o(\Delta z)V_A(\Delta z)]/V_A(\Delta z)$
where Δz is the height above the local terrain, subscript 'A' denotes a point upwind where flow is undisturbed and subscript 'o' the hill top.

(ii) For gentle ridges: ΔV_{hill} equals about: 4 × hill height/L
For isolated hills: ΔV_{hill} equals about: 3.2 × hill height/L,
where L is the hill width at half the maximum height of the hill.

(iii) For a typical, gentle hill (height = 100 m, L = 250 m), the speed-up just above the crest can be 160% or more (especially if there is an inversion above summit height).

Stull (1988)

1.3.2.6 Vertical velocities and slope (SB)

Amplitude of the vertical velocities is determined by the slope of the topography and the undisturbed wind flow.

Stull (1988)

1.3.2.7 Airflow over a series of hills (SB)

A series of hills can modify the flow to yield a new profile that behaves in accordance with the characteristics of the rougher surface of the terrain.

Stull (1988)

1.3.2.8 Airflow with a capping inversion (SB, Fig. 1.20)

1.3.2.9 Airflow over other complex terrain (SB)

1.3.2.10 Airflow over different surfaces (SB)

Stull (1988)

1.3.3 Slope and valley winds

1.3.3.1 Anabatic winds (SB)

In the United Kingdom these winds are less frequently observed than katabatic winds.

1.3.3.2 Katabatic winds (SB)

These are generally shallow flows (<30 m deep) down slopes and along valleys (donor sites) cooled by nocturnal radiation.

Bader et al. (1995)
Dawe (1982)
Moffitt (1956)

1.3.3.3 Valley wind systems (SB, Fig. 1.21)

On any occasion there may be anabatic or katabatic components complicated by the presence of a gradient wind flow above the level of the surrounding ridge tops and varying through the day as the sun's orientation changes.

Bradbury (1989)

1.3.3.4 Severe downslope winds (SB)

Two types of mountain waves can generate severe downslope winds (see *Mountain waves*):

Untrapped lee waves may result in gusty, downslope winds. Conducive atmospheric conditions of high stability accompanying strong low-level flow with little increase in speed with height are frequently found in the lee of the Pennines during:

(i) strong anticyclonic south-westerlies;
(ii) warm-sector conditions;
(iii) in the low-level zone of strong winds a few hundred kilometres ahead of a cold front.

Satellite imagery reveals dense orographic cirrus in the lee of the mountains, with a cloudless 'slot' where frontal cirrus is forced to descend in the lee wave system.

Trapped lee waves may give rise to severe downslope winds when the waves reach a critical amplitude and wavelength.

(i) UK mountain ridges are never much more than 1 km high so such winds can only occur for $V \approx 10$ m s^{-1} (**see SB**).
(ii) The streamlines of flow are concentrated above and to the lee of large mountain ridges.
(iii) These extreme winds may extend for some distance across the plain before the flow separates from the surface in an intense vertical current beyond which rotors may be found.
(iv) Surface charts may show a marked lee trough (note that mesoscale model resolution limitations may result in the effect being underestimated).

Conditions conducive to severe downslope winds resulting from trapped lee waves:

(i) strong stable layer near hill-top height;
(ii) very light winds or flow reversal at some tropospheric level;
(iii) a mountain range with steep leeward escarpment.

The 'Helm Bar' in Cumbria is a well-known example where the rotor may be indicated by a long roll of ragged cumulus or stratocumulus parallel to the ridge.

Bader et al. (1995), Chapter 8
Bradbury (1989)
Corby (1954)
Förchtgott (1949)
HAM (1994)
Klemp (1978)
Stull (1988)

1.3.3.5 Rotor streaming (see 6.2)

1.3.3.6 Föhn winds (SB, Fig. 1.22)

Bader et al. (1995), Chapter 8 **Bradbury (1989)**
Lawrence (1953)

1.3.4 Urban winds

The temperature differential due to the urban 'heat island' (2.11) can set up a 'country breeze', a low-level flow (<8 kn) of cool air from the rural area towards the city. Pollution can be transported large distances downwind in the 'urban plume' which is as wide as the city, and whose boundary-layer characteristics vary diurnally **(SB, Fig. 1.23)**.

Oke (1982) **Stull (1988)**

1.3.5 Wind-chill (see 2.10)

BIBLIOGRAPHY

CHAPTER 1 — WIND

Aanenson, C.J.M. (Editor), 1965: Gales in Yorkshire in February 1962. *Geophys Mem* No. 108, Meteorological Office

Bader, M.J., Forbes, G.S., Grant, J.R., Lilley, R.B.E. and Waters, J., 1995: Images in weather forecasting. Cambridge University Press.

Barry, R.G., 1981: Mountain weather and climate, Methuen.

Booth, B., 1980: Unusual wave flow over the Midlands. *Meteorol Mag*, **109**, 313–324.

Bradbury, T.A.M., 1989: Meteorology and flight, A & C Black.

Bradbury, T.A.M., 1990: Links between convection and waves. *Meteorol Mag*, **119**, 112–120.

Bradbury, W.M.S., Deaves, D.M., Hunt, J.C.R., Kershaw, R., Nakamura, K. and Hardman, M.E., 1994: The importance of convective gusts. *Meteorol Appl*, **1**, 365–378.

Brittain, O.W., 1970: Forecasting the inland penetration of a sea-breeze over Lincolnshire. Met. Office Forecasting Techniques Memorandum No. 20.

Carruthers, D.J. and Choularton, T.W., 1982: Airflow over hills of moderate slope. *QJR Meteorol Soc*, **108**, 603–624.

Casswell, S.A., 1966: A simplified calculation of maximum vertical velocities in mountain lee waves. *Meteorol Mag*, **95**, 68–80.

Corby, G.A., 1954: The airflow over mountains: A review of the state of current knowledge. *QJR Meteorol Soc*, **80**, 377–408.

Dawe. A.J., 1982: A study of a katabatic wind at Brueggen on 27 February 1975. *Meteorol Mag*, **111**, 491–521.

Findlater, J., 1964: The sea breeze and inland convection — an example of the interrelation. *Meteorol Mag*, **93**, 82–89.

Findlater, J., Harrower, T.N.S., Howkins, G.A. and Wright, H.L., 1966: Surface and 900 mb wind relationships. Scientific Paper No. 23. London, HMSO.

Foldvick, A., 1962: Two-dimensional mountain waves — a method for rapid computation of lee wavelength and vertical velocity. *QJR Meteorol Soc*, **88**, 271–285.

Förchtgott, J., 1949: Wave currents on the leeward side of mountain crests. *Bull met tchecoal, Prague*, **3**, 49–51.

HAM. Handbook of Aviation Meteorology, 1994: London, HMSO.

HWF. Handbook of Weather Forecasting, 1975: Met.O.875, Meteorological Office.

Holton, J.R., 1992: Introduction to dynamic meteorology (3rd edition). Academic Press.

Hunt, J.C.R., 1980: Wind over hills. Workshop on the Planetary Boundary Layer, pp. 107–144. Am Meteorol Soc.

Hunt, J.C.R., 1995: The contribution of meteorological science to wind hazard mitigation. *In* T. Wyatt (Ed), Proceedings of the Wind Engineering Society meeting on wind hazard, May 1995.

Klemp, J.B., 1978: A severe downslope windstorm and aircraft event induced by a mountain wave. *J Atmos Sci*, **35**, 59–77.

Lawrence, E.N., 1953: Föhn temperatures in Scotland. *Meteorol Mag*, **82**, 74–79.
Ludlam, F.H., 1980, Clouds and storms. Pennsylvania State University Press.

McCarthy, J. and Serafin, R., 1984: The microburst: hazard to aircraft. *Weatherwise*, **37**, 120–127.

Mason, P.J., 1986: Flow over the summit of an isolated hill. *Boundary Layer Meteorol*, **37**, 385–405.

Meteorological Glossary (MG) (6th Edition), 1991: London, HMSO.

Meteorological Office (Heathrow), 198?

Moffitt, B.J., 1956: The nocturnal wind at Thorney Island. *Meteorol Mag*, **85**, 268–271.

Oke, T.R., 1982: The energetic basis of the urban heat island. *QJR Meteorol Soc,* **108**, 1–24.

Pielke, R.A., 1984: Mesoscale meteorological modeling. Academic Press, Florida.

Scorer, R.S., 1949: Theory of waves in the lee of mountains. *QJR Meteorol Soc*, **75**, 41–56.

Shutts, G.J., 1992: Observations and numerical model simulation of a partially trapped lee wave over the Welsh mountains. *Mon Weather Rev*, **120**, 2056–2066.

Shutts, G.J. and Broad, A., 1993: A case study of lee waves over the Lake District in northern England. *QJR Meteorol Soc*, **119**, 377–408.

Simpson, J.E., 1994: Sea breeze and local wind. Cambridge University Press.

Starr, J.R. and Browning, K.A., 1972: Observations of lee waves by high power radar. *QJR Meteorol Soc*, **98**, 73–85.

Stull, R.B., 1988: An introduction to boundary layer meteorology. Kluwer Academic Publishers.

Thorpe, A.J. and Guymer, T.H., 1977: The nocturnal jet. *QJR Meteorol Soc*, **103**, 633–654.

WMO, 1969: Vertical wind shear in the lower layers of the atmosphere. Geneva, World Meteorological Organization, Technical Note 93.

WMO, 1973: Airflow over mountains. Geneva, World Meteorological Organization, Technical Note 127.

2.1 Thermodynamics and the tephigram

2.1.1 Constructions using a tephigram

Fig. 2.1 illustrates Normand's theorem and construction to obtain potential and equivalent temperatures. **Fig. 2.2** illustrates constructions to obtain vapour pressure and saturation vapour pressure. Temperatures are specified for a parcel of air at 850 hPa.

HWF (1975)

2.1.2 Calculation of heights on a tephigram

This is illustrated in **Fig. 2.3**. After modifying the profile to show the virtual temperature (T_v):

(i) divide the temperature profile into a series of layers, 100 hPa deep up to the 300 hPa isobar, and then 50 hPa deep between 300 and 100 hPa.

(ii) Use a transparent scale marked with a straight line. Lay this over the temperature profile in each of the layers, parallel to the isotherms so as to create equal positive and negative areas either side of the mean isotherm.

(iii) Read off the layer thicknesses, in decametres, as marked along the intermediate isobars at 950, 850, 750 hPa, etc. The height of a standard pressure level is the sum of all the partial thicknesses below that level, plus the height of the 1000 hPa level. The height of the 1000 hPa surface may be read off from the nomogram printed on standard tephigrams. When the MSL pressure is less than 1000 hPa, the 1000 hPa heights are negative.

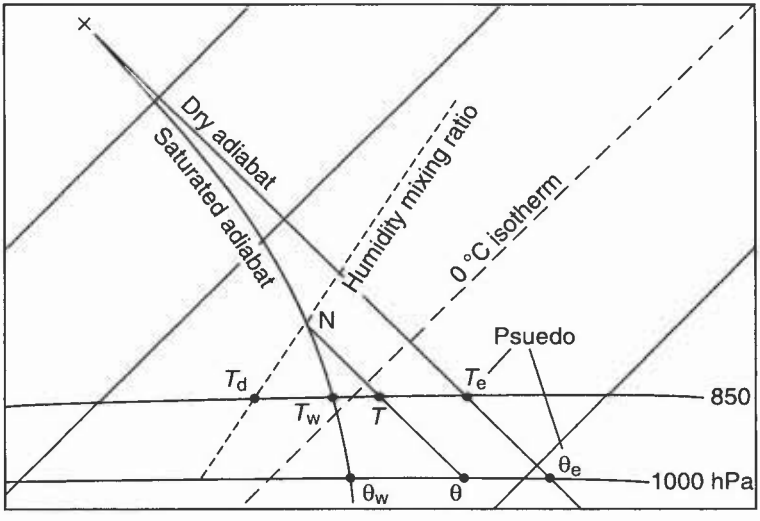

Figure 2.1. Construction on a tephigram to illustrate Normand's theorem, and to obtain potential temperature (θ, θ_w) and pseudo-equivalent temperatures (T_e, θ_e). The constructions are based on a parcel of air at 850 hPa, with temperature (T), wet-bulb temperature (T_w) and dew point (T_d).

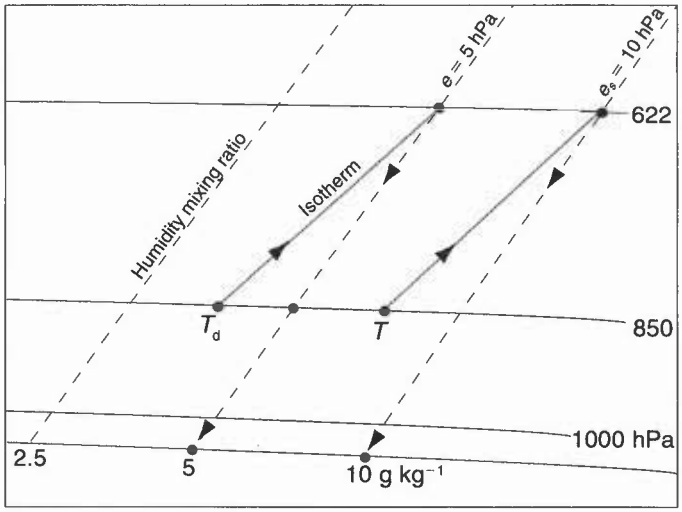

Figure 2.2. Constructions on a tephigram to obtain vapour pressure (e) and saturation vapour pressure (e_s) based on the air temperature (T) and dew point (T_d) of a parcel of air at 850 hPa.

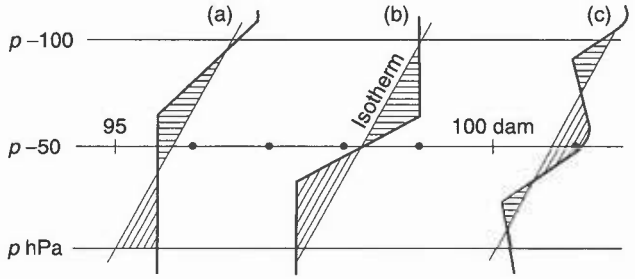

Figure 2.3. Calculating the thickness of a 100 hPa layer (base pressure = p). Shaded areas show equal positive and negative areas either side of a mean isotherm for three different shapes of environment curve. Thickness values are read off the scale on intermediate isobars. The examples show thickness values of (a) 95.7 dam, (b) 98.2 dam, and (c) 100.7 dam. See text for method of calculation.

The formula for height calculations involving layers which are not at standard levels is:

$$H = 29.27\, T_v \ln(p_0/p_1)$$

where H is in metres and T_v is the mean virtual temperature (K) of the layer $p_0 - p_1$.

2.2 Diurnal temperature variations in different air masses

(i) Statistics of temperature ranges occurring in various conditions can help in deciding whether forecast temperatures are reasonable.
(ii) In **Table 2.1** air-mass types are grouped according to whether trajectories on approaching the British Isles are curved cyclonically or anticyclonically. Data are pre-1950.
(iii) Forecasters may well have local data.

Table 2.1. Diurnal variations of temperature at Kew and Rye in different conditions

These data are summarized in the Local Weather Manual for S England, which also presents the 850 hPa WBPT by air-mass track and by season.

Belasco (1952)
Local Weather Manual for S England (1994)

2.3 Daytime rise of surface temperature

2.3.1 Forecasting the hourly rise of temperature on sunny days, using a tephigram

This method relates the amount of solar energy available for heating the lower layers of the atmosphere to an equivalent area on a tephigram.

(i) **Table 2.2** gives the thickness of the layer (Δp in hPa) which is changed from an isothermal to an adiabatic state by insolation for each hour from dawn, to the time of day maximum temperature, for the middle of each month, assuming no cloud.
(ii) Marking isobars p_o and $p_o - \Delta p$ **(Fig. 2.4)**, point I is placed on the isobar ($p_0 - \Delta p$) with IF along a dry adiabat and IH along an isotherm in such a way that it intersects the environment curve to form equal areas on either side, i.e. in this case area BAD equals area GHA plus area BIE. The point F then gives the value of the forecast surface temperature.

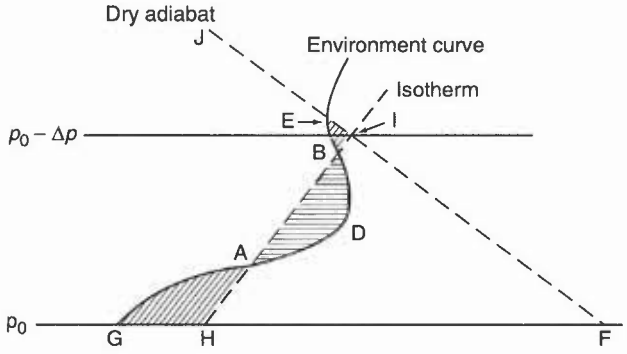

Figure 2.4. Estimating the rise of temperature on a sunny day by a tephigram construction. Δp is the thickness of the layer (hPa) and F is the forecast surface temperature. See text for details of construction.

Table 2.2 The thickness of the layer (Δp in hPa) which is changed from an isothermal to an adiabatic state by insolation at 52° N, 00° W

Month	Time (UTC)											
	05	06	07	08	09	10	11	12	13	14	15	Max
Jan.	—	—	—	—	03	18	35	48	58	61		61
Feb.	—	—	—	01	15	33	50	65	75	80		81
Mar.	—	—	02	17	35	53	68	81	90	95		97
Apr.	—	04	19	37	54	71	86	98	107	112	115	115
May	04	19	36	54	70	86	100	110	119	124	127	127
June	08	23	40	58	74	89	102	113	122	127	130	131
July	04	19	36	53	69	84	98	109	118	123	126	126
Aug.	—	08	24	41	59	75	89	101	110	116	119	119
Sept.	—	—	10	27	44	60	76	88	96	102	104	104
Oct.	—	—	01	13	29	45	60	72	80	85		86
Nov	—	—	—	—	11	25	38	49	57	61		61
Dec.	—	—	—	—	02	15	30	42	50	53		53

Notes:

(i) These values do not take into account any superadiabatic close to the surface. Add 2 °C to the resulting forecast temperature with clear skies and light winds in summer, to allow for superadiabats.

(ii) Approximate corrections to be applied to allow for cloud cover:

Table 2.3.

8/8 Ci	use	90% of depth (Δp in hPa)
8/8 As	use	60%
8/8 Sc	use	50%
8/8 Ns	use	35%

The value of Δp may be reduced if the ground is wet and/or the lowest layers of the atmosphere are very humid. In summer, if the ground is very dry and humidity in the bottom layers is low, the value of Δp may be increased. These changes are generally only significant in the first 3 or 4 hours of heating.

Inglis (1970) **Johnson (1958)**
Jefferson (1950)

2.3.2 Forecasting the temperature rise on days with fog or low cloud (Jefferson's method)

(i) Use the method in 2.3.1 to draw a curve showing the rise of temperature to be expected if the sky were clear.

(ii) Evaluate a constant 'delay factor' f. This may be done from the observation of temperature at least 3 hours after sunrise. If h_0 is the time of sunrise, h_2 is the time at which the temperature is observed and h_1 is the time at which that temperature would have been observed on a sunny day, then

$$f = (h_1 - h_0)/(h_2 - h_0)$$

(iii) Plot points C, F, etc., as shown in **Fig. 2.5**, such that:

$$AB/AC = DE/DF = \ldots f.$$

(As a first estimate, take $f = 0.25$ for deep fog or thick stratus and $f = 0.35$ for shallow fog or thin stratus). Points C, F, etc. provide a forecast temperature curve for a foggy day.

(iv) If this curve reaches the temperature (T_c) at which the fog can be expected to disperse, the subsequent temperature rise will be steeper and more in line with conditions for a clear day (dotted line in **Fig. 2.5**).

(v) A note of caution: the local advection of fog will give large errors in T_c, the calculated value not being achieved.

Grant (undated) **Jefferson (1950)**

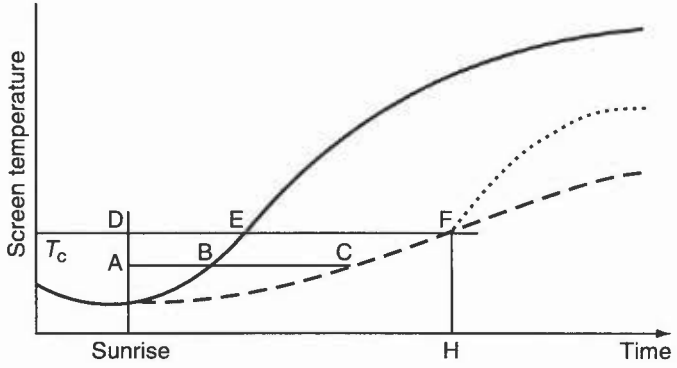

Figure 2.5. Constructing a forecast temperature curve on a foggy morning. The solid line is the forecast temperature curve for a clear day. The dashed line is the forecast for a foggy day, based on a delay factor of 0.35. The dotted line is the forecast for the later part of the day if the fog clears when the temperature reaches the critical value (T_c), at time H. See text for details of construction.

2.3.3 Forecasting T_{max} (Callen and Prescott's method, using 1000–850 hPa thickness)

This is an empirical method based on the maximum temperatures observed at Gatwick and the 1000–850 hPa thickness values at midday at Crawley.

There are three steps:

(i) Classify the cloud cover or presence of fog between dawn and 1200 UTC on a scale from 0 to 3 (**Table 2.4**), as follows:

Table 2.4.

Class 0	$C_L + C_M \leq 3/8$, $C_H \leq 5/8$; or any fog confined to dawn period.
Class 1	$C_L + C_M + C_H = 4/8$–$6/8$; or any fog clearing slowly during morning.
Class 2	$C_L + C_M \geq 6/8$; or any fog clearing before noon.
Class 3	Predominantly overcast with precipitation (not including very slight drizzle) or persistent fog.

(ii) Using **Fig. 2.6**, obtain the temperature adjustment for the month for the appropriate cloud class.

(iii) Apply this adjustment to the values given in **Table 2.5** to find the predicted maximum temperature.

The relationship between 1000–850 thickness (h) and the unadjusted maximum temperature (T_u) is given by

$$T_u = -192.65 + 0.156h.$$

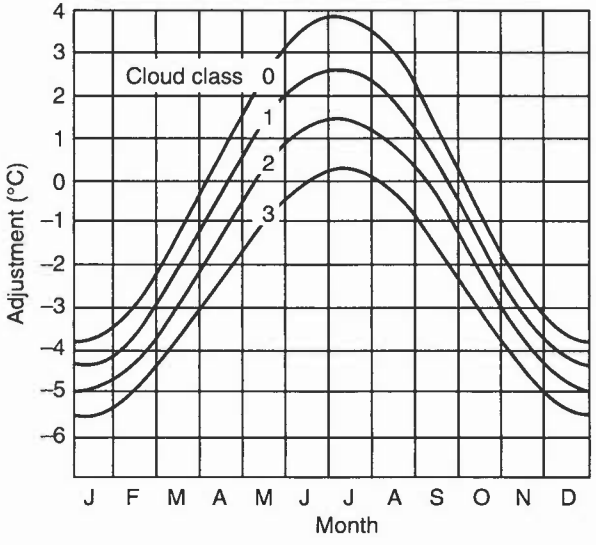

Figure 2.6. Adjustments to be applied to the values in Table 2.5 to allow for cloud classification and time of year.

Table 2.5. Unadjusted maximum temperature (°C) in terms of 1000–850 hPa thickness

Thickness (gpm)	Maximum temperature									
	0	1	2	3	4	5	6	7	8	9
1230	−0.8	−0.6	−0.5	−0.3	−0.1	0.0	0.2	0.3	0.5	0.6
1240	0.8	0.9	1.1	1.3	1.4	1.6	1.7	1.9	2.0	2.2
1250	2.3	2.5	2.7	2.8	3.0	3.1	3.3	3.4	3.6	3.8
1260	3.9	4.1	4.2	4.4	4.5	4.7	4.8	5.0	5.2	5.3
1270	5.5	5.6	5.8	5.9	6.1	6.2	6.4	6.6	6.7	6.9
1280	7.0	7.2	7.3	7.5	7.7	7.8	8.0	8.1	8.3	8.4
1290	8.6	8.7	8.9	9.1	9.2	9.4	9.5	9.7	9.8	10.0
1300	10.1	10.3	10.5	10.6	10.8	10.9	11.1	11.2	11.4	11.6
1310	11.7	11.9	12.0	12.2	12.3	12.5	12.6	12.8	13.0	13.1
1320	13.3	13.4	13.6	13.7	13.9	14.0	14.2	14.4	14.5	14.7
1330	14.8	15.0	15.1	15.3	15.5	15.6	15.8	15.9	16.1	16.2
1340	16.4	16.5	16.7	16.9	17.0	17.2	17.3	17.5	17.6	17.8
1350	17.9	18.1	18.3	18.4	18.6	18.7	18.9	19.0	19.2	19.4
1360	19.5	19.7	19.8	20.0	20.1	20.3	20.4	20.6	20.8	20.9
1370	21.1	21.2	21.4	21.5	21.7	21.8	22.0	22.2	22.3	22.5
1380	22.6	22.8	22.9	23.1	23.3	23.4	23.6	23.7	23.9	24.0
1390	24.2	24.3	24.5	24.7	24.8	25.0	25.1	25.3	25.4	25.6
1400	25.7	25.9	26.1	26.2	26.4	26.5	26.7	26.8	27.0	27.2
1410	27.3	27.5	27.6	27.8	27.9	28.1	28.2	28.4	28.6	28.7
1420	28.9	29.0	29.2	29.3	29.5	29.6	29.8	30.0	30.1	30.3
1430	30.4	30.6	30.7	30.9	31.1	31.2	31.4	31.5	31.7	31.8
1440	32.0	32.1	32.3	32.5	32.6	32.8	32.9	33.1	33.2	33.4

Callen et al. (1982)

2.3.4 Forecasting T_{max} from the 850 hPa wet-bulb potential temperature

The maximum temperature derived from the 850 WBPT is presented in **Table 2.6**, with corrections for wet and sunny conditions (based on London Weather Centre data for southern England).

Table 2.6. Maximum temperatures derived from 850 hPa wet-bulb potential temperatures

850 hPa θ_w	Equivalent thickness (m) 1000–850 hPa	Jan.	Feb.	Mar.	Apr.	May	Jun.	Jul.	Aug.	Sept.	Oct.	Nov.	Dec.	Correction Wet	Correction Sunny
18	1390	19	20	21	23	25	26	26	25	24	22	20	19	−5	+3
16	1380	17	19	19	21	23	25	25	23	23	21	19	17	−5	+2
14	1370	16	17	18	20	22	23	23	22	21	19	17	16	−4	+2
12	1360	15	15	17	19	21	21	21	21	19	17	15	17	−4	+2
10	1350	13	14	15	17	19	20	20	19	18	16	14	13	−4	+2
8	1340	11	13	13	15	17	19	19	17	17	15	13	11	−3	+2
6	1325	9	10	11	13	15	16	16	15	14	12	10	9	−3	+1
4	1320	8	9	10	12	14	15	15	14	13	11	9	8	−3	+1
2	1305	6	7	8	10	12	13	13	12	11	9	7	6	−3	+1
0	1295	4	5	6	8	10	11	11	10	9	7	5	4	−2	+1
−2	1285	3	4	5	7	9	10	10	9	8	6	4	3	−2	+1
−4	1270	−1	1	1	4	6	7	7	6	5	3	1	1	−2	+1

2.4 Nocturnal fall of surface temperature

(i) Empirical methods depend on solving an equation of the form: $T_{min} = aT + bT_d + C$, where T is an afternoon temperature, T_d is the dew point at a particular time or a mean dew point over a cooling period and C is a quantity depending only on wind speed and cloud amount. a and b are constants. A useful approach is to estimate the dusk temperature as one of the points on the Saunders' cooling curve.

(ii) The methods are applicable only when the ground is not snow covered; the effect of fresh snow cover is discussed later. Exceptionally low minima may also occur when there is a large catchment area for katabatic drainage and when the lowest layers (950–850 hPa) are very dry (dew-point depressions >20 °C).

Boyden (1937)
McKenzie (1944)

2.4.1 Forecasting dusk temperature, T_R, by Saunders' method

Saunders based his graphical method for determining a cooling curve on the idea of a discontinuity occurring in the rate of cooling at grass level within an hour after sunset, an effect particularly well defined on clear, windless nights (and possibly related to the deposition of dew). (**SB, Table 2.7.**)

Barthram (1964)
Saunders (1952)

2.4.2 Forecasting minimum temperature

2.4.2.1 Forecasting T_{min} (McKenzie's method)

(i) The night-time minimum air temperature (T_{min}) can be forecast as follows:

$$T_{min} = 0.5(T_{max} + T_d) - K$$

where T_{max} = maximum temperature, T_d = air-mass dew point at time of T_{max}, and K = local constant depending on forecast surface wind and low cloud amount).

(ii) K values have been calculated for most airports in the United Kingdom; forecasters should insert appropriate values (widely available from forecast offices).

Table 2.8(a). Values of local constant (K) for Birmingham Airport

Mean overnight surface wind (kn)	Average cloud amount overnight (oktas)				
	0	1–2	3–4	5–6	7–8
Calm	8.8	8.0	7.3	6.7	3.2
1–3	8.2	7.7	6.7	5.1	2.8
4–6	6.5	5.8	5.2	4.0	2.3
7–10	4.7	4.3	3.9	3.1	1.8
11–16	2.3	2.8	2.5	2.1	1.4
17–21	0.5	0.8	2.0	1.1	0.8

Monthly variations have been found which apply at all stations. The value of K may usefully be corrected by the following amounts:

Table 2.8(b).

	Jan.	Feb.	Mar.	Apr.	May	June	July	Aug.	Sept.	Oct.	Nov.	Dec.
A	−1.0	−0.5	+0.5	0.0	0.0	0.0	0.0	0.0	+0.5	+1.0	0.0	−1.0
B	−0.5	−0.5	0.0	0.0	+0.5	+0.5	+0.5	+0.5	0.0	0.0	−0.5	−0.5

A = 'Good radiation nights' B = 'Poor radiation nights'

Kensett (1983) **McKenzie (1944)**

2.4.2.2 Forecasting T_{min} (Craddock and Pritchard's method)

(i) The following regression equation was obtained from a statistical investigation of 16 stations in eastern England not close to the sea; it is considered valid for a wide area of eastern England:

$$T_{min} = 0.316\,T_{12} + 0.548\,T_{d12} - 1.24 + K$$
$$= X + K$$

where T_{12} = screen temperature at 1200 UTC and T_{d12} = dew-point temperature at 1200 UTC.

(ii) For ease of use, the value for X may be obtained from **Table 2.9** while the values for K, which depend on forecast values of the mean geostrophic wind and mean cloud amount, are given in **Table 2.10.** The means are forecast values for 1800, 0000 and 0600 UTC.

Table 2.9. Computation of the value of X (°C)

Air temp. at 1200	Dew-point at 1200 UTC																			
	−3	−2	−1	0	1	2	3	4	5	6	7	8	9	10	11	12	13	14	15	16
27	5.7	6.2	6.7	7.3	7.8	8.4	8.9	9.5	10.0	10.6	11.1	11.7	12.2	12.8	13.3	13.9	14.4	15.0	15.5	16.1
26	5.4	5.9	6.4	7.0	7.5	8.1	8.6	9.2	9.7	10.3	10.8	11.4	11.9	12.5	13.0	13.6	14.1	14.6	15.2	15.7
25	5.1	5.6	6.1	6.7	7.2	7.8	8.3	8.9	9.4	9.9	10.5	11.0	11.6	12.1	12.7	13.2	13.8	14.3	14.9	15.4
24	4.8	5.2	5.8	6.3	6.9	7.4	8.0	8.5	9.1	9.6	10.2	10.7	11.3	11.8	12.4	12.9	13.5	14.0	14.6	15.1
23	4.5	4.9	5.5	6.0	6.6	7.1	7.7	8.2	8.8	9.3	9.9	10.4	11.0	11.5	12.1	12.6	13.2	13.7	14.2	14.8
22	4.1	4.6	5.2	5.7	6.3	6.8	7.4	7.9	8.5	9.0	9.5	10.1	10.6	11.2	11.7	12.3	12.8	13.4	13.9	14.5
21	3.8	4.3	4.8	5.4	5.9	6.5	7.0	7.6	8.1	8.7	9.2	9.8	10.3	10.9	11.4	12.0	12.5	13.1	13.6	14.2
20	3.5	4.0	4.5	5.1	5.6	6.2	6.7	7.3	7.8	8.4	8.9	9.5	10.0	10.6	11.1	11.7	12.2	12.8	13.3	13.8
19	3.2	3.7	4.2	4.8	5.3	5.9	6.4	7.0	7.5	8.1	8.6	9.1	9.7	10.2	10.8	11.3	11.9	12.4	13.0	13.5
18	2.9	3.4	3.9	4.4	5.0	5.5	6.1	6.6	7.2	7.7	8.2	8.8	9.4	9.9	10.5	11.0	11.6	12.1	12.7	13.3
17	2.6	3.0	3.6	4.1	4.7	5.2	5.8	6.3	6.9	7.4	8.0	8.5	9.1	9.6	10.2	10.7	11.3	11.8	12.4	12.9
16	2.3	2.7	3.3	3.8	4.4	4.9	5.5	6.0	6.6	7.1	7.7	8.2	8.7	9.3	9.8	10.4	10.9	11.5	12.0	12.6
15	1.9	2.4	3.0	3.5	4.0	4.6	5.1	5.7	6.2	6.8	7.3	7.9	8.4	9.0	9.5	10.1	10.6	11.2	11.7	
14	1.6	2.1	2.6	3.2	3.7	4.3	4.8	5.4	5.9	6.5	7.0	7.6	8.1	8.7	9.2	9.8	10.3	10.9		
13	1.3	1.8	2.3	2.9	3.4	4.0	4.5	5.1	5.6	6.2	6.7	7.3	7.8	8.3	8.9	9.4	10.0			
12	1.0	1.5	2.0	2.6	3.1	3.6	4.2	4.7	5.3	5.8	6.4	6.9	7.5	8.0	8.6	9.1				
11	+0.7	1.1	1.7	2.2	2.8	3.3	3.9	4.4	5.0	5.5	6.1	6.6	7.2	7.7	8.3					
10	+0.4	+0.8	1.4	1.9	2.5	3.0	3.6	4.1	4.7	5.2	5.8	6.3	6.9	7.4						
9	−0.0	+0.5	1.1	1.6	2.2	2.7	3.2	3.8	4.3	4.9	5.4	6.0	6.5							
8	−0.4	+0.2	+0.7	1.3	1.8	2.4	2.9	3.5	4.0	4.6	5.1	5.7								
7	−0.7	−0.1	+0.4	1.0	1.5	2.1	2.6	3.2	3.7	4.3	4.8									
6	−1.0	−0.4	+0.1	+0.7	1.2	1.8	2.3	2.8	3.4											
5	−1.3	−0.8	−0.2	+0.3	+0.9	1.4	2.0	2.5	3.1											
4	−1.6	−1.1	−0.5	+0.0	+0.6	1.1	1.7	2.2												
3	−1.9	−1.4	−0.8	−0.3	+0.3	+0.8	1.4													

Table 2.10. Values of K (°C) based on mean forecast values of wind speed and cloud amount for 1800, 0000 and 0600 UTC

Mean geostrophic wind speed (kn)	Mean cloud amount (oktas) 0–2	2–4	4–6	6–8
0–12	−2.2	−1.7	−0.6	0
13–25	−1.1	0	+0.6	+1.1
26–38	−0.6	0	+0.6	+1.1
39–51	+1.1	+1.7	+2.8	—

The development of appropriate regression equations is required if the method is to be applied to other areas of the country.

Craddock et al. (1951)

2.4.2.3 Forecasting the hourly fall of temperature during the night (Barthram's method)

The following steps are used in conjunction with the Night Cooling Nomogram **(Fig. 2.7)**, to obtain a cooling curve, drawn realistically through T_{max}, T_R (the Saunders' discontinuity temperature) and T_{min}:

(i) Use a representative upper-air sounding to determine whether there is an inversion with its base below 900 hPa at the time of maximum temperature.
(ii) Decide if nocturnal cloud cover will be best described as cloudless or 8/8.
(iii) From steps (i) and (ii), select one of the four rows marked 'Dew-point at time of maximum temp'. A series of vertical lines descends from these dew-point values.
(iv) Follow a horizontal line from the value for the maximum temperature (marked on the left-hand side) until it cuts the vertical line descending from the dew-point value selected in step (iii). From this point, follow one of the diagonal lines to the line marked 'Saunders' discontinuity temperature T_R'. Ignore T_R on cloudy, windy nights.
(v) The time of this discontinuity depends on the date. Use the small graph at the bottom of the nomogram where the months are marked. Find the time of T_R for the required date from the curve marked 'time of discontinuity'.
(vi) Follow the vertical line upwards from the time of T_R and extend it to the main graph to meet the value of T_R established in step (iv).
(vii) The next stage brings in a correction for the forecast gradient wind overnight. Select one of the diagonal lines on the right-hand side of the nomogram marked 'gradient wind speed'.
(viii) Follow the horizontal line from T_R until it cuts the selected diagonal line marked 'gradient wind speed'. From this point of intersection, descend along a vertical line to the diagonal marked 'Minimum temp. under clear skies'. The preliminary value for T_{min} can be read off here.
(ix) The preliminary value for T_{min} needs corrections for cloud amount and wind speed. The two small graphs (lower left) show amounts to be added to the preliminary T_{min} value to allow for the effect of nocturnal cloud cover and wind.
(x) In summer a further correction is needed because the short nights give a reduced period for cooling. Use the small graph (lower right, **Fig. 2.7(b)**) to find this value.

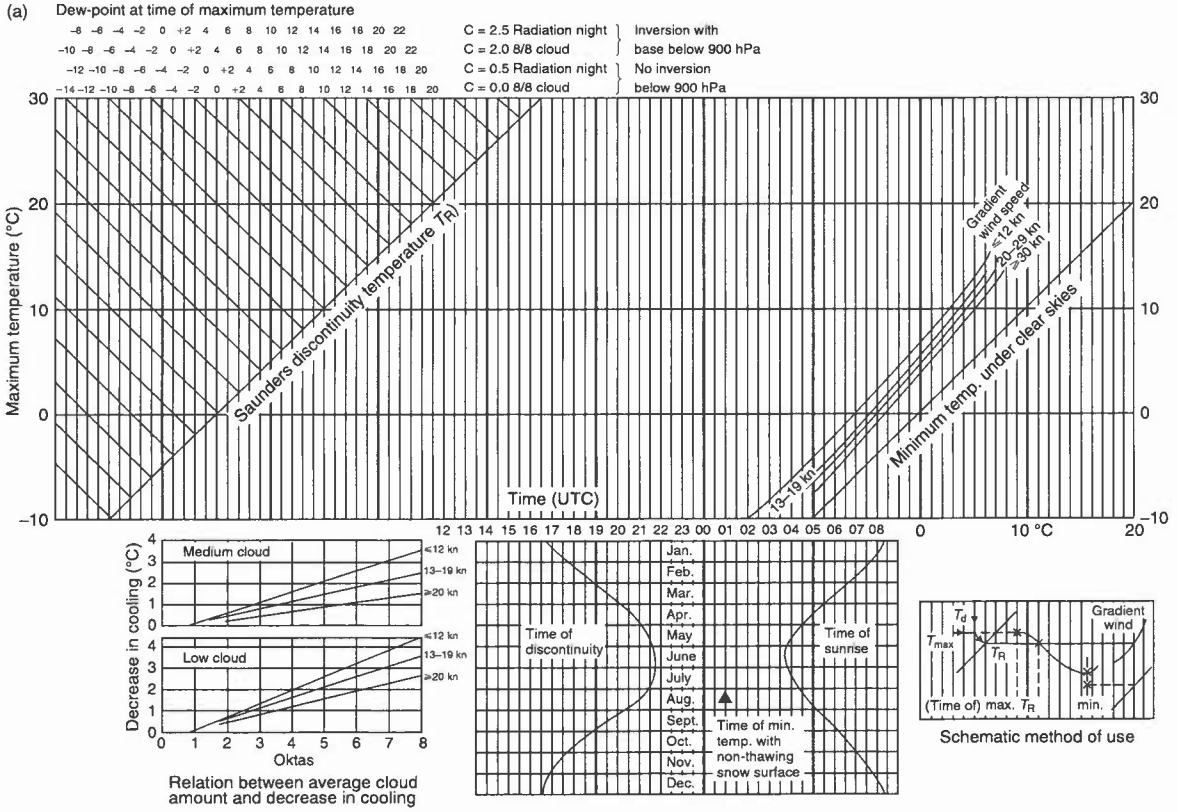

Figure 2.7(a). Night cooling nomogram for winter (October–March). See text for method of use.

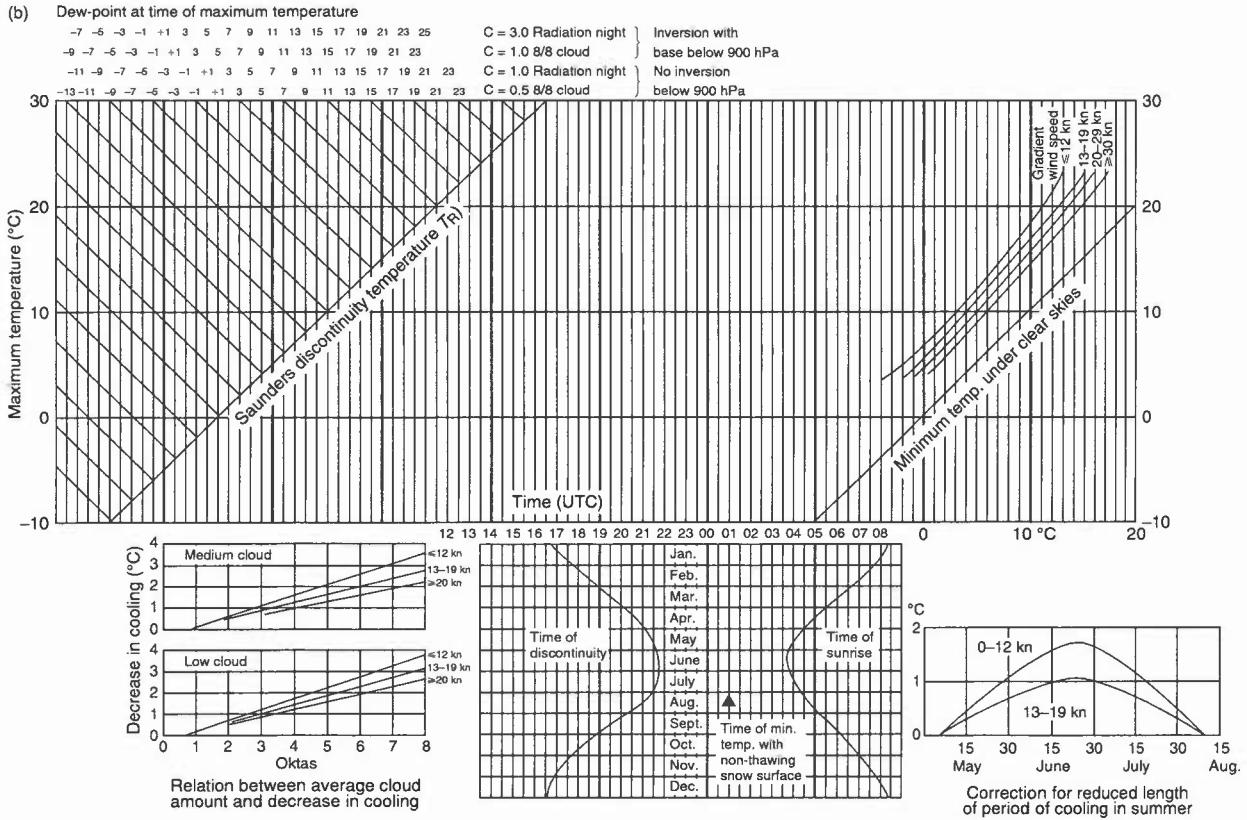

Figure 2.7(b). Night cooling nomogram for summer (April–September). See text for method of use.

(xi) After raising the preliminary T_{min} by adding the corrections in steps (ix) and (x) the final value of T_{min} is plotted on the main graph above the time for sunrise shown on the lower graph.

(xii) This fixes three points on the cooling curve: T_{max} at approximately mid afternoon, T_R and T_{min}. The cooling curve can be drawn through these three points.

There are small differences between cooling for summer and winter and separate diagrams are provided for winter (October to March) (**Fig. 2.7(a)**) and for summer (April to September) (**Fig. 2.7(b)**).

Notes:

(a) The method applies to nights without fog.

(b) Effect of snow cover is discussed next.

Barthram (1964)

2.4.3 Effect of snow cover

(i) Under clear skies and light winds, screen temperature over a snow surface is likely to fall 2 to 4 °C below the minimum calculated by the methods in 2.4 and to be reached earlier than if snow free.

(ii) With cloud present the minimum is likely to be about 1 °C lower than over snow-free surface; it may be less than that for wind speeds of 15 kn or so.

HWF (1975), Chapter 17.7.4

2.4.4 Description of the severity of air frost

When actual or forecast air temperatures fall below 0 °C, the severity of the frost is described arbitrarily by the terms 'Slight', 'Moderate', 'Severe' or 'Very severe' according to the temperature and the surface wind speed at the time, as illustrated in **Fig. 2.8.**

2.5 Grass- and concrete-minimum temperatures

2.5.1 Forecasting the grass-minimum temperature, using the geostrophic wind speed and cloud amount

T_g, the grass-minimum temperature is calculated from:

$$T_g = T_n - K$$

where T_n is the air-minimum temperature, and K is a constant which depends on forecast values of geostrophic wind speed and cloud amount.

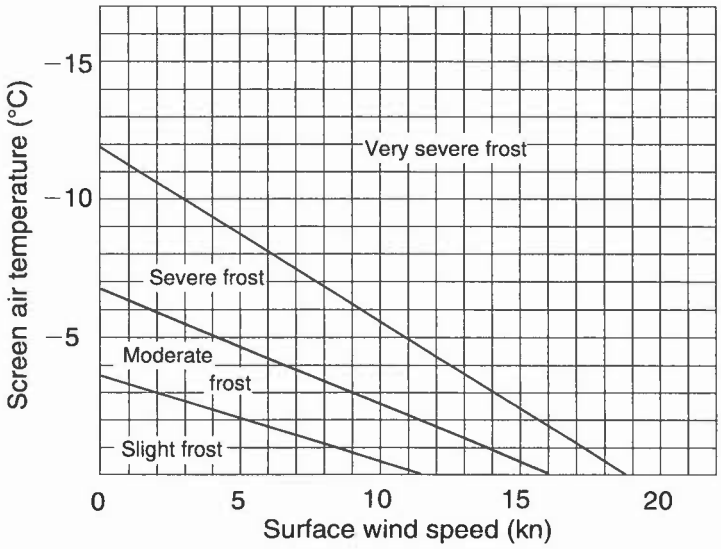

Figure 2.8. Diagram for determining the severity of air frost for actual or forecast wind speeds and air temperatures.

Table 2.11. Values of K (°C)

V_g	N (oktas)			
(kn)	0–2	2–4	4–6	6–8
0–12	5.0	5.0	4.0	4.0
13–25	4.0	4.0	3.0	2.0
26–38	3.5	3.0	2.5	2.5
39–52	2.5	2.5	2.5	3.0

Values of V_g and N are means of the 1800, 0000 and 0600 UTC values.

Craddock & Pritchard (1951)
HWF (1975) Chapter 14.7.3

2.5.2 Forecasting the grass-minimum temperature from the geostrophic wind speed (graphical method)

Fig. 2.9 shows isopleths of the depression of the grass-minimum temperature below the air-minimum temperature at Cottesmore in eastern England. Only low-cloud cover is considered, and 'sky obscured' is taken to be the same as 8 oktas.

Sills (1969)

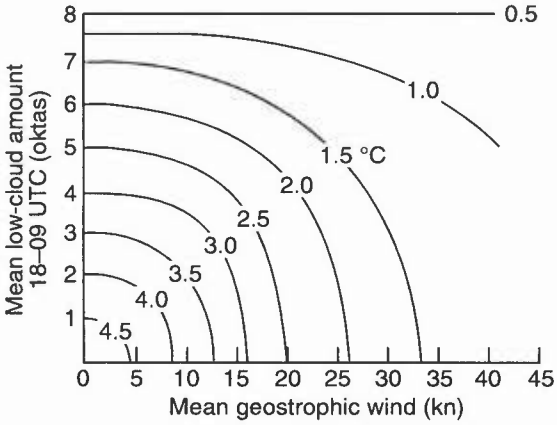

Figure 2.9. Depression (°C) of the grass-minimum temperature below the air-minimum temperature at Cottesmore.

2.5.3 Forecasting the grass-minimum temperature from the surface wind speed

Use the same formula as in 2.5.1 above but with values of K as follows:

Table 2.12. K values (°C) as a function of surface wind speed and cloudiness

Surface wind (kn)	Clear sky (up to 2/8)		Cloudy (8/8 cloud)
	Mean	(Max)	Mean
1–5	5.0	(8.0)	1.0
6–10	3.5	(8.6)	1.0
11–15	2.5	(3.5)	1.0
>15	1.5	(2.8)	1.0

Cloud cover is C_L, C_M or $C_L + C_M$

The mean values, averaged for six stations in England, have been rounded to 0.5 °C.

FRB (1993)

2.5.4 Minimum temperature on roads

At Watnall (near Nottingham), it was found that the difference between screen minimum, T_{min}, and (concrete) road minimum temperatures varied with the length of night. The following regression equation was obtained **(Table 2.13)**:

$$T_{min} - T_r = 0.28t - 2.9$$

where T_r = minimum temperature on the road, t is the length of night (in hours).

Table 2.13. Minimum temperature on roads (°C)

	Jan.	Feb.	Mar.	Apr.	May	Jun.	Jul	Aug.	Sep.	Oct.	Nov.	Dec.
$T_{min} - T_r$ (observed)	2.0	1.5	1.0	0.0	—	—	—	—	—	0.5	1.5	2.0
From the formula for length of night for 52° N	1.5	1.1	0.5	0.0	−0.6	−1.1	−0.7	−0.3	0.3	0.8	1.4	1.6

Parrey (1969)
Ritchie (1969)

2.6 Forecasting road surface conditions

Forecasting the temperature of road surfaces is not straightforward, because of the wide variations in meteorological conditions which are found over short distances on the same night as well as variations in the thermal capacity and conductivity of different types of road and the road state (**SB**).

2.6.1 Site differences

Site-specific ice prediction lies at the core of forecasting road surface conditions. There are three types of night for which forecasts are required: *Extreme, Damped and Intermediate.* (**SB, Fig 2.10**).

2.6.1.1 Urban, rural and coastal sites and bridges

Important meteorological, locational and traffic factors are listed in **SB**.

Astbury (1994) **Perry & Symons (1991)**

2.6.2 Forecasting for icy roads

Forecasting for the sources of moisture leading to road icing (precipitation; dew; hoar frost; freezing fog; moisture advection; melting snow) as discussed in the **SB**.

Astbury (1994) **Hewson & Gait (1992)**

2.6.2.1 Forecasting hoar frost

The following are necessary for hoar frost:
RST to be below air-mass dew point and to be at or near freezing; breeze sufficient to cause mixing.

These conditions are likely if five or more of the following conditions are satisfied:
(i) long night;
(ii) low road-depth temperature (RDT) (≤4.5 °C);
(iii) clear sky ≤2/8 cloud cover;
(iv) wind ≥4 kn at 10 m;
(v) high dew point ≥1 °C;
(vi) small dew-point depression ≤1.5°C;
(vii) cold and clear previous night.

Adjacent moisture sources, such as small lakes, rivers, edges of woods, etc. are important.

Local variations: more likely to be encountered on higher ground, in coastal regions, on bridge decks.

Note that:
(i) Hoar frost is unlikely in very cold, dry air; early or late in the season.
(ii) The five conditions are most likely during polar maritime and arctic maritime outbreaks when the higher, colder more exposed sites become frosty first.
(iii) Most severe events occur when moister air with RDT higher than RST is being advected over a cold surface after a cold spell.
(iv) During several days of clear skies north facing slopes, sheltered urban and rural roads can accumulate hoar frost over several days and nights.

Thermal maps can aid the forecaster in constructing the likely spatial variability to be anticipated in road-surface temperatures under clear, cloudy, windy, wet, etc. nights.

Astbury (1994)
Hewson & Gait (1992)
Perry & Symons (1991)

2.7 Modification of surface air temperature over the sea

2.7.1 Advection of cold air over warm sea

2.7.1.1 Frost's method (SB)

Frost (1941)

2.7.1.2 Blackall's method (SB, Fig. 2.11, Table 2.14)

This empirically based method takes into account both the duration of the sea crossing and the depth of convection.

Blackall (1973)

2.7.1.3 Grant's method (SB, Figs 2.12 and 2.13)

This method of forecasting coastal temperatures in cold-air advection with onshore winds appears to perform better than Blackall's method, though giving no real improvement in showery northerlies.

Grant (1975)

2.7.2 Advection of warm air over a cold sea (Lamb and Frost's method) (SB, Table 2.15)

Lamb (1943)

2.8 Cooling of air by precipitation

2.8.1 Cooling of air by rain

A dry-bulb temperature close to the wet-bulb value is reached after about half an hour of very heavy rain or about 1 to 2 hours of rain of lesser intensity.

HWF (1975) Chapter 14.9.3

2.8.2 Cooling of air by snow

Falling snow gradually lowers the 0 °C level. However, the reduction of the surface temperature to 0 °C is unlikely if:

(i) the wet-bulb temperature at the surface is higher than 2.5 °C in prolonged frontal precipitation;

(ii) the wet-bulb temperature at the surface is higher than 3.5 °C within extensive areas of moderate or heavy instability precipitation.

Note: The relation between wet-bulb temperature and the form of precipitation is given in 5.10.1.

Lumb (1963)

2.8.3 Downdraught temperatures in non-frontal thunderstorms

The temperatures of strong downdraughts reaching the ground are very close to the surface temperature of the saturated adiabatic through the intersection of the wet bulb and the 0 °C isotherm (6.2.2.4) **(Fig. 6.4)**.

Fawbush & Miller (1954)

2.9 Ice accretion

2.9.1 Types of icing

See Table 2.16.

2.9.2 Airframe icing

Ice accretion on an airframe is possible whenever flight occurs through cloud or rain at sub-zero temperatures **(Fig. 2.14)**, and on a rapid move from regions of low temperature to warm, moist regions (**SB**).

Pike (1995)

2.9.2.1 Icing risks for helicopters

Ice on rotating blades is especially dangerous, as they are more heavily loaded than a fixed aircraft wing (**SB**). For commercial operations, principally in the North Sea, forecasts of liquid-water content and temperature are made available from numerical models.

HAM (1994)

Table 2.16. Types of icing

Type	Source	Formation and properties
Hoar frost	Vapour	Direct deposition on surface with temperature below frost point of ambient air. White crystalline coating.
Rime	Supercooled droplets	Impact on surface with temperature <0 °C. Variable properties. Two extreme forms are: (a) *Opaque rime*: Drops freeze rapidly without much spreading; light porous texture with a lot of entrapped air; the smaller the droplets and the lower the temperature the rougher and more cloudy will be deposit. (b) *Clear, or glazed, ice*: Drops spread and freeze more slowly; smooth and glassy deposit sticks strongly to surface (temperatures near 0 °C).
Rain ice	Supercooled	Formation similar to clear ice. Substantial deposits may form over an extensive region. The resulting low-level icing may be severe; it is not common, but is a very important forecasting challengs in the UK and near continent (see 2.9.9).
Cloudy or mixed ice	Supercooled and ice	Ice crystals may adhere to wet surface and freeze in with droplets to give a rough, cloudy ice.
Pack snow	Supercooled drops and snowflakes	Drops freeze on impact, embedding the snowflakes, giving deposit like tightly packed snow.

HAM (1994)

2.9.2.2 'Cold-soak' icing as a result of 'Hi-Lo' profile flying

Fast descent of military aircraft after prolonged flight at high levels with sub-zero temperatures can result in 'cold-soak' icing in no-cloud conditions (**SB**).

HAM (1994)

2.9.3 Engine icing

Engine icing can occur at temperatures above zero and in clear air (**SB**).

2.9.3.1 Piston engines

In addition to *impact icing*, piston engines are subject to *Fuel icing* — not common — and *Carburettor icing*.

CAA (1991)

2.9.3.2 Turbine and jet engines

Susceptible parts are intake rim and struts (**SB**).

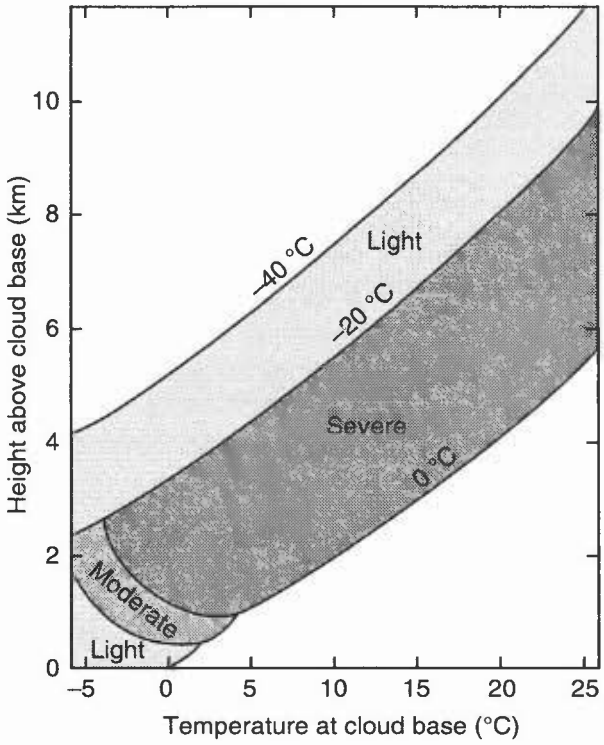

Figure 2.14. Airframe icing in convection cloud. Approximate thickness of layers within which various degrees of icing may be expected to occur. Base of cloud = 950 hPa, ambient relative humidity = 70%.

2.9.4 Intensity of ice accretion

Terms used to describe ice accretion are: Trace of icing, light, moderate and severe icing.

(i) These terms can be used to *report* ice accretion but not for *forecasting* purposes since icing intensity is dependent on aircraft type and velocity vector.

(ii) The *depth* of the icing layer ('icing band') is always required by aircrew in order to plan for avoidance or rapid transit of the band.

HAM (1994)
WMO (1968)

2.9.5 Icing and liquid-water content

(i) The relationship between the intensity of icing in clouds and supercooled liquid water content (LWC) is not simple.

(ii) It depends on the integral of the LWC (or rather that fraction that consists of droplets large enough to accrete to the aircraft) along the aircraft trajectory. Thus Fig. 2.14 is only a guide.

(iii) Critical value of the integral is 7.5 g cm^{-3}.
(iv) Forecasters should, in principle, forecast LWC using model guidance and/or methods in 2.9.6 and 2.9.7.5, allowing the user to calculate integrals along aircraft trajectories (consistent methodology required of the user).
(v) Forecasters must be aware that the propensity for droplets to accumulate on an aircraft depends critically on both drop size and the size of the aircraft component; a large proportion of cloud drops are of sizes that are efficiently collected by small components (e.g. pitot-static tubes) on fast aircraft but are collected much less efficiently on large components on slow-moving aircraft.

2.9.6 Estimating the maximum liquid-water content of a cloud (SB)

On a tephigram:
(a) Plot the pressure and temperature at cloud base.
(b) Ascend along a saturated adiabat to the cloud-top level.
(c) The difference in HMR between the base and top of the cloud gives the maximum (adiabatic) liquid-water content of the cloud, in units of g kg^{-1}.
(d) Mixing with dry air at cloud top may reduce the actual cloud water content to around half the theoretical maximum value.

Since at 800 hPa (a typical wet-cloud level) 1 kg of air occupies about 1 m^3, the number obtained in (c) may simply be relabelled in units of g m^{-3}, which is a more useful measure of liquid water content for practical measurement.

Note that orographic uplift can significantly lower the freezing level, giving icing at unexpectedly low levels. The importance of the increase in icing severity thus encountered cannot be overemphasized.

2.9.7 Cloud temperature and icing risk

2.9.7.1 Convective clouds

(i) Cloud-base temperature influences the risk and severity of ice accretion; the average liquid-water content/unit volume shows little variation with that over most of the cloud depth.
(ii) However, there is a higher liquid-water content in newly developing parts of a Cu cloud than in the more mature regions; liquid droplets predominate down to about −15 °C.
(iii) Large cloud-water mixing ratios can exist at high altitude. Incidents of severe icing have been reported in developing Cb anvils, the tropopause restricting vertical development, thereby producing an extensive layer of liquid and frozen water.

The following rules are generally accepted:

Table 2.17.

Cloud temperature (°C)	Nature of cloud particles: Supercooled water	Nature of cloud particles: Ice crystals	Icing risk
0 to −20	many	few	High
−20 to −40	few	many	Low (but High in Cb cells and see (iii) above))
<−40	nil	all	nil

Fig. 2.14 illustrates the potential for airframe icing in convective clouds under various cloud-base temperature conditions, but see 2.9.4, 2.9.5.

Lunnon et al. (1994)

2.9.7.2 Layer cloud

Generally the icing severity in layer clouds of about 3000 ft thickness and tops at 850 hPa is:

(a) *moderate* for tops between 0 and −10 °C;
(b) *light* for tops <−10 °C.

Satellite imagery is useful in pinpointing the rapid build-up of cloud frequently responsible for icing.

It is important to note:

(i) The risk of icing increases above the lowest 300 m of the cloud.
(ii) Even in layer cloud, such as anticyclonic stratocumulus forming over the sea in winter, the icing in the upper part of the cloud may be severe. This is due both to the high liquid-water content and to duration of flight possible within extensive cloud layers. A capping inversion will further encourage the maintenance of a high liquid-water content by restricting the depth for drop growth by the Bergeron–Findeisen method.
(iii) Altocumulus and nimbostratus, formed by mass ascent, may be extensive and deep; icing will be further enhanced by orographic lifting. Severe icing has been reported at temperatures as low as −20 to −25 °C.

2.9.7.3 Cirrus

Cirrus clouds seldom constitute an icing hazard.

2.9.7.4 Orographic cloud

Icing is likely to be more severe in clouds subject to orographic lift than in similar clouds away from high ground.

2.9.7.5 Cloud type: summary table of icing probability and intensity

Liquid water content increases from zero at just below cloud base roughly linearly for the first 200–300 m above cloud base. In this region there is little or no icing, unless there is orographic uplift or embedded convective cloud.

Table 2.18.

Cloud type	Probability of icing	Intensity	Water content ($g\ m^{-3}$)
Cb, Ns	High	May be severe	0.2–4.0
Cu, Sc, Ac, AcAs	50%	Rarely more than moderate	0.1–0.5
As	Low	Moderate or light	0.1–0.3
St	Low	Light	0.1–0.5
Upper regions of layer cloud	High	May be severe	0.5–1
Orographic	High	probably moderate	0.1–0.5

Note that the severity is also a function of other non-meteorological factors: aircraft type and duration of flight within the cloud(2.9.4).

HAM (1994)

2.9.8 Freezing rain in elevated layers (Chapter 5.8 and SB)

Ahmed et al. (1993)

2.9.9 Severe low-level icing (rain ice) (Chapter 5.8)

HWF (1994), Chapter 7.8

2.9.10 Slantwise convection (conditional symmetric instability)

Severe icing events are often associated with this slantwise convection up to θ_w surfaces **(SB)**.

Bohorquez & McCann (1995)

2.9.11 Icing on ships

(i) In rough seas when the wind is strong and the air temperature below -2 °C, spray may freeze on the superstructure of a vessel. The weight of accumulated ice may eventually become a considerable hazard.

(ii) The degree of icing depends on both temperature and wind speed, as shown in **Fig. 2.15**. The icing is classified in terms of thickness of accumulation per day:

Table 2.19.

Degree of icing	Accumulation (cm per 24 hours)
Light	1–3
Moderate	4–6
Severe	7–14
Very severe	15 or more

HWF (1975), Chapter 21.5.2

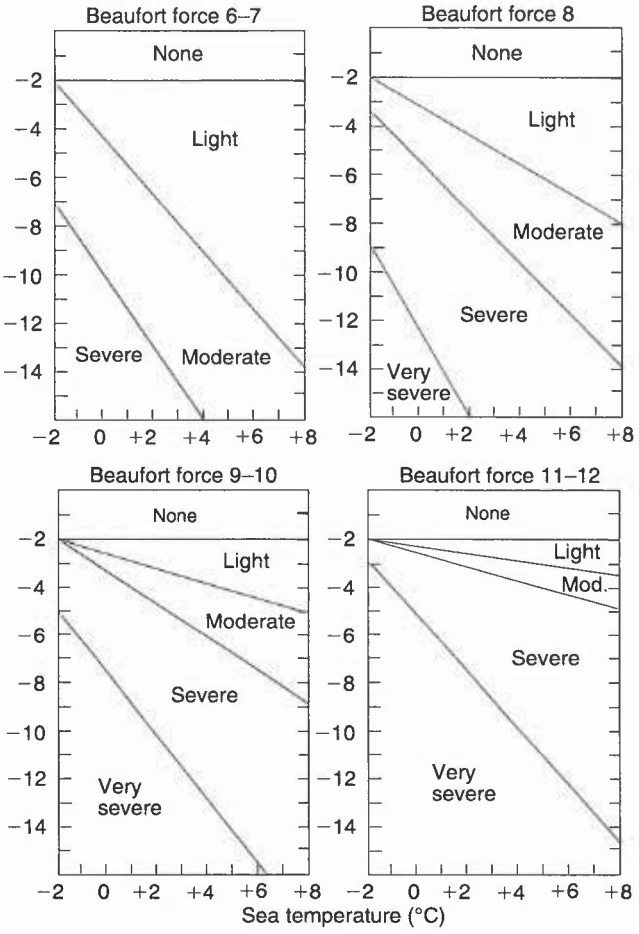

Figure 2.15. Icing on slow-moving fishing vessels in various wind conditions.

2.10 Wind chill and heat stress in man and animals

2.10.1 Human perception of wind chill

The influence of wind on the human perception of temperature gives rise to an 'equivalent temperature' (not applicable to inanimate objects). Steadman's data (**Table 2.20, Fig. 2.16**) relate to the still air temperature for which the rate of heat loss from a human is the same as that for the observed wind and temperature.

C & PSH, Chapter 3.10.3
Dixon & Prior (1987)
Steadman (1984)

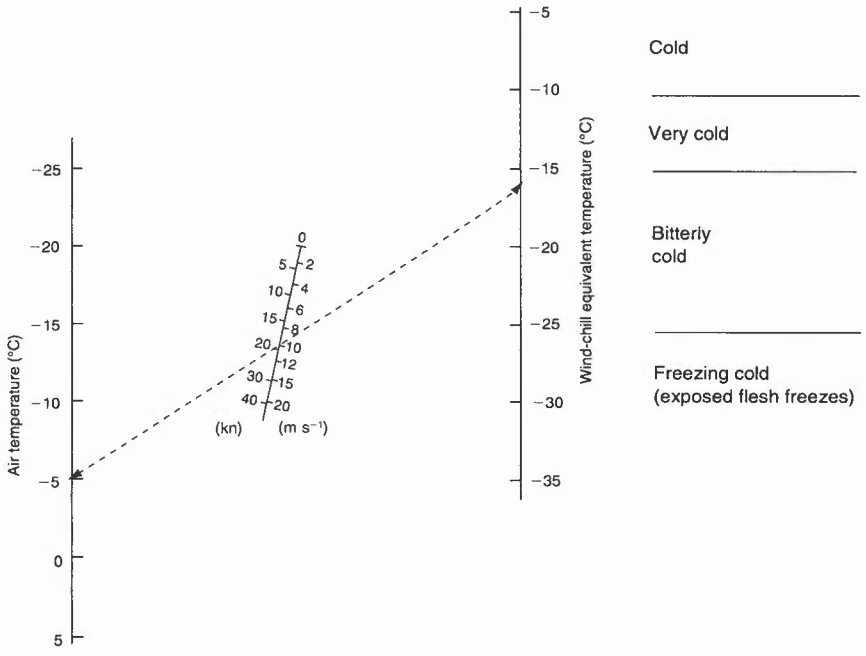

Figure 2.16. Nomogram for obtaining Steadman (1984) wind-chill equivalent temperatures and associated sensations for various combinations of air temperature and 10 m wind speed. The example shows an equivalent temperature of −16 °C, which would be termed 'bitterly cold', resulting from an air temperature of −5 °C and a wind speed of 20 kn.

2.10.2 Heat stress, mass participation events

Many heat stress indices have been devised. The Temperature–Humidity Index (THI) is applicable to sedentary workers indoors, or outside in the shade in light winds and can be forecast from the dry- and wet-bulb temperatures (T and T_w) as follows:

$$\text{THI} = 0.4(T + T_w) + 4.8 \text{ (in °C)}.$$

As THI increases above 20, increasing discomfort is felt; at THI = 24 some 50% of people are expected to feel discomfort; for THI >27 all are likely to be distressed.

The potential for heat stress in mass participation 'fun-run' events is considerable and this must be pointed out in any forecasts specifically for such events; crowding restricts the ability of the body to dissipate the heat load imposed by high levels of temperature, humidity and solar radiation.

Driscoll (1985) **Kerslake (1972)**
de Freitas et al. (1985) **Steadman (1984)**

Table 2.20.

(a). Wind-chill equivalent temperatures (Steadman)

Screen temp. (°C)	10-metre wind (knots)							
	5	10	15	20	25	30	35	40
20	19.1	17.4	15.9	14.9	14.0	13.3	12.8	12.3
18	17.0	15.2	13.7	12.5	11.5	10.8	10.2	9.7
16	14.9	13.0	11.4	10.1	9.0	8.2	7.6	7.0
14	12.9	10.8	9.1	7.6	6.5	5.6	4.9	4.2
12	10.8	8.6	6.7	5.2	4.0	3.0	2.1	1.4
10	8.7	6.4	4.4	2.7	1.4	0.2	−0.6	−1.4
8	6.7	4.2	2.0	0.2	−1.2	−2.5	−3.4	−4.2
6	4.6	2.0	−0.4	−2.3	−3.9	−5.2	−6.3	−7.0
4	2.5	−0.3	−2.8	−4.8	−6.5	−7.9	−9.1	−10.0
2	0.4	−2.5	−5.2	−7.3	−9.1	−10.7	−11.9	−12.9
0	−1.7	−4.8	−7.5	−9.9	−11.8	−13.3	−14.6	−15.8
−2	−3.7	−7.1	−9.9	−12.3	−14.4	−16.1	−17.4	−18.6
−4	−5.8	−9.3	−12.3	−14.8	−17.0	−18.8	−20.2	−21.4
−6	−7.9	−11.6	−14.6	−17.3	−19.6	−21.3	−22.9	−24.2
−8	−10.0	−13.9	−17.0	−19.9	−22.2	−24.0	−25.6	−27.0
−10	−12.1	−16.1	−19.4	−22.4	−24.7	−26.6	−28.3	−29.5
−12	−14.2	−18.3	−21.7	−24.9	−27.3	−29.3	−31.0	−32.6
−14	−16.3	−20.6	−24.1	−27.3	−29.9	−31.9	−33.8	−35.3
−16	−18.3	−22.8	−26.5	−29.7	−32.4	−34.6	−36.5	−38.0
−18	−20.4	−25.0	−28.9	−32.2	−34.9	−37.2	−39.1	−40.8
−20	−22.5	−27.2	−31.2	−34.7	−37.4	−39.7	−41.7	−43.5

2.10.3 Wind chill and heat stress in livestock (SB)

C & PSH, Chapter 6
Starr (1988)

2.11 The urban 'heat island'

The urban environment will influence heat storage and the radiation balance; the result is a modified local (micro-) climate compared with the surrounding rural environment **(SB, Fig. 2.17, Table 2.21)**

Landsberg (1981)
Oke (1987)

2.12 Model Output Statistics (MOS)

(i) MOS models match observations and forecast parameters; a statistical relationship is established, the MOS technique thus allowing for bias in the model forecast by the post-processing of model data. Station-specific maximum and minimum temperatures are available.

(ii) Current parameters used in MOS regressions are:
MSLP (of little value);
level 1 (997 hPa): temperature, dew point, wind speed and direction;
level 4 (870 hPa): temperature, dew point, wind speed and direction;
vertical shear parameter (of minor significance).

(iii) MOS are not well equipped to forecast extreme temperatures.

(iv) MOS temperatures from the LAM are occasionally misleading due to poor representation of boundary layer cloud, particularly when Sc is trapped below an inversion lower than model level 4, with dry air above (giving too low minima).

(v) Changes in model formulation can affect maximum temperatures, giving a temporary deterioration in accuracy until the new model characteristics have been 'learnt' by the MOS model.

(vi) Forecasters must examine structure of low-level flow before using MOS values.

(vi) MOS forecasts are based on midday and midnight ascents for maximum and minimum temperature, respectively. Changes after these times, e.g. the passage of a cold front in the early hours of the morning, cannot be taken into account; beware situations when the base of an inversion is lower than 870 hPa (level 4).

(vii) MOS algorithms are updated monthly.

(viii) Around equinoxes rapid changes in insolation may lead to inaccurate forecasts, e.g. too cold at beginning of September, too warm at end of that month.

Glahn & Lowry (1972)
Ross (1989)

BIBLIOGRAPHY

CHAPTER 2 — TEMPERATURE

Ahmed, M., Graham, R.J. and Lunnon, R.W., 1993: Creating a global climatology of freezing rain using numerical model output. Proc. of Fifth Conference on Aviation Weather Systems, Am Meteorol Soc, Vienna (Virginia), USA.

Astbury, A., 1994: OpenRoad Manual, Meteorological Office (continuously updated).

Barthram, J.A., 1964: A method of forecasting a radiation night cooling curve. *Meteorol Mag*, **93**, 246–251.

Belasco, J.E., 1952: Characteristics of air masses over the British Isles. *Geophys Mem*, No. 87, London, Meteorological Office.

Blackall, R.M., 1973: Warming of the lower troposphere by the sea. *Meteorol Mag*, **102**, 65–73.

Bohorquez, M.A. and McCann, D.W., 1995: Model proximity soundings near significant aircraft icing reports. Proc. of Sixth Conf. on Aviation Weather Systems, Am Meteorol Soc, Dallas, Texas, USA.

Boyden, C.J., 1937, A method for predicting night minimum temperatures. *QJR Meteorol Soc,* **63**, 383–392.

CAA, 1991: Piston engine icing. Safety Sense Leaflet No. 14, Civil Aviation Authority.

Callen, N.S. and Prescott, P., 1982: Forecasting daily maximum surface temperatures from 1000–850 mb thickness lines and cloud cover. *Meteorol Mag*, **111**, 51–58

C&PSH: Commercial and Public Services Handbook, Met.O.868, Meteorological Office (continuously updated).

Craddock, J.M. and Pritchard, D.L., 1951: Forecasting the formation of radiation fog — a preliminary approach. *Meteorological Research Paper* No. 624. Meteorological Office (unpublished).

de Freitas, C.R., Dawson, N.J., Young, A.A. and Mackey, W.J., 1985: Microclimate and heat stress in runners in mass participation events. *J Clim Appl Meteorol*, **24**, 184–191.

Dixon, J.C. and Prior, M.J., 1987: Wind-chill indices: a review. *Meteorol Mag*, **116**, 1–16.

Driscoll, D.M., 1985: Human health. Handbook of Applied Meteorology, pp. 778–814. John Wiley & Sons.

Fawbush E.J. and Miller, R.C. 1954: A basis for forecasting peak wind gusts in non-frontal thunderstorms. *Bull Am Meteorol Soc*, **35**, 14–19.

Frost, R., 1941: The influence of the North Sea on winter temperatures and dew points. Meteorological Office (unpublished).

Glahn, H.R. and Lowry, D.A., 1972: The use of MOS in objective weather forecasting. *J Appl Meteorol*, **11,** 1203–1211.

Grant, K., Fog frequencies in the UK relative to time of sunrise. *Special Investigations Paper*, Meteorological Office, (unpublished).

Grant, K., 1975: The warming and moistening of cold air masses by the sea. *Meteorol Mag*, **104**, 1–9.

HAM. Handbook of Aviation Meteorology, 1994: London, HMSO.

Hewson, T.D. and Gait, N.J., 1992: Hoar-frost deposition on roads. *Meteorol Mag*, **121**, 1–21.

HWF. Handbook of Weather Forecasting, 1975: Met.O.875, Meteorological Office.

Inglis, G.A., 1970: Maximum temperatures on clear days. *Meteorol Mag*, **99**, 355–363.

Jefferson, G.J., 1950: Temperature rise on clear mornings. *Meteorol Mag*, **79**, 33–41.

Johnson, D.W., 1958: The estimation of maximum day temperatures from the tephigram. *Meteorol Mag*, **87**, 265–266.

Kensett, C.H., 1983: Forecasting night minimum temperatures — a revision of McKenzie's method for 90 stations in the UK. Forecasting Techniques Memorandum No. 21. Meteorological Office.

Kerslake, D. McK., 1972: The stress of hot environments. Cambridge University Press.

Lamb, H.H., 1943: Haars or North Sea fogs on the coast of Great Britain. Meteorological Office (unpublished).

Landsberg, H.E., 1981: The Urban Environment. Academic Press.

Local Weather Manual (S England), 1994: Meteorological Office (PSP) publication.

Lumb, F.E. 1963: Downward penetration of snow in relation to the intensity of precipitation. *Meteorol Mag*, **92**, 1–14.

Lunnon, R.W., Holpin, G.E. and Anderson, S., 1994: Study of the meteorological conditions pertaining to 25 January 1994 BAe ALF502 rollback incident. Meteorological Office Research Tech. Report No. 102.

McKenzie, F., 1944: A method of estimating night minimum temperatures. *SDTM* No. 68. Meteorological Office, London (unpublished).

Oke, T.R., 1987: Boundary layer climates (2nd edition). Methuen.

Parrey, G.E., 1969: Minimum road temperatures. *Meteorol Mag*, **98**, 286–290.

Perry, A.H. and Symons, L.J., 1991: Highway meteorology. E & F.N. Spon.

Pike, W.S., 1995: Extreme warm frontal icing on 25 February 1994 causes an aircraft accident near Uttoxeter. *Meteorol Appl*, **2**, 273–279.

Ritchie, W.G., 1969: Night minimum temperatures at or near various surfaces. *Meteorol Mag*, **98**, 297–304.

Ross, G.H., 1989: Model Output Statistics. An updatable scheme. Am Meteorol Soc. 11th Conference on Probability and Statistics in the Atmospheric Sciences, Monterey, Ca, USA.

Saunders, W.E., 1952, Some further aspects of night cooling under clear skies. *QJR Meteorol Soc,* **78**, 603–612.

Sills, A.G., 1969: An investigation into the depression of the grass minimum temperature below the air minimum at Cottesmore. *Meteorol Mag*, **98**, 348–351.

Starr, J.R., 1988: Weather, climate and animal performance. Geneva, World Meteorological Organization, Technical Note 190.

Steadman, R.G., 1984: A universal scale of apparent temperatures. *J Clim Appl Meteorol,* **23,** 1674–1687.

WMO, 1968: Ice formation on aircraft. Geneva. (Reprint of 1961 publication). World Meteorological Organization, Technical Note 139.

CHAPTER 3 — VISIBILITY

3.1 Factors reducing visibility (SB)

Reduction in visibility depends on the concentration and size of hydrometeors, particulates or moisture in the atmosphere as well as the viewing path and the time of day.

AWDC (1960)
Local Weather Manual for Southern England (1994)

3.2 Fog (SB)

Fog forms as a result of air near the surface becoming saturated and being cooled below its dew point. The basic fog classifications are: air mass fog((i) to (iii)) and frontal fog (iv):
(i) *Radiation fog.*
(ii) *Advection fog* (warm and cold).
(iii) *Upslope fog.*
(iv) *Frontal fog.*

On many occasions the development of fog is due to more than one factor.

Bader et al. (1995), Chapter 7
Perry & Symons (1991)
Thomas (1995)

3.3 Radiation fog

The three stages of formation are summarized in **Fig. 3.1**.

3.3.1 Physics of formation of radiation fog (SB, Figs 3.1 and 3.2))

Bradbury (1989) **Findlater (1985)**
Brown (1987) **Roach (1994, 1995)**

3.3.2 Conditions observed during radiation fog formation

Factors favourable for formation:
(i) Clear skies or just thin, high cloud.
(ii) Moist air in the lowest 100 m or so.
(iii) Moist ground (e.g. after rain, or over marshes).
(iv) Favourable local topography.
(v) Slack pressure gradient, allowing the surface wind (preferably measured at 2 m) to decrease to near calm.

The frequency of geostrophic wind speeds (V_g) at Cardington during periods of fog were found to be as shown in **Tables 3.1 and 3.2**).

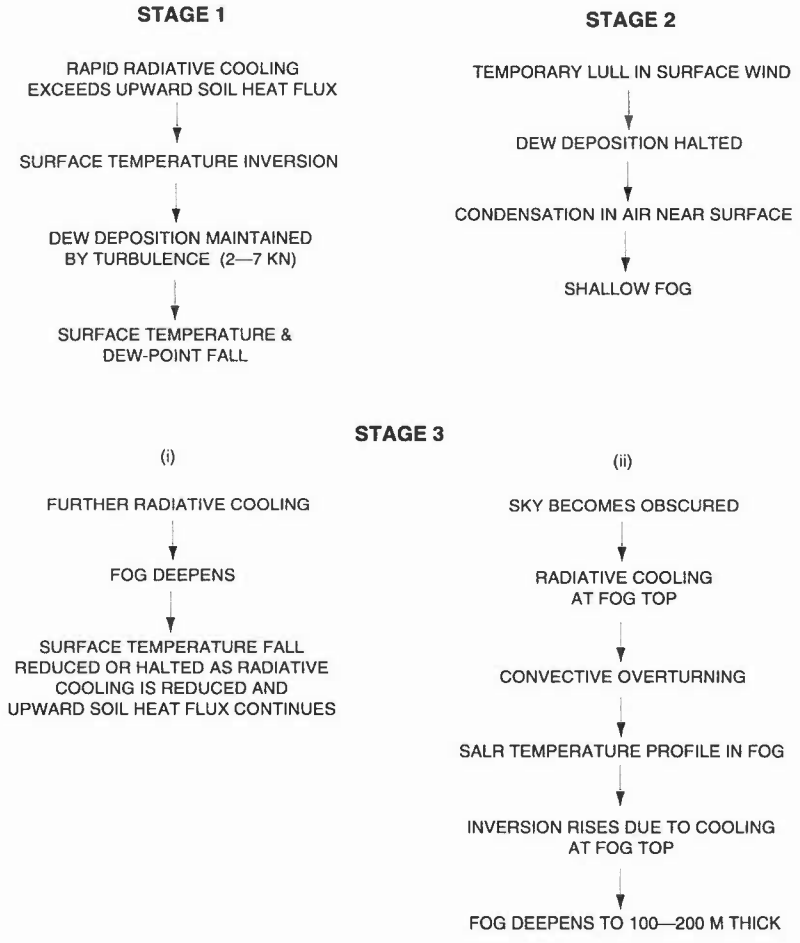

Figure 3.1. The three stages in the formation of radiation fog.

Table 3.1. Percentage frequency of V_g in various speed ranges

	knots										
	0–2	3–5	6–8	9–11	12–14	15–17	18–20	21–23	24–26	27–29	30+
A	7.1	16.7	23.8	23.0	18.3	10.3	0.8	—			
B	6.7	16.0	18.0	20.0	16.3	11.3	6.7	2.5	1.5	0.5	0.7

A = when fog first formed, B = while fog persisted

The wind speed at 10 m during the same fogs had the following frequency distribution:

Table 3.2. Percentage frequencies of surface wind in various speed ranges

knots	0–2	3–5	6–8	9–11	12–14	15–17
%	58.5	28.6	10.5	2.1	0.3	—

The stronger winds occurred when North Sea stratus spread inland replacing local radiation fog with widespread advection fog.

(i) Recent studies have shown that the wind speed at 1–2 m is more important than the 10 m wind. Fog forms when the 2 m wind falls below 2 kn. The wind at 10 m may be significantly stronger than the 2 m wind on radiation nights.
(ii) Synoptic studies demonstrate the preferred occurrence of radiation fog to be with anticyclonic pressure patterns, particularly on the western side (to where, generally, air of higher RH is moving).
(iii) Only about one fog in seven occurs in a cyclonic situation. Within these pressure patterns there is a greater tendency for fog to form in those sectors where there is a southerly component to the geostrophic wind (East Anglia/Lincolnshire) by a factor of about 3 to 1.

Findlater (1985)

3.3.2.1 Height of fog top (Findlater's method)

(i) During the period of fog deepening, and with minimum advective effects, the temperature at the base of the inversion was observed by Findlater to remain constant to within ± 0.5 °C while the screen temperature rose slightly. In many cases, however, screen temperatures continue to fall, in which case the following technique is not appropriate.
(ii) Findlater's technique (based on only a small number of cases) is to draw the SALR temperature profile from the known screen temperature T_t at time t after sky obscuration to intersect an assumed temperature at the inversion base (i.e. the screen temperature when sky became obscured). The height of the inversion base, H_1, may then be estimated and fog top is taken as: $H_1 + 25$ m.

Findlater (1985)

3.3.2.2 Factors modifying fog formation (SB)

Four specific factors which complicate and modify the radiative progress of fog formation are:
Advective effects: *Sunrise*: *Fog aloft*: *Fog forming in smoky boundary layers.*

Findlater (1985)

3.3.3.1 Forecasting the formation of radiation fog

3.3.3.1 Calculation of fog point (Saunders' method)

The method takes account of moisture throughout the cooling layer; it is based on Mk. IIb radiosonde profiles; Mk. III T_d data may differ.

(i) Select a representative upper-air sounding and find the condensation level from the maximum temperature and the dew point at that time, using Normand's theorem (2.1.1).

(ii) Find the humidity mixing ratio at the condensation level and read off the temperature where the humidity mixing ratio line cuts the surface isobar. This is the expected fog-point temperature.

This procedure needs modification to allow for different types of sounding (see **Fig. 3.3**):

(a) *Type I* has a constant dew-point lapse rate except near the ground where the surface dew-point lies on, or to the right of, a downward extension of the upper dew-point curve. T is the maximum temperature and T_d is the surface dew-point. If there is a superadiabatic, use the value T_c instead of T to eliminate the superadiabatic section. The pecked lines through T_c and the dew point T_d meet at the condensation level A. The humidity mixing ratio at this level is at B and the fog point is at C.

(b) In *Type II* the dew-point lapse rate increases aloft. Point B is found by extrapolating the lower part of the dew-point curve above the point at which the lapse rate increases.

(c) In *Type III* the surface dew point lies to the left of the downward extension of the upper dew-point curve, two possibilities are illustrated:

  (i) If the temperature lapse in the lowest layers is less than a dry adiabatic, the construction follows the basic principles as for *Type I*.

  (ii) If the temperature lapse rate in the lowest layer is equal to or greater than a dry adiabat, then no Normand construction is drawn and the fog point is taken to equal the dew-point.

Normally, if the boundary layer is mixed at the time of the midday sounding, extending the mean mixing-ratio through the boundary layer to the surface will give an acceptable fog point. As a rough guide, the afternoon dew point at screen level minus 2 °C gives a good first guess for $T_f > -2$ °C.

Notes:

(i) If a subsidence inversion has brought dry air down to within 30 hPa of the ground, use the dew point (T_d) as the fog-point.

(ii) If rain falls during the afternoon leaving the ground wet, the actual fog point may be higher than the calculated value.

(iii) If a sea-breeze reaches the area later in the day, the fog point may be much higher than calculated; use the coastal dew point.

(iv) The dew-point temperature 60 hPa above the surface nearly always gives a fog-point value close to Saunders' value, exception being *Type IIIb* when the surface dew-point is used.

(v) If the calculated temperature is ≤ 0 °C, then the actual fog point may well be lower (due to deposition by hoar frost).

Saunders (1950)

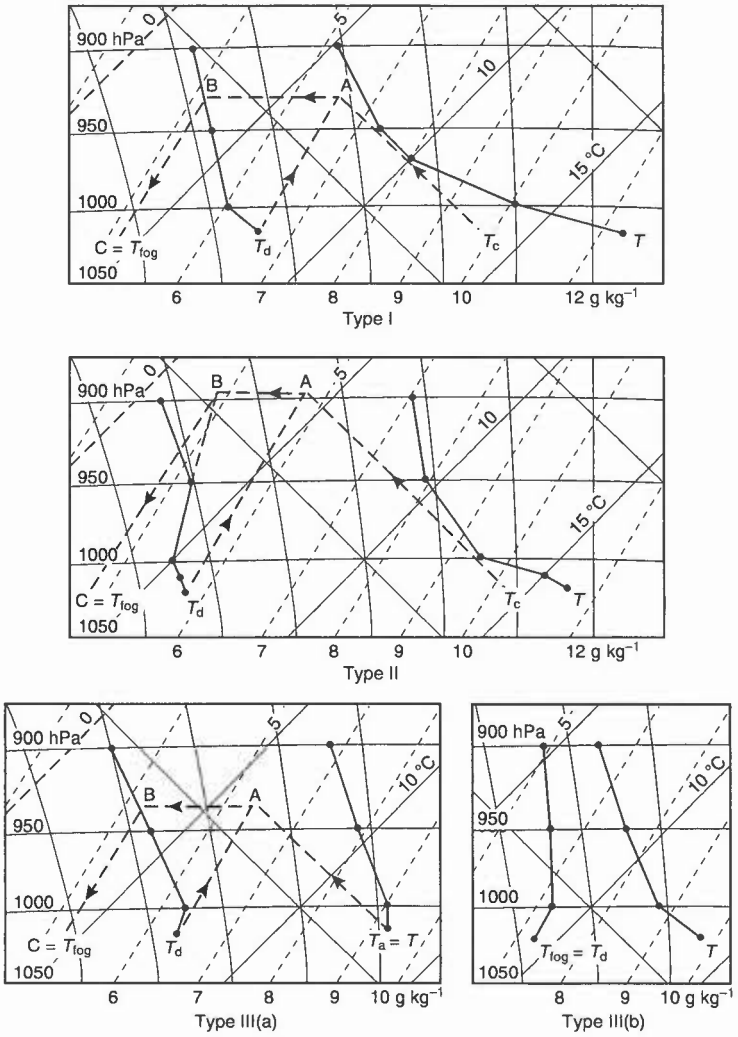

Figure 3.3. Estimation of fog-point (Saunders' method) with adjustments to midday soundings under various conditions. See text for explanation of types.

3.3.3.2 *Calculation of fog-point (Craddock and Pritchard's method)*

If T_f is the fog point, T_{12} is the screen temperature at 1200 UTC, and T_{d12} is the dew point at 1200 UTC, then

$$T_f = 0.044\ (T_{12}) + 0.844\ (T_{d12}) - 0.55 + A = Y + A.$$

Values of A and Y can be obtained from **Table 3.3**.

Table 3.3(a). Values of Y (°C) corresponding to the observed values of T_{12} and T_{d12}

T_{d12} \ T_{12}	30	25	20	15	10	5	0	−5	−10
20	17.7	17.4	17.2						
18	16.0	15.7	15.5						
16	14.3	14.1	13.8						
14	12.6	12.4	12.1	11.9					
12	10.9	10.7	10.5	10.2					
10	9.2	9.0	8.8	8.6	8.3				
8	7.5	7.3	7.1	6.9	6.6				
6	5.8	5.6	5.4	5.2	5.0				
4	4.1	3.9	3.7	3.5	3.3	3.0			
2	2.5	2.2	2.0	1.8	1.6	1.4			
0	0.8	0.6	0.3	0.1	−0.1	−0.3	−0.6		
−2	−0.9	−1.1	−1.4	−1.6	−1.8	−2.0	−2.2		
−4	−2.6	−2.8	−3.0	−3.3	−3.5	−3.7	−3.9		
−6	−4.3	−4.5	−4.7	−5.0	−5.2	−5.4	−5.6	−5.8	
−8	−6.0	−6.2	−6.4	−6.6	−6.9	−7.1	−7.3	−7.5	
−10	−7.7	−7.9	−8.1	−8.3	−8.6	−8.8	−9.0	−9.2	−9.4

The number A (°C) is an adjustment which depends upon the forecast cloud amount and geostrophic wind speed, as tabulated below.

Table 3.3(b).

*Mean cloud amount (oktas)	*Mean geostrophic wind speed (kn) 0–12	13–25
0–2	0.0	−1.5
2–4	0.0	0.0
4–6	+1.0	+0.5
6–8	+1.5	+0.5

*Mean of forecast values for 1800, 0000 and 0600 UTC.

Notes:

(a) The equation for T_f was derived from the combined data for 13 widely separated stations in England. There was considerable variation from station to station in their proximity to major smoke sources.

(b) Account was not taken of variations in atmospheric pollution so that, in effect, an average degree of pollution is assumed in using this technique (in contrast to Saunders' method which refers mainly to fog in clean air).

(c) If the minimum temperature is predicted using Craddock and Pritchard's method it is suggested that:
   (i) if T_f is 1 °C or more above T_{min}, forecast fog;
   (ii) if T_f is 0.5 °C above to 1.5 °C below T_{min}, forecast a risk of fog;
   (iii) if T_f is 2 °C or more below T_{min}, do not forecast fog.

(d) When forecasting for a region, rather than a specific airfield, allow a larger safety margin, since there is always more low-level moisture present near streams and in lush valleys than over flat airfields with trimmed grass.

Craddock & Pritchard (1951)

Other fog prediction techniques (Banks, Swinbank) are given in HWF; a 'probability predictor' diagram for Waddington, while not being statistically rigorous has operational credibility.

HWF (1975) Chapter 20.7

3.3.3.3 Inferred fog prediction from $T_f - T_{min}$

Table 3.4. Fog prediction summary

$T_f - T_{min}$ (°C)	Inferred fog prediction
$\geq +1$	widespread fog expected
$=0.5$	fog probable late in the night
$=0$	patchy fog likely by dawn
-0.5 to -1.5	fog patches possible in fog-prone areas
≤ -2	fog not expected

If T_f is significantly greater than T_{min} the time of formation can be predicted from the night cooling curve.

Craddock& Pritchard (1951)

3.3.3.4 The fog point in relation to the 850 hPa wet-bulb potential temperature

(i) The 850 hPa wet-bulb potential temperature is useful as a means of identifying air masses.

(ii) The probability of fog occurring increases as the temperature difference of the surface temperature below the 850 hPa WBPT increases, see **Fig. 3.4**.

3.3.3.5 Summary of forecasting procedures for fog formation

(i) Forecast the synoptic situation overnight.

(ii) Consider history — e.g. did fog form last night in the same air mass? How will conditions differ tonight?

(iii) Consider local factors — topography, smoke sources, etc.

(iv) Estimate the fog point — Craddock–Pritchard; Saunders' technique; any others available?

(v) Will the fog point be reached? — construct night cooling curve.
(vi) Once the fog forms, what will the visibility be? — usually less than 200 m in clean air; decrease in visibility may be slower in smoky air; if temperature <0 °C, 200 to 1000 m more common
(vii) Keep the forecast under review

The potential of a given location for thick radiation fog (visibilities <200 m) can be assessed by a Fog Potential Index.

Meteorological Office (1985)

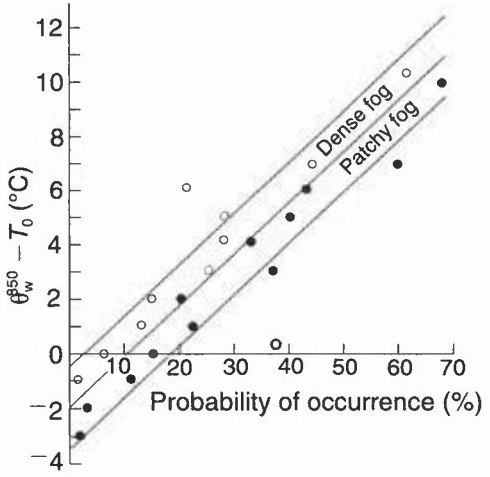

Figure 3.4. The probability of fog corresponding to a given depression of the surface temperature (T_0) below the 850 hPa wet-bulb potential temperature (θ_w^{850}).

3.3.4 Forecasting the clearance of radiation fog

3.3.4.1 Fog clearance by insolation

Satellite imagery shows that extensive areas of radiation fog and stratus dissipate from their outer edges inward due to mixing generated by insolation (**SB**).

Bader et al. (1995), Chapter 7
Gurka (1986)

The fog depth must be known or estimated, together with a fog-clearance temperature.

(a) *Estimation of fog top.*
  (i) Visual estimation: if the sky is visible, the fog depth is probably about 5 hPa in dense fog, and 10 hPa in thin fog.
  (ii) If the sky is obscured at dawn, and no local mini-sonde ascent is available, the most representative midnight sounding should be modified as in (b) below to allow for changes between midnight and the time of minimum temperature (note height of fog top is 25 m above top of inversion).

(b) *Modifying the temperature profile on a tephigram.*
Heffer's estimate is probably appropriate:

(i) If the nose has already formed on the temperature ascent curve, the level is raised by 5 hPa and the temperature decreased by 1.5 °C; this point is joined to the night-minimum temperature by a straight line on the tephigram. The point where this line and the downward extension of the dew-point curve intersect (O in **Fig. 3.5(a)**) represents the fog top.

(ii) If a nose has not yet formed on the midnight ascent, the point 35 hPa above the ground is joined to the night minimum surface temperature and the fog top at dawn estimated as before (O in **Fig. 3.5(b)**).

(c) *Estimation of fog-clearance temperature (Jefferson).*

(i) From the fog-top estimate, the clearance temperature is estimated on the assumption of a dry adiabat from the surface to fog top. Temperature rise is estimated from 2.3 **(Fig. 2.5)**.

(ii) The surface temperature thus obtained represents the probable value above which the fog will lift to very low stratus.

(iii) The fog or low stratus should disperse entirely when the condensation level reaches the level of the inversion base (fog top will rise as fog lifts into stratus).

Caution: During winter when the sun is at a very low angle, the fog top will continue to radiate after sunrise. The fog will increase in depth for some time before the absorption of insolation is effective in starting the clearance process.

Barthram (1964) **Heffer (1965)**
Brown (1987) **Jefferson (1950)**
Findlater (1985) **Kennington (1961)**

(d) *A nomogram for forecasting clearance of fog by insolation*
Fig. 3.6 is a nomogram, due to Barthram, for predicting the time of fog clearance due to insolation, where:
T_1 = surface temperature at dawn
T_2 = fog-clearance temperature
d = depth of fog at dawn in hectopascals.

To use the nomogram:

(i) Enter the fog-depth on the left-hand diagram and move to the right to meet the vertical from the value $(T_2 - T_1)$. From this point move downwards and to the right following the curved lines representing Q to the right-hand edge of the diagram.

(ii) Move horizontally across to the middle diagram and then as far as the vertical from the value $T_2 + T_1$. Then follow the curves for fQ to the right-hand edge of the diagram.

(iii) From this point move horizontally across to the right-hand diagram to meet one of the curves marked with dates. From this curve go down to the baseline where the time of clearance is marked.

If the fog is thin (visibility more than 600 m or depth <20 hPa) the insolation needed is reduced by one third. Take the value on the left-hand margin and follow one of the diagonal pecked lines down to the inner (thin fog) scale and continue as before.

Barthram (1964)

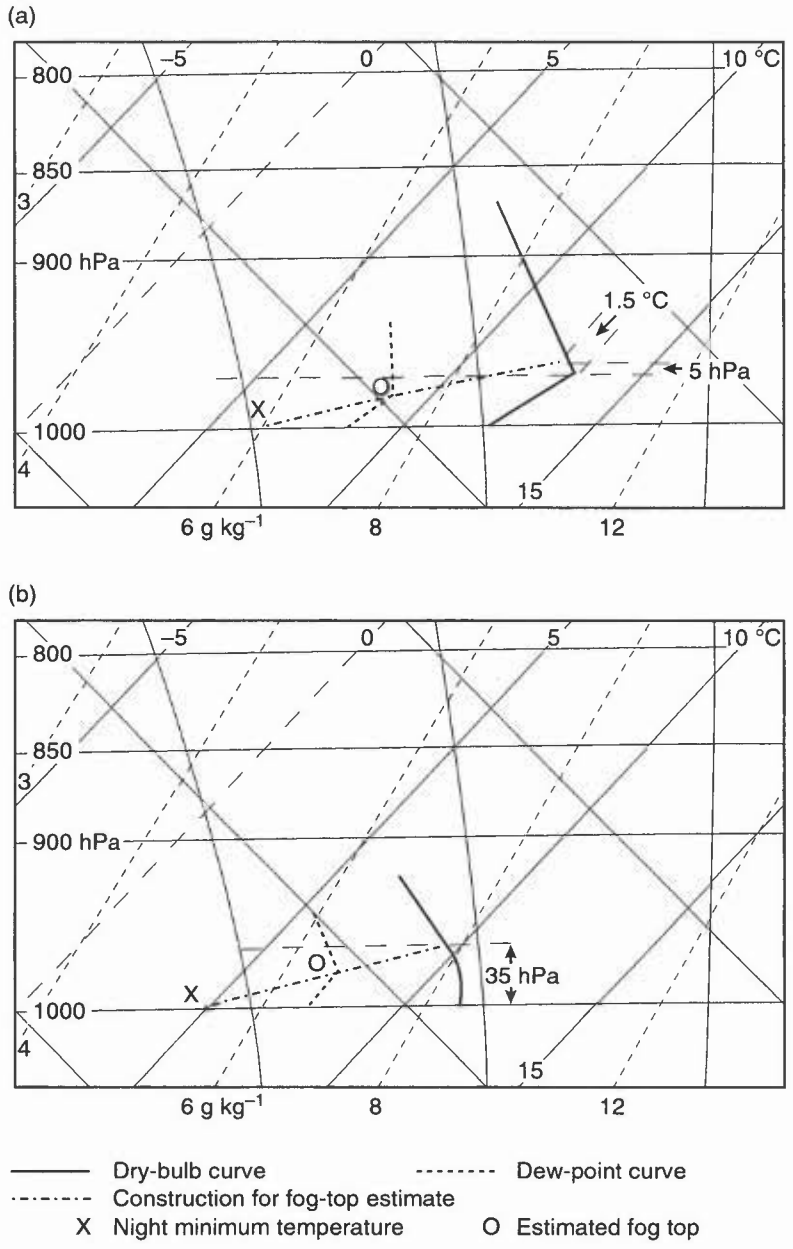

Figure 3.5. Construction for fog-top estimate from a midnight BALTHUM when (a) the inversion nose has already formed, and (b) the inversion nose has not yet formed.

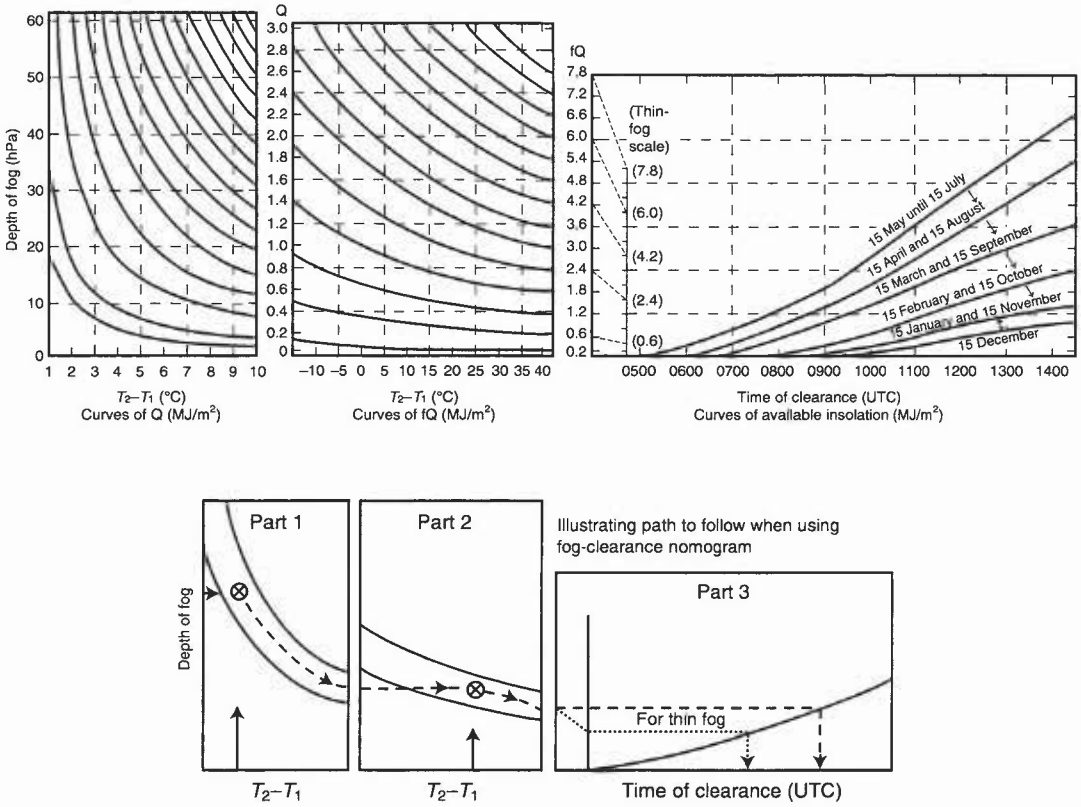

Figure 3.6. Nomogram for forecasting the clearance of radiation fog by insolation.

3.3.4.2 *Fog clearance without insolation*

(a) *Fog clearance following the spread of cloud*

(i) The arrival of a cloud sheet over water fog often leads to the most rapid and efficient clearance of the fog because it stops, or reverses, the continual radiative cooling of the fog.

(ii) The lower the cloud sheet the more effective it is in clearing the fog, provided the ground is not frozen.

(iii) Heat flux from the soil, causing warming of the air by weak convective motions, may lift the fog into low stratus before its complete dispersal.

(iv) The time taken for fog to clear decreases with higher temperatures, as is shown by the following observations (**Table 3.5**) made at Exeter Airport (south-west England).

Table 3.5.

	Initial grass temp. (°C)					
	<0	0–2	3–5	6–8	9–10	11–13
Average time (hours) for fog to clear after arrival of cloud sheet	3.1	2.2	1.1	1.5	0.9	0.5
Number of cases	10	10	5	10	5	3

Saunders (1957, 1960)

(b) *Fog clearance due to increase of gradient wind*

Although fog does not normally form unless the wind falls very light, its dispersal may be delayed until the winds aloft are quite strong. Mature fog has a well developed inversion capping it; through this mixed layer, a strong wind shear can be maintained. The more intense the inversion, the greater must be the wind above in order to produce turbulent mixing and dispersal of fog.

As a guide, the geostrophic wind speed required for fog to be dispersed by the increasing wind is:

(i) 15–20 kn over flat coastlands;

(ii) 20–25 kn inland;

(iii) 30–40 kn in deep valleys lying across the wind flow.

Even over the flat terrain at Cardington a peak geostrophic wind of 37 kn was estimated on one occasion before the fog cleared.

While increasing winds may lift fog into a layer of low stratus, localities downstream, especially where the ground has a gradual slope upwards, are liable to experience a delay in clearance, or the arrival of stratus if there was no fog initially.

HWF (1975) Chapter 20.8.5

(c) *Fog clearance due to dry-air advection*

(i) Local variations in air-mass surface characteristics and moisture content can create mesoscale patches of drier air which cannot be detected on synoptic-scale charts.

(ii) Unexpected nocturnal clearance of fog may occur when advection brings in drier air.

(iii) The gradual advection of progressively drier air can be effective in fog clearance.

(iv) The passage of a cold front can produce rapid fog clearance, by combining effects of dry air advection, increasing cloud cover and, often, increased wind speed.

3.3.4.3 Persistent fogs (SB)

Persistent fogs commonly occur in eastern districts of England in winter.

(i) In December and January, one third of all fogs are persistent.

(ii) In November and February the proportion is about one sixth.

(iii) Only 5–10% persist beyond 1700 UTC on the second day

(v) Fog clearance in the summer half-year is well defined in time; fog is generally most likely just after sunrise,

(vi) In autumn/winter it may persist overnight, although it tends to disperse next day.

Brown (1979)
Kennington (1961)
HAM (1994) Fig. 59

3.3.4.4 Summary of forecasting procedures for fog clearance

(i) Study the synoptic situation. Will fog clear by any other mechanism?

(ii) Obtain a dawn temperature

(iii) Choose a representative upper-air sounding

(iv) Modify the sounding — based on: sky visible or obscured? Station dawn temperature

(v) Find fog clearance temperature and time. Kennington–Barthram or other technique

(vi) Find stratus clearance temperature — if fog is deep and widespread

(vii) Will local factors delay or advance clearance?

(viii) Keep the forecast under review

3.3.4.5 Large temperature falls associated with periods of weak advection on radiation nights

Sudden, large temperature falls ($\geq$3.5 °C) have been recorded on radiation nights (**SB**).

Booth (1982)

3.4 Advection fog

3.4.1 Warm advection fog

Typical examples are sea fog and fog over very cold land. Thawing snow is commonly associated with advection fog over land.

(a) Factors favourable for *formation*:

(i) Air-mass dew point greater than temperature of surface.

(ii) Stable lapse rate, slight hydrolapse in lowest layers.

(iii) Moderate winds (10–15 kn) — low stratus likely in winds greater than 15 kn.
(iv) Suitable wind direction.

Note that: The advection of moist air also renders *radiation fogs* more frequent.

(b) Factors favourable for *clearance*:
(i) Change of air mass — the most common and reliable means.
(ii) Change of track of air mass to drier source.
(iii) Over land — solar heating; radiation fog clearance techniques may be used. (Over snow the surface temperature may not rise above 0 °C).

HWF (1975), Chapter 20.9

3.4.1.1 Sea fog

There are four main sources of warm, moist air giving sea fog over coasts and waters around the British Isles:

(i) A south-westerly flow from the Atlantic west of the Iberian Peninsula; the air should have originated from, or spent some time over, warm waters south of 40° N. It is often associated with the warm sector of a frontal depression; it gives rise to widespread fog around southern and western coasts.
(ii) With high pressure to the west of the British Isles, mild air may circulate around northern Britain and come southwards as a north to north-east wind, bringing low stratus and fog ('haar') to exposed eastern coasts of Scotland and north-east England.
(iii) Warm continental air during spring and early summer in a south-easterly flow from the Mediterranean across Europe may become sufficiently moist and stable at low levels to affect east coast areas of the United Kingdom.
(iv) In summer very high dew-point air often accompanies thundery lows moving north from France, giving rise to sea fog in the English Channel and southern North Sea which may spread inland at night.

Bader et al. (1995), Chapter 7 **Roach (1995)**
HWF (1975), Chapter 20.9

3.4.1.2 Prediction of sea fog (SB)

Satellite imagery (VIS) is invaluable for locating the boundaries of existing areas of sea fog:

3.4.1.3 Advection of fog from land to sea (SB)

3.4.1.4 Advection of fog from sea to land (SB)

3.4.1.5 Advection fog over land (SB)

3.4.2 Cold advection fog

Cold advection fog forms when cold dry, stable air flows over a much warmer water surface (warmer by 10–15 °C at least).

(i) The evaporating vapour immediately condenses again to form *steam fog*, with convective whirls and a top at a few metres.
(ii) In polar regions the same process gives rise to 'Arctic Sea Smoke'.

HWF (1975) Chapter 20.9

3.5 Upslope fog

3.5.1 Requirements

(i) flow of moist air over gently rising ground over a wide area **(SB, Fig. 3.7)**;
(ii) a stable lapse rate in the lowest layers.

(Very stable air may be deflected around the edge of steeply rising ground if there are gaps in the escarpment.)

On radiation nights, weak moist advection may be combined with gentle upslope motion producing multiple conditions favourable for fog; the likelihood of formation of upslope fog may be determined from a representative tephigram — the height of the base being given by the lifting condensation level of the upwind air.

3.5.2 Hill fog (SB, Fig. 3.8)

In the presence of strong winds the empirical relationship is suggested for the height of the cloud base in kilometres:

$$\text{Cloud base (km)} = \text{dew-point depression (°C)}/8;$$

thus in a southerly airstream ahead of a depression, with dew-point depression near a coast of <2 °C, cloud base may develop only 250 m asl.

Pedgley (1967)

3.6 Frontal fog (SB, Fig. 3.9)

3.6.1 Summary of factors favourable for frontal fog development:

(i) Ahead of active warm front or warm occlusion.
(ii) Very cold (or snow-covered) ground.
(iii) Large temperature contrast between cold and warm air masses.
(iv) Light surface winds.

3.7 Convective activity above fog (SB)

Although fog is normally associated with a stable air mass, the top of the inversion may be below the level of adjacent hills. During the day fog-free high ground may become warm enough to set off cumulus clouds.

3.8 Guidance on the formation and detection of fog through imagery (SB)

Satellite imagery will help to determine several atmospheric conditions that can lead to fog formation/dissipation: *Low-lying moisture*; *Cloud cover*; *Snow cover*; *Precipitation*.

Extra information may be deduced from satellite multi-spectral channels.

Bader et al. (1995), Chapter 7

3.9 Haze

3.9.1 Haze particles (SB)

3.9.2 Haze occurrence (RH)

Haze is often concentrated where RH is high (e.g. under an inversion); hygroscopic particles can result in haze at relatively low RH.

AWDC (1960) **HAM (1994)**
Bradbury (1989) **Hänel (1976)**

3.9.3 Depth of haze (SB, Fig. 3.9)

Bradbury (1989)

3.9.4 Diurnal variation of haze (SB, Fig. 3.10)

HWF (1975), Chapter 20

3.9.5 Dispersal of haze

Continuous rain is effective in washing out most of the haze particles from the air. Showers, and even heavy thunderstorms, are much less effective.

3.9.6 Synoptic situations favourable for haze

(i) Haze is usually thickest in anticyclonic conditions when low-level winds are light. An increase in surface wind often leads to improved visibility, and a decrease in wind to poorer visibility at the surface.

(ii) Ahead of a warm front, when the clouds are increasing, the visibility from the air often deteriorates in the layer extending about 300 ft below the cloud base.

(iii) In the United Kingdom a high proportion of haze days are associated with winds from Europe (**Fig. 3.11**). Surface wind directions from 060–120° commonly bring the worst haze.

3.9.7 Visibility forecasting methods

3.9.7.1 The File method

Based upon data for five stations in southern England, the method is intended to be used 6–8 hours before the forecast time. Part I requires prediction of afternoon and evening wind speed and relative humidity. Forecast values are read from **Fig. 3.12.** In Part II a correction factor for those results is obtained by considering the surface chart and inspecting upwind humidity and wind speed and then applying these to the nomogram.

Example: actual visibility is 20 km, relative humidity about 60% and surface wind 10 kn. **Fig. 3.12(a)** gives a visibility of 13 km. The correction factor is then 20/13 = 1.5; this is applied to all subsequent forecasts. (A good forecast of advective changes to the airstream is necessary.) File recommends that in highly polluted airstreams visibility derived from the graphs be halved.

File (1985)

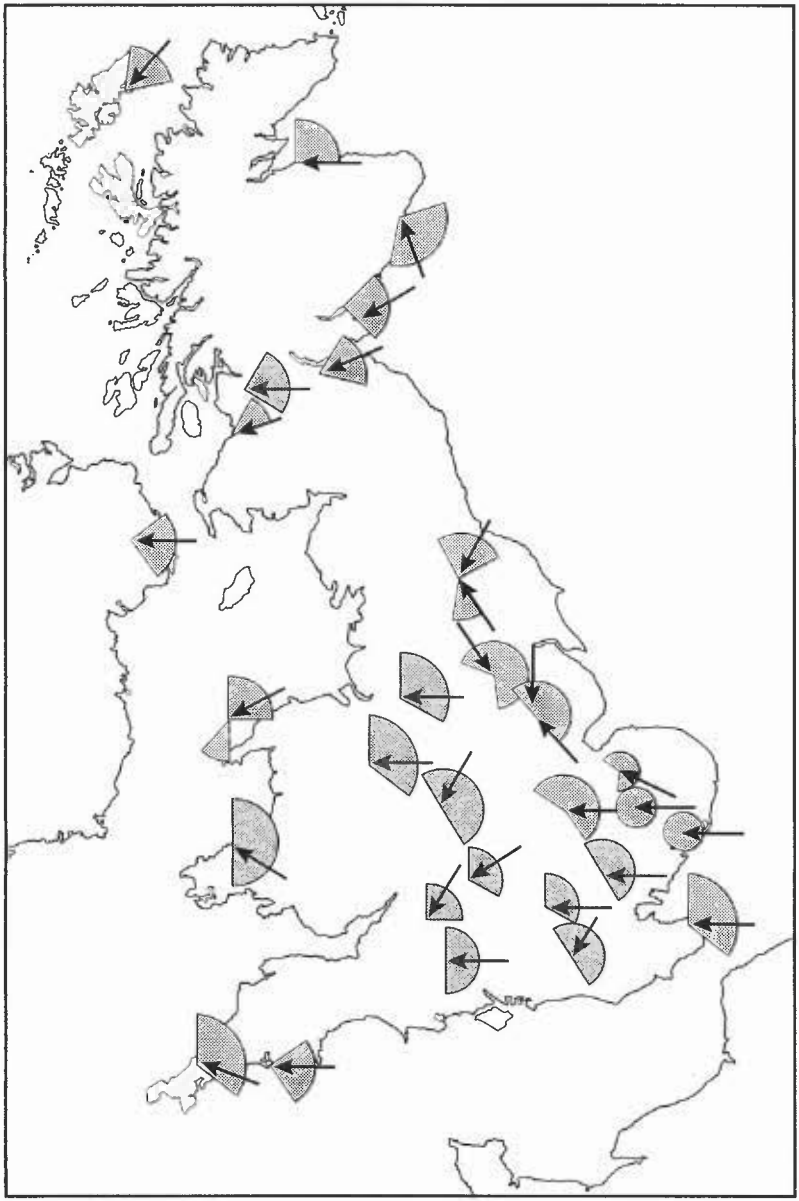

Figure 3.11. Surface wind direction and summer haze. Shaded sectors show the range of directions most often associated with visibilities in the range 1.8 to 9.9 km. Where variations are small the area shown is circular, and the arrows denote the worst directions. The radius of the sector arcs has no significance.

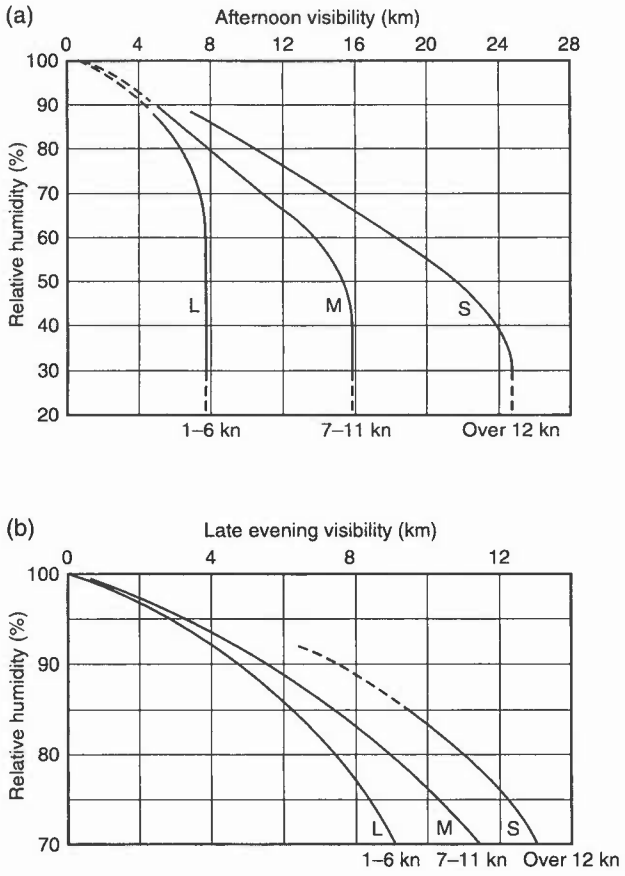

Figure 3.12. (a) Afternoon visibility against relative humidity for three classes of wind speed in 'easterly' synoptic situations. Median values are represented by L, M and S for light, moderate and strong wind speeds, respectively. The curves should be regarded as provisional for relative humidities above 87% and below 30%. (b) Late evening visibility against relative humidity for three classes of wind speed in 'easterly' synoptic situations. Median values are represented by L, M and S for light, moderate and strong wind speeds, respectively. The curve for strong winds should be regarded as provisional for relative humidities above 87% where data were sparse.

3.9.7.2 A (non-frontal) visibility forecasting method devised at Middle Wallop

(i) Construct a forecast night-cooling curve; find intercept of expected air-mass dew point with cooling curve.

(ii) Find out visibility at time of the maximum temperature (Vis_{max}); allow for areas of differing visibilities advecting across area.

(iii) Forecast overnight surface wind.

Then visibility, when temperature has fallen to air-mass dew point, depends on wind speed (**Table 3.6(a)**):

Table 3.6(a).

Wind (kn)	Visibility
0–5	1/3 of Vis_{max}
6–9	1/2 of Vis_{max}
≥10	3/4 of Vis_{max}

Thereafter for each °C below the intercept temperature halve the visibility, noting time from curve.
For example, dew point at T_{max} is +4 °C, when visibility was 25 km; forecast wind speed: 3 kn.

Table 3.6(b).

At forecast temperature of 4 °C, forecast visibility is 8 km
At forecast temperature of 3 °C, forecast visibility is 4 km
At forecast temperature of 2 °C, forecast visibility is 2 km

A further proposition is that visibility at dusk is 80% of Vis_{max}.

Perry & Symons (1991)

3.9.7.3 Changes in horizontal visibility with height associated with relative-humidity changes

An untested, but theoretically sound, method for inferring the variation of visibility with height from a given surface observation is presented in **SB (Fig. 3.13)**

Hänel (1976)
Reichert (1978)

3.10 Visibility in precipitation and spray

Rain — visibility is inversely proportional to total water content and number of raindrops; thus deterioration is greatest in heavy rain and in drizzle. **Fig. 3.14** summarizes experience in various countries; in moderate rain visibility is between 5 and 10 km, while heavy showers can reduce visibility to 1000 m, assuming no pre-existing pollution.

Snow — has a greater impact, visibility commonly falling below 1000 m even in moderate snow; in heavy snow this may fall to 200 m or less. Dry snowflakes result in visibilities only about one half of those illustrated in **Fig. 3.14** (wet snowflakes collapse to a smaller volume and become translucent). Blowing snow gives very low visibilities. It is most likely to occur when snow is dry and powdery.

In drizzle visibility ranges from about 3000 m to 500 m although simultaneous presence of fog droplets will still further reduce range.

In *low cloud* (hill fog) visibility is reduced to below 30 m.

In *spray* at sea and at coastal sites — winds >50 kn reduce visibility to <5 km
winds >70 kn reduce visibility to <1 km.

Jefferson (1961)

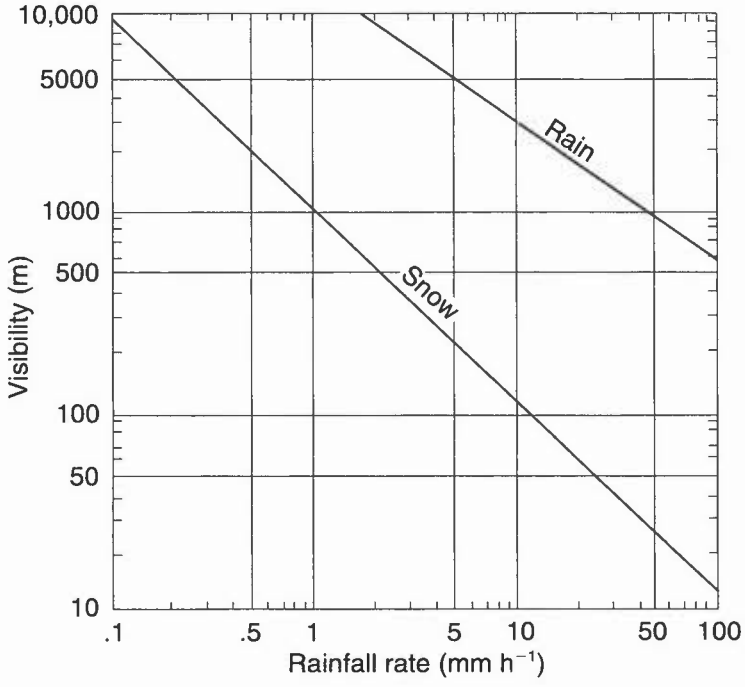

Figure 3.14. Visibility in rain and snow.

BIBLIOGRAPHY

CHAPTER 3 — VISIBILITY

Aerodrome Weather Diagrams and Characteristics (AWDC), 1960: Meteorological Office, London, HMSO (also Airfield Weather Diagrams, Met.O.564).

Bader, M.J., Forbes, G.S., Grant, J.R., Lilley, R.B.E. and Waters, J., 1995: Images in weather forecasting. Cambridge University Press.

Barthram, J.A.,1964: A diagram to assess the time of fog clearance. *Meteorol Mag,* **93**, 51–56.

Booth, B.J., 1982: An analysis of sudden, large falls in temperature at Lyneham during periods of weak advection. *Meteorol Mag,* **111**, 281–290.

Bradbury, T., 1989: Meteorology and flight. A & C Black.

Brown, A.A., 1979: The clearance of persistent fog. *Meteorol Mag,* **108**, 201–208.

Brown. R., 1987: Observation of the structure of a deep fog. *Meteorol Mag,* **116**, 329–338.

Craddock, J.M. and Pritchard, D.L., 1951: Forecasting the formation of radiation fog — a preliminary approach. Meteorological Research Paper No. 624. Meteorological Office (unpublished).

File, R.F., 1985: Forecasting visibility over southern England in polluted easterly airstreams. *Meteorol Mag,* **114**, 13–23.

Findlater, J., 1985: Field investigations of radiation fog formation at outstations. *Meteorol Mag,* **114**, 187–201.

Gurka, J.J., 1986: The role of inward mixing in the dissipation of fog and stratus. *Meteorol Monogr*, 2-86, Satellite imagery interpretation for forecasters, Vol. 3, National Weather Assoc. Temple Hills, MD.

HAM. Handbook of Aviation Meteorology, 1994: London, HMSO.

Hänel, G., 1976: The properties of atmospheric aerosol particles as functions of the relative humidity at thermodynamic equilibrium with the surrounding air. *Adv in Geophys*, **19**, 73–188.

Heffer, D.J., 1965: A test of Kennington's method of forecasting the time of clearance of radiation fog. *Meteorol Mag,* **94**, 259–264.

HWF. Handbook of Weather Forecasting, 1975: Met.O.875, Meteorological Office.

Jefferson, G.J., 1950: Method for forecasting the time of decrease of radiation fog or low stratus. *Meteorol Mag,* **79**, 102–109.

Jefferson, G.J., 1961: Visibility in precipitation. *Meteorol Mag,* **96**, 19–22.

Kennington, C.J., 1961: An approach to the problem of fog clearance. *Meteorol Mag,* **90**, 70–73.

Local Weather Manual for Southern England, 1994: Meteorological Office.

Meteorological Office, 1985: The susceptibility of fog on the M25 motorway. Met O 3, Building, Construction Climat Unit.

Pedgley, D.E., 1967: Weather in the mountains. *Weather*, **22**, 266–275.

Perry, A.H. and Symons, L.J., 1991: Highway meteorology. E. and F.N. Spon.

Reichert, B, 1978: A method of forecasting flight visibility in bad weather. Porz-Wahn, *Amt Wehrgeoph*, Fachl. mitt. Nr. 187, 157–162.

Roach, W.T., 1994/95: Back to basics: Fog.
1994: Part 1: Definitions and basic physics. *Weather*, **49,** 411–415.
1995: Part 2: Formation and dissipation of land fog. *Weather*, **50**, 7–11.
1995: Part 3: Formation and dissipation of sea fog. *Weather*, **50**, 80–84.

Saunders, W.E., 1950: A method of forecasting the temperature of fog formation. *Meteorol Mag,* **79**, 213–219.

Saunders, W.E., 1957: Variation of visibility in fog at Exeter airport and the time of fog dispersal. *Meteorol Mag,* **86**, 362–368.

Saunders, W.E., 1960: The clearance of water fog following the arrival of a cloud sheet during the night *Meteorol Mag,* **89**, 8–10.

Thomas, N., 1995: Fog and fog forecasting. MSc dissertation, University of Reading (also available as Meteorological Office NWP publication).

CHAPTER 4 — CONVECTION AND SHOWERS

4.1 Forecasting convective cloud

The initial upward motion of an air parcel is provided by buoyancy from surface heating, convergence on a range of scales, mass ascent or orographic forcing. Condensation and entrainment mark the subsequent progress of the parcel upwards under various instability criteria until it achieves its upper limit. A simple model of the thermodynamic processes which occur can be represented on the tephigram which, however, shows only the static stability which does not always give a complete description of the true stability of moving air.

4.1.1 Instability definitions (SB)

Met. Glossary (1991)

4.2 Constructions on a tephigram

4.2.1 Parcel method

Fig. 4.1 illustrates the general 'parcel' method, using a temperature sounding made before dawn (usually midnight) to forecast cumulus cloud during the day. ABCD is the environment curve. T and T_d are the surface temperature and dew point expected as a result of daytime heating. BU is the condensation level, CV is the level where the lapse-rate of the environment decreases to less than the SALR. Areas DWX and WVUBCW are equal.

Summary:

- U is Normand's point
- V is taken as the tops of most of the clouds
- W is forecast for the tops of occasional large clouds
- X is forecast only when conditions seem favourable for exceptionally vigorous and deep convection (e.g. θ_w lapse rate ≥ 0).

4.2.2 Forecasting the cloud base of cumulus

4.2.2.1 Estimating the condensation level

The surface temperature (T) and dew-point (T_d) may be used to estimate the condensation level (H).

As a rough approximation:

$$H = 4\,(T - T_d)$$
$$H_m = 1.22\,(T - T_d)$$

where T, T_d are in degrees Celsius and H in hundreds of feet (H_m in hundreds of metres).

On a tephigram, Normand's theorem gives the condensation level at the intersection of a dry adiabat through T and a humidity mixing ratio (HMR) line through T_d. This is the level BU in **Fig. 4.1**. During the afternoon, when convective upcurrents are strongest, the base of cumulus may be up to 700 ft (25 hPa) above the condensation level as the moisture flux from the surface causes the mixing ratio to decrease in the lowest tens of metres near the ground.

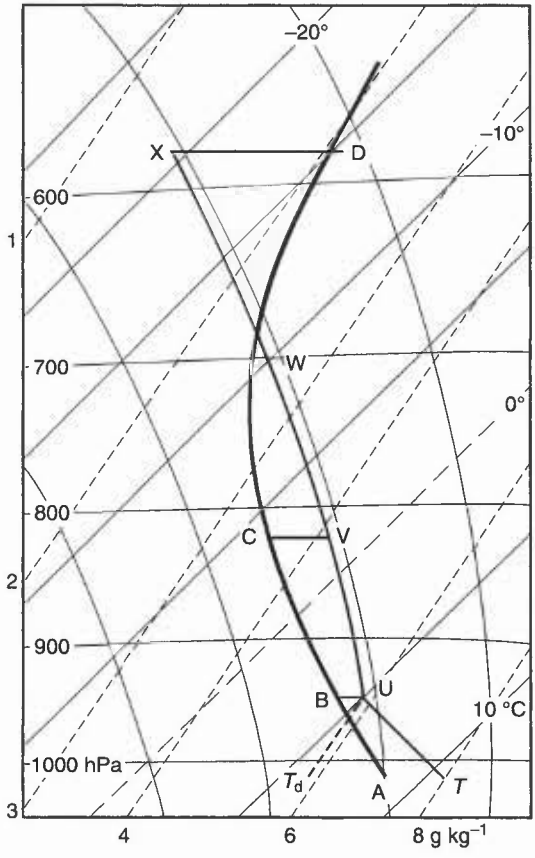

Figure 4.1. Tephigram construction for estimating the base and tops of convection cloud. See text for method of use.

4.2.2.2 Relationship between condensation level and cloud base (SB)

4.2.3 Forecasting the heights of convective cloud tops (SB)

Local Weather Manuals (1994)

4.2.3.3 Prediction of surface dew points

(i) **Fig. 4.2** shows a tephigram construction for finding a representative daytime dew point from a night-time sounding.

(ii) The full line is the dry-bulb curve and the pecked line is the dew-point curve at dawn. The maximum surface dew point may be found by extrapolating down to the surface that part of the dew-point curve (DX) which has been unaffected by nocturnal cooling in the

boundary layer. The dew point so obtained, A, is the maximum daytime value of the dew point. This will occur in the late morning when cumulus cloud first forms. The temperature T_{Cu} and height, h, at which the first Cu form is estimated by drawing up a constant HMR from A to the environment curve (for h) and then down to the surface along a DALR (for T_{Cu}).

(iii) With the onset of vigorous convection, at midday or soon after, the boundary layer develops an almost constant HMR. The afternoon value of the dew point (B) may be found by drawing a line of constant HMR (CXB) such that the total moisture content represented by the values along DX equals that represented by the values along XA. Since the HMR scale is not linear, DX should be slightly longer than XA. In practice it may be assumed that DX equals XA to a first approximation.

(iv) In this example it has been assumed that the mixed layer extends up to 900 hPa. In midsummer it may be necessary to raise this level to a point 150 hPa above the surface.

(v) On days with strong heating the reported dew points may show wide differences between adjacent inland stations by mid afternoon, especially if winds are light. Stations on or near the coast report much higher dew points when there is an influx of air from the sea.

4.3 Forecasting considerations

4.3.1 Synoptic-scale indicators of enhanced or suppressed convection (SB)

Bader et al. (1995), Chapter 6

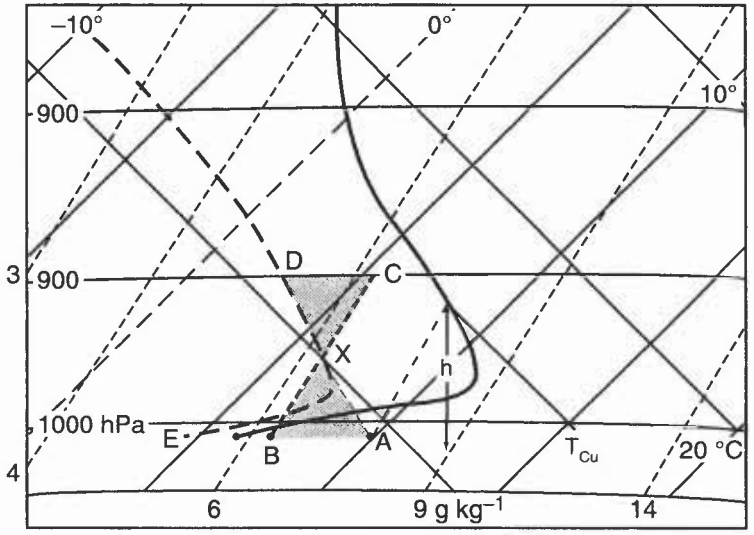

Figure 4.2. Tephigram construction for estimating a representative daytime value of the surface dew point, and temperature of first formation of cumulus. See text for method of use.

4.3.1.1 Summary of forecasting pointers — convective cloud

Decide which air mass will affect the station. Look at its history: did showers develop in it yesterday? If so:

Where? Over sea/coasts/hills/inland?
When? Throughout 24 hours or only at the time of maximum temperature?
At what temperature?
What factors since yesterday have changed the stability?
Heating/cooling from below — advection over warm sea, etc.
Warming/cooling aloft — warm or cold advection.
Increase/decrease in moisture content — by evaporation from a surface/advection of moister air aloft.
Wind direction change may have brought air with markedly different low-level characteristics into the local area, or may do so later in the day.

From representative ascents: what factors might release potential/latent instability?

Low-level convergence due to:
(i) Cyclonic curvature of isobars.
(ii) Along sea-breeze front or where two sea-breeze fronts meet.
(iii) Falling surface pressure.
(iv) Coastal convergence.

Forced mass ascent due to:
(i) Orographic uplift.
(ii) Divergence aloft — upper troughs, etc.
(iii) Along a front.
(iv) Intense surface heating — over a plateau.

HWF (1975), Chapter 19.7

4.3.2 Organization of shallow convection (SB and 1.3)

4.3.2.1 Convection and waves (SB and 1.3)

Thermal activity can be modified by the gravity waves that have, in turn, been generated by the convective activity.

Booth (1980)
Bradbury (1990)
Ludlam (1980)

4.3.2.2 Sea breezes and other convergence zones (SB and 1.3)

4.3.2.3 Convection over the sea (see 10.3.1.2)

4.3.3 Forecasting thermals for glider flights

The best gliding conditions usually occur when the top of the convective layer is marked by an inversion between 5000 and 8000 ft, and thermals are marked by shallow Cu.

Thermal strengths are classified as nil, weak, moderate or strong as follows:

Table 4.1.

Thermal category	Max. rate of climb (kn)	Max. rate of climb ($m\ s^{-1}$)	Cu bases at, or dry adiabatic conditions to (feet agl)
Nil	0	0	<2000
Weak	≤3	≤1.5	≥2000<3000
Moderate	>3≤6	>1.5≤3	≥3000<5000
Strong	>6	>3	≥5000

Mean rate of ascent will be less.

Fig. 4.3 illustrates maximum lift (a) in cloudless thermals, and (b) in cumulus clouds, the latter deduced from the tracking of free balloons by radar. Thermal activity begins to decrease about an hour after maximum surface temperature has been reached. After 1700 UTC thermals usually subside quickly; lift may still be found over towns and south-west facing slopes well into the evening.

An empirical method for estimating thermal strength, based on numerous French glider pilot reports, is illustrated in **Fig. 4.4.** The prediction requires an estimate of cloud base:

(i) Move horizontally across from an estimate of cloud base (e.g. 5500 ft) to one of the diagonal line labelled with the cloud amount (e.g. 1/8).
(ii) Follow line from intersection vertically to the Average Lift scale (e.g. 4.25 kn).
(iii) Continue down to intersect the diagonal lie and read off the Max Lift (e.g. 7 kn).

Summary: a prediction of 1/8 cloud at 5500 ft gives a forecast average lift of 4.25 kn, peaking at about 7 kn.

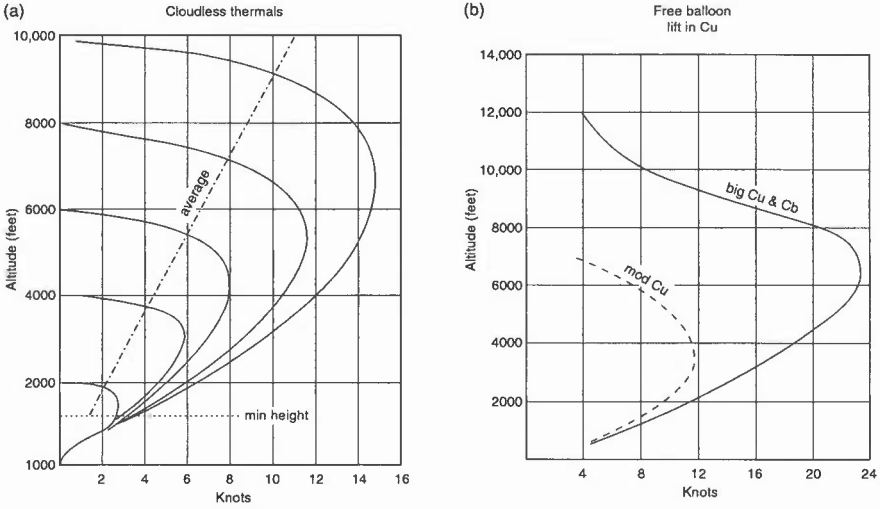

Figure 4.3. (a) Lift in cloudless thermals, and (b) lift in cumulus cloud.

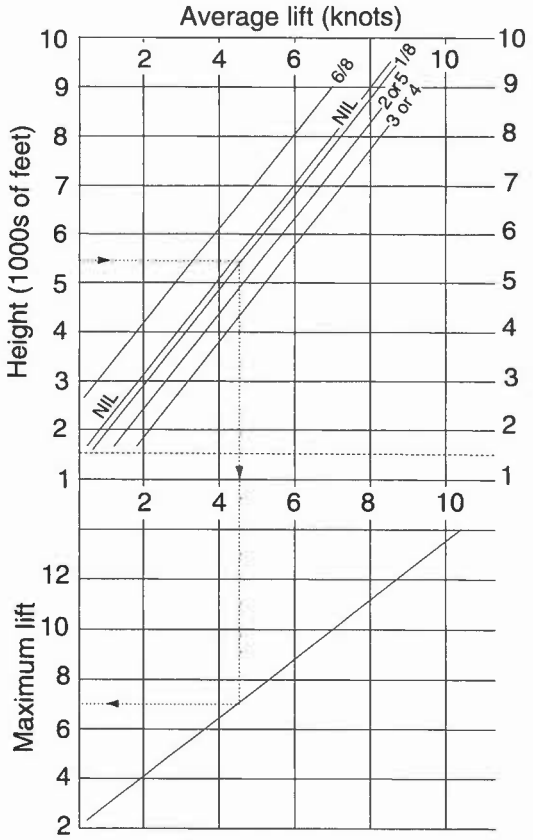

Figure 4.4. Empirically derived average and maximum thermal lift as a function of cloud base and cloud cover (see text for details).

Lee waves enable gliding to high altitudes in the lee of quite moderate hills; vertical velocities are generally between 5 and 10 kn (2.5 to 5 m s^{-1}), exceptionally speeds >25 kn (12.5 m s^{-1}) and heights in excess of 30,000 ft have been recorded. Often associated with such systems, however, are flight hazards such as rotors and severe downslope winds (1.3.3.4). Waves above isolated cumulus, cumulus streets and waves, enhanced by cumulus over mountains, offer good opportunities, for example, for cross-country flights.

4.3.3.1 Cross-country flights

Prediction diagrams of air trajectory, isobaric curvature, 850 hPa wind speed/direction, and potential temperature/dew-point depression data (due to Bradbury) may be 'scored' to assess long-distance prospects. **Table 4.2** summarizes favourable conditions over closed-circuit routes.

Table 4.2. Long cross-country flights over closed-circuit routes: favourable conditions

Previous air trajectory	From NW, N or NE (never from S).
Curvature of isobars	Anticyclonic.
Mean sea-level pressure	1023 hPa (±7 hPa).
850 hPa wind	Speed not more than 16 kn, direction between WNW and ENE through N.
Stability	Potential temperature decreasing about 3 °C between surface and 850 hPa at the time of maximum temperature. Depth of instability restricted to a stable layer below 700 hPa to prevent any shower activity.
Surface dew-point depression	11 to 18 °C by mid-afternoon.
Surface moisture and rainfall	State of ground dry at 06 UTC, no overnight rainfall.
Sunshine	At least 8 hours bright sunshine.
Visibility	More than 20 km.

Booth (1978) **Met O 6 Gliding Notes (1989)**
Bradbury (1978, 1991a, 1991b)

4.4 The spreading out of cumulus into a layer of stratocumulus

4.4.1 Cloud cover beneath an inversion

When the depth of convection is limited by an inversion, cumulus tops may spread out to form an almost unbroken sheet which covers large areas and persists for long periods. This is common in subsided polar maritime air masses, particularly on the eastern flanks of anticyclones. **Fig. 4.5** illustrates an empirical method for estimating the cloud cover beneath an inversion. B is the condensation level, derived from the expected surface temperature, *T*,

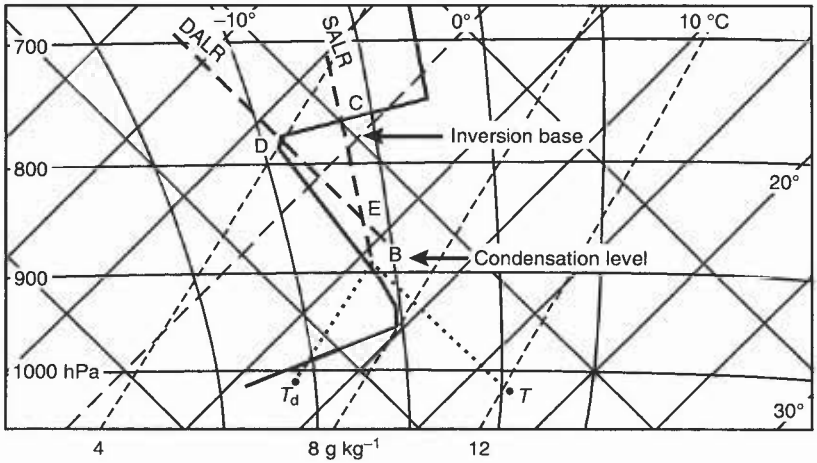

Figure 4.5. Estimating the spread out of cumulus cover beneath an inversion. See text for method of construction.

and dew point, T_d, BC is a saturated adiabat from cloud base to cloud top. DE is a dry adiabat from the base of the capping inversion, cutting BC at E.

The expected cloud amount equals CE divided by CB, where the depths are conveniently measured in hectopascals and the answer is a fraction which can be expressed in terms of oktas.

4.4.2 Criteria for development of stratocumulus spread-out (see 5.8)

(i) An inversion or well-marked stable layer strong enough to halt all convective upcurrents even at the time of maximum insolation.
(ii) A lapse-rate close to the DALR from the surface to near the base of the inversion when convection starts.
(iii) Condensation level at least 2000 ft below the level of the inversion.
(iv) A dew-point depression of 5 °C or less in the layer between the condensation level and the base of the inversion.

4.4.3 Criteria for break-up of cloud sheet

(i) Decreasing surface dew points, lifting the condensation level to within 30 hPa of the inversion.
(ii) Increasing surface temperatures, sufficient to lift the condensation level to within 30 hPa of the inversion.
(iii) Continued subsidence, bringing the inversion down to within 30 hPa of the condensation level.
(iv) A weakening of the inversion, allowing cumulus tops to break through to a higher level.
(v) If the cloud layer is formed due to diurnal heating over land, nocturnal cooling usually results in the dispersal of the layer.
(vi) Cloud formed by convection over the sea shows no such diurnal variation.

HWF (1975)

4.5 Forecasting showers

4.5.1 Precipitation processes within continental and maritime clouds (SB)

4.5.2 Depth of cloud needed for showers

(i) The diagram at **Fig. 5.15** may be used as a rough guide to the intensity of both convective and non-convective precipitation, even though cloud-top temperature is not considered.
(ii) Showers are likely to be heavier in intensity than layer-cloud precipitation for the same thickness of cloud.
(iii) The diagram only applies if the difference in water content at the base and top of a shower cloud exceeds 1.5 g kg^{-1}.
(iv) Moderate Cu of maritime origin may give more precipitation than indicated.
(v) If the cloud depth is <5000 ft (1500 m) with cloud-top temperature warmer than −12 °C there is a 10% probability of showers; the figure rises to 90% for cloud depth >10,000 ft (3000 m). Exceptions to this rule are the 'drizzly' showers from warm maritime clouds and the shallow winter maritime/coastal showers common in northern areas in northerly polar flows with limited instability.

(vi) It is important that the top should certainly be < -4 °C, and generally < -10 °C, for any likelihood of showers by the Bergeron–Findeisen mechanism.

See 4.7.1.2 for guidance on the probability of thunderstorms related to the height of cumulonimbus tops.

Pettersen et al. (1945)

4.5.2.1 Cloud cover and lifetime

(i) Cover — if RH at cloud level is 50% suggest 2 oktas;
if 75% suggest 5 oktas.

(ii) Surface observations routinely give larger amounts of convective cloud than are seen from the air or satellite, since the gaps between distant Cu are obscured from the ground-based observer by adjacent Cu.

Table 4.3. Depths, updraughts and lifetimes of Cu and Cb

Cloud type	depth (ft)	updraught ($m\ s^{-1}$)	lifetime
Small Cu	1500	1–5	20 min
Large Cu	6000–15,000	5–10	1 hour
Cb	15,000 upwards	10–20	>1 hour
Supercell Cb	15,000 upwards	>50	>>1hour

4.5.2.2 Intensities of showery precipitation (UK Met. Office definitions)

Table 4.4.

Rain showers	Intensity ($mm\ h^{-1}$)
Slight	<2.0
Moderate	2.0 to 10.0
Heavy	10.0 to 50.0
Violent	>50.0

Meteorological Glossary (1991)
Observer's Handbook (1982)

4.5.3 Showers and wind shear (SB)

The wind shear in the cloudy convective layer is a useful key to the persistence of individual showers:

HWF (1975), Chapter 19.7.3.3
Ludlam (1980)

4.6 Topographically related convection

Satellite and radar imagery confirm that the distribution of convection is rarely random. Cloud bands and precipitation repeatedly occur in similar air masses relative to the same topographic features and may be seasonal, diurnal or tied to wind direction (**SB, Figs 4.6, 4.7, 4.8 and 4.9**).

Bader et al. (1995), Chapter 6
Browning et al. (1985)
Hill (1983)
Monk (1987)
Orographic Processes (1993)

4.7 Forecasting cumulonimbus and thunderstorms

4.7.1 Main factors

At around −20 °C a significant proportion of cloud particles in an air parcel will be composed of ice crystals, giving the cloud boundary a fibrous appearance. This marks the transition of the cloud from large cumulus to cumulonimbus. The vertical wind structure will determine the lifetime and severity of the storm and whether it exists as a single cell or develops as a multicell storm.

4.7.1.1 Movement of thunderstorms: the steering level

With a cumulonimbus extending through a deep layer in which there is marked wind shear, the storm cloud is steered by the wind at the level approximately one third of its depth, measured from the base of the cloud, i.e.

$$H_{base} + 1/3\ (H_{top} - H_{base}).$$

In the United Kingdom, the steering level is often around 700 hPa. However, for a storm with a 5000 ft (1500 m) base and top at 40,000 ft (12,000 m) this gives a steering level of 16,600 ft (5000 m; 550 hPa).

Ludlam (1980)

4.7.1.2 Depth of cumulonimbus giving thunder

A useful guide is given by:

Table 4.5.

If cumulonimbus tops are at:	
<13,000 ft	— thunder unlikely
14,000–18,000 ft	— thunder probable
>18,000 ft	— thunder highly probable

A better guide may be: cloud-top temperature ≤ −18 °C.

HWF (1975), Chapter 19.7.5

4.7.2 *Forecasting thunderstorms — instability indices*

(a) *Boyden Index*

A measure of the instability below 700hPa is:

$$I = (Z - 200) - T$$

where Z = 1000–700 hPa thickness (dam); T = 700 hPa temperature (°C).

Thunder is probable if $I \geq 94/95$ (in the UK).

Forecasts should be made assuming that index isopleths move with the 700 hPa wind. A main advantage claimed for this method is its usefulness in mobile situations, regardless of whether fronts are involved. It should not be used in Mediterranean or tropical areas, or where the ground level is high.

Boyden (1966)

(b) *Rackliff Index*

The index is related to temperature as well as instability:

$$T = \theta_{w900} - T_{500}$$

where θ_{w900} is the 900 hPa wet-bulb potential temperature (°C); T_{500} is the 500 hPa temperature (°C).

In non-frontal situations significant showers accompanied by thunder are probable if $T \geq 29/30$ in the UK.

Rackliff (1962)

(c) *Modified Jefferson Index*

An amended form of Rackliff's index: values of that index for neutral stability air decrease almost linearly as WBPT increases. Jefferson's index gives an index independent of temperature (with same thunderstorm threshold value over a wide range of temperature). The formula was later amended to incorporate the 700 hPa dew-point depression to allow for middle-level humidity:

$$T_{mj} = 1.6\theta_{w900} - T_{500} - 0.5D_{700} - 8$$

where D_{700} = dew-point depression (°C) at 700 hPa.

Thunder is probable if T_{mj} = 27 to 28, in the United Kingdom although 26 to 27 is better in returning polar maritime air.

The formula can be reduced to $T_{mj} = \Delta T + X$ and computed more easily by using **Fig. 4.10,** where the value of $(-0.5D_{700} - 8)$ is replaced by the constant -11.

(i) From the values of 500 hPa temperature (x-axis) and 900 hPa θ_w (y-axis), obtain a value of ΔT given by the sloping lines.

(ii) Correct this value of ΔT, according to the actual 700 hPa dew-point depression, using the small graph (top right) to obtain the correction X.

Jefferson (1963)

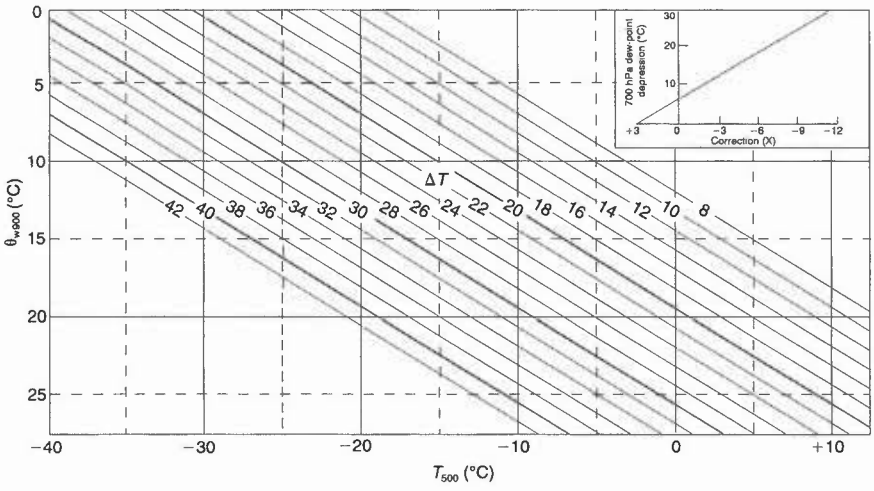

Figure 4.10. Computing the modified Jefferson Instability Index. See text for method of use.

(d) *Potential instability index*

$$P = \theta_{w500} - \theta_{w850}$$

Thunder is possible if: P is ≤ -2 °C (summer)
P is $\leq +3$ °C (winter)

Bradbury (1977)

(e) *K index*

$$K = (T_{850} - T_{500}) + T_{d850} - (T_{700} - T_{d700}),$$

where: T_{d850} is 850 hPa dew-point temperature etc.
Thunder possible for K≥20

George (1960)

4.7.2.1 Tests of different instability indices

Operationally indices offer only a guide to the degree of static instability at the time of a sounding. Other measures of convective development, such as radar and satellite imagery, as well as numerical weather prediction models, must provide supporting information.

Bradbury (1977)
Collier & Lilley (1994)

4.7.3 Hail

Deep and vigorous convection is required. The following criteria are a guide:

(i) Cumulonimbus tops are colder than −20 °C.

(ii) The 'parcel' path curve is warmer than the environment curve by 4 °C at some level (CV in **Fig. 4.1**) and gives cloud tops of 15,000 ft (4500 m) or more.

A similar method, based on the parcel curve, is:

(i) At the point where the curve reaches −20 °C measure the difference between this temperature and the environment temperature.

(ii) If this difference is:

≥5 °C	forecast hail;
from 5 °C to 2.5 °C	forecast soft hail or rain;
if difference ≤2.5 °C	forecast rain.

(large hail requires a 'steady state', but not necessarily slow-moving, storm).

In both methods vertical wind shear exists between the base and top of cumulonimbus.

Browning (1963) **Ludlam (1980)**

4.7.4 Lightning

Lightning occurs in vigorous convective cloud; ice particles and hail are considered to play a key role in charge generation and, indeed, the vast majority of lightning emanates from thunderstorms extending well above the freezing level. However, there are well documented UK observations of lightning discharges from all-water clouds.

4.7.4.1 Detection and forecasting

(i) Often it is a reliable assurance that lightning is not going to occur that is required.

(ii) The Arrival Time Difference (ATD) system can detect both ground and cloud-to-cloud lightning strokes.

(iii) The current system detects about one third of all strokes, being limited by computer processing speed and station locations; the low false-alarm rate allows the detection of smaller thunderstorms earlier.

Atkinson et al. (1989) **Ludlam (1980)**
Lee (1986) **Mason (1971)**

4.7.4.2 Static risk for towed targets (SB)

Many incidents of aerial-towed targets glowing and then disintegrating are due, apparently, to static discharge: the influence of the conducting nature of the tow line has yet to be determined.

Aberporth Met. Office (1993)
Rogers (1967)

4.7.5 Gust fronts (SB and 6.2, Fig. 6.4)

4.7.6 Squall lines (SB)

Associated with *thunderstorms* and with *cold active fronts* with rearward-sloping warm conveyor belt (7.1): see also 6.2 — *Gust forecasting in strong wind conditions*)

HWF (1975) Chapter 16
Ludlam (1980)

4.7.7 Single- and multi-cell development (SB)

4.7.7.1 Effect of vertical wind shear (SB)

4.7.7.2 Changing wind direction and speed with height (SB, Figs 4.1 .and 4.12)

4.7.7.3 MCC systems: characteristics (SB)

Bader et al. (1995), Chapter 6

4.7.7.4 Supercells (SB, Fig. 4.11(a))

The 'supercell' is responsible for the most severe summertime thunderstorms with localized flooding. Southern England is a favoured location with a low-level flow of warm, continental south-easterly winds overridden by cooler, oceanic south-westerlies aloft. In extreme cases with light winds storms may persist at a particular place for several hours with heavy rain and hail, although such storms are not common in the UK.

Typical synoptic-scale environment for supercell storms:

(i) Strong instability with parcel theory indicating >4 °C excess buoyancy at 500 hPa.
(ii) Strong mean sub-cloud winds (order of 10 m s^{-1}).
(iii) Strong environmental shear through cloud layer of 2.5 to 4.5 m s^{-1} per km (hence strong upper winds).
(iv) Strong veer of wind with height.

Bader et al. (1995), Chapter 6
Browning & Ludlam (1962)
Ludlam (1980)

4.7.7.5 CAPE and development of severe storms

Severe storms may spawn 'daughter cells' to their north-east flank, due to convergence; the maximum area of convective activity (as tracked, for example, by radar) will move to the right of the individual cell motion, typically by 20 to 30° **(SB, Fig. 4.12)**.

Development of severe storms depend on:

(i) Vertical wind shear through the depth of the convective layer ΔU **(Figs 4.11 and 4.13)**.

(ii) Large quantities of Convectively Available Potential Energy (CAPE), which can be released through convection. On a tephigram this energy is represented by the area between the environment curve and the path curve of a rising parcel (ATUVWCB in **Fig. 4.1**). The severity of the storms depends on whether the CAPE is released by many small cumulonimbus clouds or by a few giant ones.

(iii) A measure of whether or not a storm will be single- or multi-cell is estimated from:
$R>3$ — storms likely to be multi-celled;
$0.5<R<1$ — single cell likely,

where: R (the bulk Richardson number)= $\text{CAPE}/[0.5(\Delta U)^2]$, i.e a measure of the wind shear required to organize flow, against buoyancy forces tending to disrupt the flow.

Collier & Lilley (1994)
Galvin et al. (1995)
Ludlam (1980)

4.7.8 Forecasting thunderstorms — synoptic features (SB)

The objective forecasting techniques should not be used in isolation. Their value is greatly enhanced when they are used in conjunction with features which can be analysed on synoptic charts. Upper-air soundings alone do not always reveal the extent of the thunder risk, the soundings available before a thundery outbreak failing to show exceptional instability.

Consideration should be given to factors likely to release the energy available for convection, such as: the position and movement of upper-level troughs or lows: the existence and movement of low-level convergence lines, such as surface fronts,or sea-breeze fronts; areas of high ground prone to warning.

Other useful synoptic tools are: dew-point analysis: charts of θ_w at 850 hPa: these serve a similar purpose as surface dew-point analyses; charts of the difference between θ_w at 500 and 850 hPa;:cyclonic curvature of surface isobars.

4.7.8.1 Conditions favouring severe thunderstorms

Over Britain, severe storms are often associated with a cold front over, or close to, north-western parts with an attendant upper trough to the west.. A representation of the synoptic-scale airflow associated with such storms over southern Britain is shown in **Fig.4.14**.

Pointers to forecasting thunderstorms over southern England:

(i) *Upper-air soundings*
Some of the most severe and widespread outbreaks of thunder have occurred some 12–18 hours after a sounding showed a layer of warm air capping a shallow convective layer. This cap can prevent the early release of the convective energy, allowing it to build up with continued surface heating and be released explosively in one big storm later.

(ii) *Advection of low-level moisture*
Surface dew points should exceed 13 °C, but often reach 18 °C or more in severe storms over southern England. At 850 hPa, similar values of θ_w are experienced. The winds at this level are usually in the sector SE–SSW, with a speed of 20–30 kn, often in a narrow tongue.

(iii) *Medium-level advection of dry air*
With potential instability present, θ_w values at 500 hPa may be 2–5 °C lower than at 850 hPa. Winds at 500 hPa should be 20–40° veered from those at 850 hPa, with speeds of 35–50 kn.

(iv) *Upper-level strong winds*
Further veering above 500 hPa, with 300 hPa winds in the sector SSW–W and speeds 50–85 kn, are good conditions for positioning the downdraughts in the favoured position for generating severe storms.

(v) *Positive vorticity advection (PVA) at 500 and 300 hPa*
This usually occurs in the region in advance of an upper trough or upper low. Isopleths of vorticity cross the contour lines at an angle of 30° or more.

(vi) *'Dry lines'*
Mesoscale areas of dry air within an otherwise moist air mass, and the resulting production of strong horizontal moisture gradients (*dry lines*) by deformation in the air ahead of a (summer) cold front, may provide a preferred position for triggering intense thunderstorm activity in the already unstable air. Satellite, radar and model data should distinguish the deep, dry areas well before the outbreak.

Bader et al. (1995), Chapter 6
Grant (1995)
Ludlam (1980)
Morris (1986)
Scorer & Verkaik (1989)
Young (1995)

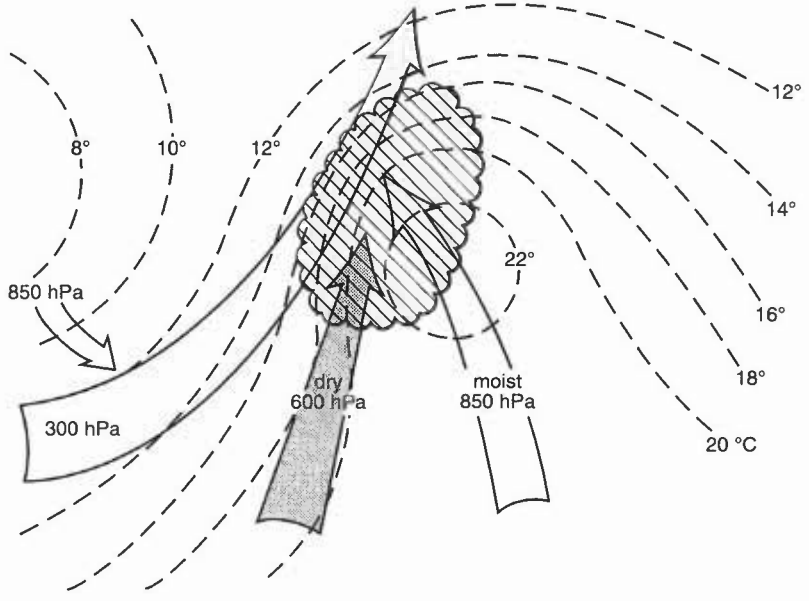

Figure 4.14. A schematic diagram of the three main synoptic-scale currents associated with the development of severe thunderstorms over southern England, together with typical isopleths of θ_w at 850 hPa. The hatched area indicates the the location of the storms.

BIBLIOGRAPHY

CHAPTER 4 — CONVECTION AND SHOWERS

Aberporth Met. Office, 1993: Local Staff Instructions.

Atkinson,N.C, Blackburn, M.R. and Kitchen, M., 1989: Wide area lightning location using the UK Met. Office arrival time difference system. International Conference on Lightning and Static Electricity, University of Bath, 26/28 September 1989.

Bader, M.J., Forbes, G.S., Grant, J.R., Lilley, R.B.E. and Waters, J., 1995: Images in weather forecasting. Cambridge University Press.

Booth, B.J., 1978: On forecasting dry thermals for gliding. *Meteorol Mag*, **107**, 48–61.

Booth, B., 1980: Unusual wave flow over the Midlands. *Meteorol Mag*, **109**, 313–324.

Boyden, C.J., 1966: A simple Instability Index for use as a synoptic parameter. *Meteorol Mag*, **92**, 198–210.

Bradbury, T.A.M., 1977: The use of wet-bulb potential temperature charts. *Meteorol Mag*, **106**, 233–251.

Bradbury, T.A.M., 1978: Weather conditions for long glider flights over England. *Meteorol Mag*, **107**, 340–353.

Bradbury, T.A.M., 1990: Links between convection and waves. *Meteorol Mag*, **119**, 112–120.

Bradbury, T.A.M., 1991a: Thermal prediction from the tephigram. *Sailplane & Gliding*, **June/July**, 122–126.

Bradbury, T.A.M., 1991b: Meteorology and flight. A & C Black.

Browning, K.A., 1963: The growth of large hail within a steady updraught. *QJR Meteorol Soc*, **89**, 490–506.

Browning, K.A. and Ludlam, F.H., 1962: Airflow in convective storms. *QJR Meteorol Soc*, **88**, 117–135.

Browning, K.A., Eccleston, A.J. and Monk, G.A., 1985: The use of satellite and radar imagery to identify persistent shower bands downwind of the North Channel. *Meteorol Mag*, **114**, 325–331.

Collier, C.G. and Lilley R.B.E., 1994: Forecasting thunderstorm initiation in NW Europe using thermodynamic indices, satellite and radar data. *Meteorol Appl*, **1**, 75–84.

Galvin, J.F.P., Bennett, P.H. and Couchman, P.B., 1995: Two thunderstorms in summer 1994 at Birmingham. *Weather*, **50**, 239–250.

George, J.J, 1960: Weather forecasting for Aeronautics. Academic Press (K Index).

Grant, K., 1995: The British 'dry line' and its role in the genesis of severe local storms. *J Meteorol*, **20**, 241–259.

Hill, F.F., 1983: The use of average annual rainfall to derive estimates of orographic enhancement of frontal rainfall over England and Wales for different wind directions. *J Climatol*, **3**, 113–129

Jefferson, G.J., 1963: A further development of the Instability Index. *Meteorol Mag*, **92**, 313–316.

Lee, A.C.L., 1986: An operational system for the remote location of lightning flashes using a VLF arrival time difference technique. *J Atmos and Oceanic Technol*, **3**, 630–642.

Local Weather Manual for Southern England, 1994: Meteorological Office.

Ludlam, F.H., 1980: Clouds and storms. Pennsylvania State University Press.

MacIntosh, D.H. and Thom, A.S., 1972: Essentials of meteorology. London, Wykeham Pubs.

Mason, B.J, 1971: The physics of clouds (2nd edition). Clarendon Press, Oxford.

Met O 6, 1989: Notes on the preparation of gliding forecasts for RAF gliding schools. Meteorological Office (Met O 6), Unpublished.

Meteorological Glossary, 1991: London, HMSO.

Monk, G.A., 1987: Topographically-related convection over the British Isles. *In* Workshop on 'Satellite and Radar Imagery Interpretation' at the Meteorological Office College, Shinfield, Ed: M. Bader and A. Waters; pub: EUMETSAT.

Morris, R.M., 1986: The Spanish plume — testing the forecaster's nerve. *Meteorol Mag*, **115**, 349–357

Observer's Handbook, 1982: London, HMSO.

Orographic Processes in Meteorology (Pre-prints), 1993: Summer School, Meteorological Office College.

Pettersen, S., Knighting, E., Jones, R.W. and Herlofson, N., 1945: Convection in theory and practice. *Geofys Publ*, Oslo, **16**, No. 10.

Rackliff, P.G., 1962: Applications of an Instability Index to regional forecasting. *Meteorol Mag*, **91**, 113–120.

Rogers, M.E., 1967: Interim report reviewing the present position on helicopter static electrification. RAE Technical Report 67292.

Scorer, R.S. and Verkaik, A., 1989: Spacious skies. David and Charles.

Young, M.V., 1995: Severe thunderstorms over south-east England on 24 June 1994: A forecasting perspective. *Weather*, **50,** 250–256.

CHAPTER 5 — LAYER CLOUDS AND PRECIPITATION

5.1 Layer cloud formation

Low stratus forms when air with a lapse rate less than the SALR is either cooled below its dew point or has extra moisture added by the evaporation of falling precipitation or by evaporation from wet surfaces, especially when snow or heavy frost begins to thaw.

Much information on the relation of stratus to local wind direction is available in *Aerodrome Weather Diagrams and Characteristics* (extracts in Local Weather Manuals).

AWDC (1960)
Mansfield (1988)

5.2 Large-scale ascent

5.2.1 Frontal cloud

Gentle ascent will often produce layer clouds throughout an extensive tropospheric depth; the following are forecasting techniques for short and longer term:

(a) Short term:
  (i) Tephigram analysis — **Table 5.1** may give an indication of cloud structure; high cloud may obscure lower cloud on satellite imagery; a general sense of cloud structure may be inferred from radar rainfall.
  (ii) Advection — apply gradient wind component normal to front; actual/forecast winds at cloud level; speed of warm/cold advection from hodograph.
  (iii) Development — refer to pressure tendencies; frontal waves; upper-air development; local effects.

(b) Longer term — beyond 12 hours:
  (i) Model output to position systems and indicate their likely activity.
  (ii) Conceptual models (7.1) and local knowledge to estimate likely cloud structure.

Table 5.1. Cloud structure from a tephigram

The following guidelines should give a reasonable assessment of the likely cloud structure from dew-point depressions on a representative tephigram.

Dry bulb >0 °C	
$(T - T_d) \leq 1$ °C	8/8 layer
$(T - T_d)$ 1 to 5 °C	Thin layers
$(T - T_d) > 5$ °C	No cloud
Dry bulb <0 °C	
$(T - T_d) < 3$ °C	8/8 layer
$(T - T_d)$ 3 to 5 °C	Thick layers
$(T - T_d)$ 6 to 10 °C	Thin layers
$(T - T_d) > 10$ °C	No cloud

5.2.2 Cloud formed in precipitation

(a) In rain:

(i) Evaporation of precipitation can cool the air to its wet-bulb temperature. A temperature close to the wet-bulb value is reached after about half an hour of very heavy rain or 1–2 hours of moderate rain and results in ragged stratus *pannus*. A rough guide to the base of the stratus *pannus* is:

2 hours continuous rain — base 800 feet (245 m)

3 hours continuous rain — base 400 feet (120 m) (no account taken of upslope or advective effects).

(ii) Prolonged drizzle and light winds frequently lead to the formation of very low stratus even when upslope motion is apparently negligible.

Advection of warm air across lying/thawing snow often results in stratus forming at or very near the surface.

(b) In snow:

(i) Melting of falling snow into warm sub-cloud layer will produce an isothermal (along 0 °C isotherm) 600 feet deep after 1 hour, increasing to a maximum of 1200 feet after 4 hours.

(ii) Extension of the 0 °C isotherm results in a DALR between cooled and unmodified air; at saturation instability causes fractocumulus of a few hundred feet thickness to form near the 0 °C isotherm below cloud base. The modified temperature profile is illustrated in (**SB, Fig. 5.1**); the surface temperature will fall as a result of the cooling.

(iii) If snow reaches the ground, *pannus* forms at or very near the ground.

5.2.3 Non-frontal medium and high cloud (SB)

Non-frontal cloud is often associated with medium- or upper-level instability or wind shear.

HWF (1975), Chapter 19.5

5.2.4 Cirrus forecasting

James' technique requires scores to be allotted to a series of questions for (a) 6–12 hours ahead, and (b) 24–36 hours ahead (**SB, Table 5.2**)

James (1957)

5.2.4.1 Tops and bases of cirrus

(i) 50% of all cirrus is likely to be within 5000 ft (1500 m) of the tropopause.

(ii) Thickness is likely to fall within the three ranges: 0–2000 ft, 2000–4000 ft or 4000–6000 ft (0–600, 600–1200 or 1200–1800 m) on roughly an equal number of occasions.

(iii) Mean tops reach the tropopause for tropopause heights up to about 30,000 ft (9 km), becoming relatively lower, until at 39,000 ft (12 km) they are some 4000 ft (1200 m) below the tropopause.

(iv) Mean bases tend to be about 1200 m below the tropopause up to 9 km; at higher levels mean base seems to be in the region of 9 km.

(v) Occurrence of cirrus is favoured in a layer through which wind speed increases rapidly with height (**Fig. 5.2**).

HWF (1975), Chapter 19.6.4.2

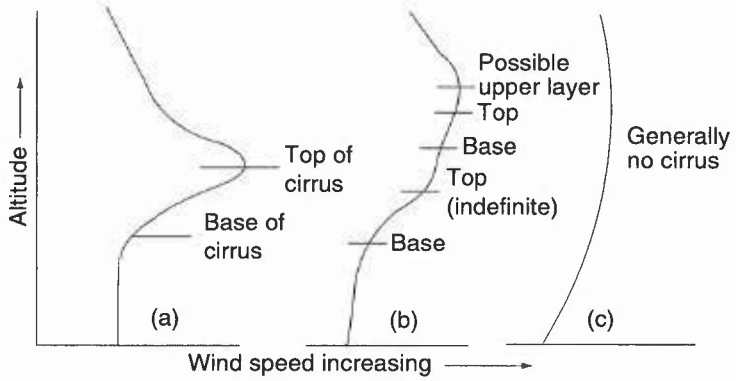

Figure 5.2. Association between cirrus levels and profiles of wind speed.

5.3 Condensation trails (SB, Fig. 5.3)

The MINTRA line represents the limiting temperature above which contrails are unlikely. In **SB, Fig. 5.3(b) and (c)**, updated nomograms are illustrated for low- and high-bypass turbofan engine categories (e.g. fighters and transport refuelling aircraft, respectively).

HAM (1994)

5.3.1 Forecasting contrails

5.3.2 Revised rules for modern engines

Appleman (1953)
Ferris (1996)
HAM (1994)

5.4 Orographic uplift

5.4.1 Upslope stratus (SB, Figs 5.4 and 5.6)

Where turbulent mixing maintains extensive low stratus over low-lying terrain, base will be at the mixing condensation level (MCL); the base on windward slopes is often lower (lifting condensation level, LCL).

To determine stratus base:

(i) From selected representative sounding modify temperature and moisture profiles near ground to fit local values.
(ii) Find LCL for a series of levels near the surface **(Fig. 5.6)**.
(iii) Upslope base is given by lowest LCL.

5.4.2 Orographic clouds

Cap, lenticular, rotor and banner clouds are discussed in 1.3.3 and 10.3.2.

Browning (1975)
Smith (1989)

5.5 Turbulent mixing

(i) Turbulence tends to establish DALR and constant HMR profiles; RH increases with height, with any cloud base being at the mixing condensation level (MCL) of the layer.

(ii) To assess the MCL requires knowledge of the mixing layer depth, d, comparatively easy if top is marked by a sharp inversion. If this is not the case, there are several empirical techniques available, for example:

for surface wind, $V_S \leq 16$ kn, $d = 200\ V_S$ feet;
for surface wind, $V_S \geq 16$ kn, $d = 3300$ to 3600 feet by night
$d = 4000$ feet by day.

(iii) In view of difficulty in deriving the MCL, locally derived empirical methods may prove more satisfactory.

HWF (1975), Chapter 19

5.5.1 Air-mass stratus (SB, Figs 5.7 and 5.8)

Three principal regimes identified for the cooling of a turbulent boundary layer below its dew point are illustrated in **SB, Fig. 5.8.**

5.6 Stratus forecasting techniques

5.6.1 Formation of low stratus (SB)

5.6.2 Forecasting the temperature of stratus formation over land

Formation temperature may be found from a number of sources, the choice of which depends on location and synoptic situation. Stratus may form at:

(i) temperature at which stratus is already present on the chart;
(ii) the stratus clearance temperature earlier in the day (minus 1 or 2 °C);
(iii) the sea temperature if advection is likely;
(iv) the temperature derived from a representative ascent; a technique is given below.

To forecast the temperature at which stratus will form as a result of nocturnal cooling over land (**Fig. 5.9**):

(i) Obtain the fog-point T_f by Saunders' method (3.3.3.1) from a representative ascent.
(ii) Assess the pressure level at which stratus is expected to form.
(iii) On a tephigram draw the constant mixing ratio line through the fog-point temperature (plotted on the surface isobar).
(iv) From the intersection of this line with the isobar corresponding to the top of the surface turbulent layer (point A), draw a dry adiabatic. The intersection of this adiabatic with the surface isobar indicates the temperature at which stratus will form. This is T_{st}.

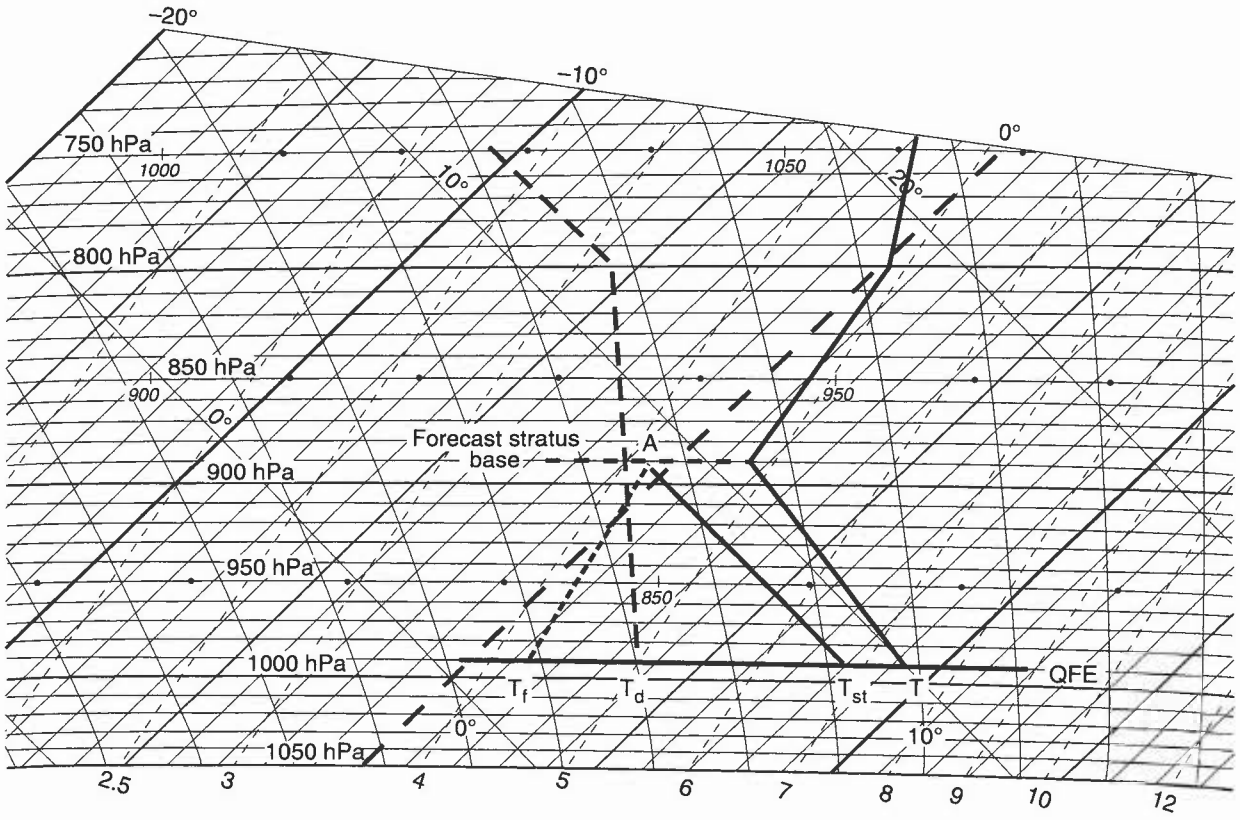

Figure 5.9. Determination of the stratus formation temperature (T_{st}) from a representative ascent. See text for details.

A technique based on constructing a 'Critical θ_w' (CTW) is illustrated in **SB (Fig. 5.10)**.

HWF (1975), Chapter 19.6
Warne (1993)

5.6.3 Forecasting the stratus base

The base height is principally a function of wind, which affects the efficiency of turbulent mixing, and RH, which determines the height of the MCL. Generally, the stronger the wind, the higher the base, as given by the guide:

$$h \text{ (ft)} = 75\ V_S, \text{ for forecast surface wind in knots.}$$

The surface temperature/dew-point difference may be used: $h = \alpha(T - T_d)$, $\alpha = 420$ feet (130 m), although work at Shawbury has given values between 395 and 450 (the latter for tropical maritime air). However, surface dew-point depression may not be representative of the mixing layer, and base estimates will be under- or over-estimated depending on whether the ground is cooling or warming. The observed base of stratus that has already formed upwind may be a more useful guide, adjusted to local effects.

HWF (1975), Chapter 19.6

5.6.4 Forecasting stratus tops

The top of the mixing layer will mark the stratus tops; it should be noted that, in most situations, stratus is likely to be no more than a few hundred feet thick. The 'critical θ_w' technique also gives stratus tops.

5.6.5 Forecasting the advection of stratus from the sea

(i) If there has been little change in the synoptic situation during the day, the temperature at which stratus cleared in the morning (minus 1 or 2 °C) is a good estimate of the threshold temperature at the coast when the stratus will start again to move inland from the coast. (If coastal temperature is not known use the (representative) sea temperature.)

(ii) The movement of stratus inland can be forecast from the direction and speed of the 10 m wind at the time when convection and turbulence are still operative in the lowest layers, and before the surface temperature begins to fall towards evening. Valleys aligned at right angles to the coast facilitate deep inland advances.

(iii) If there is upslope motion, stratus may form over higher ground before the main cloud sheet spreads in from the coast (giving the impression that the movement inland occurs at greater than the geostrophic speed).

(iv) The level at which stratus will form can be determined from a representative vertical profile of temperature and dew-point. Use a Normand construction to determine the condensation levels of air lifted from several levels. The lowest condensation level represents the pressure at the base of any orographic stratus.

(v) Studies around the Eden estuary (E Scotland) have shown that 'haar' may recede with the ebbing tide as estuarine muds and sands are exposed and warm rapidly; the haar advances with the next tide.

Alexander (1964) **Lamb (1945)**
Sparks (1962)

5.6.6 Stratus clearance (SB, Fig. 5.11)

The three main clearance mechanisms are: *Insolation; Increased wind; Advection of drier air.*

Mansfield (1988)

5.7 Stratocumulus: physical and dynamical processes of formation and dissipation (SB, Figs 5.12, 5.13 and 5.14)

The latest thinking on the physical and dynamical processes of formation and dissipation of stratocumulus is presented in the SB; the section concentrates on radiatively driven convection; other forms of mixing may also be important, but the cloud will then have a different structure and behaviour.

Bennetts et al. (1986)
James (1959)
Kraus (1943)

5.8 Non-frontal stratocumulus

In the formation of stratus, the turbulence is generally purely mechanical; in the case of stratocumulus, convection and radiation often play major roles.

5.8.1 Formation and dispersal (SB)

Two main categories of Sc are:
Sc formed by spreading out of Cu (4.4); Anticyclonic Sc.

Formation: is by mechanical turbulence in the mixing zone, by convection due to surface heating, or a combination of both.

Dispersal: prediction is difficult, especially in winter
Forecasting notes:

(i) Look for rear edge and advect with wind at cloud level, or by continuity (from satellite pictures or upwind observations)
(ii) If surface temperatures rise to give DALR profile to cloud top, break-up may start but re-form when temperature drops.
(iii) Continued subsidence may lower the inversion sufficiently to bring down drier air and disperse the cloud (unusual).
(v) James', and Kraus' rules are two forecasting techniques discussed next; neither is particularly reliable.

Bennetts et al. (1986)

5.8.2 Dispersal of stratocumulus

5.8.2.1 Nocturnal dispersal of stratocumulus over land (James' rule)

Only use this technique if the stratocumulus sheet is bounded by a dry inversion, there is no surface front within 400 miles and the cloud sheet is extensive, giving almost complete cloud cover (>6/8 for 2 or more hours).

The cloud will break if: $D_m > D_c$

where:

D_m is the maximum dew-point depression (°C) in the 50 hPa layer above cloud

D_c is the value given in the **Table 5.4** below, in which

b is the difference (g kg^{-1}) between HMR at top and bottom of the 50 hPa layer below cloud

z is the cloud thickness (hPa).

Table 5.4. Values of D_c (°C) for use with James' rule

z	b (g kg^{-1})					
(hPa)	0.25	0.50	0.75	1.00	1.25	1.50
10	—	—	1	3	6	8.5
20	0	2.5	5	8	10	13
30	4	7	9	12	14.5	17
40	9	11	14	16	19	21
50	13	15	18	20.5	23	26
60	17	20	22	25	27	30
70	21	24	26.5	29	32	34

Note: a linear hydrolapse in the layer is assumed.

James (1959)

5.8.2.2 Dispersal of stratocumulus by convection (Kraus' rule)

A cloud layer will not disperse by convective mixing with the air above if the pressure (hPa) at the cloud top is less than P_c, as given below. (If the pressure at cloud top is greater than P_c the cloud may or may not disperse.)

$$P_c = P + a(P_0 - 1000)$$

where P_0 is the surface pressure (hPa) and P and 'a' are given in **Table 5.5** below.

Kraus (1943)

Table 5.5. Values of P and 'a' (for use with Kraus' rule) for given cloud-top temperatures (water or ice cloud) and strength of inversion.

	Temp. at cloud top (°C)	Magnitude of inversion containing the cloud layer (°C)									
		10		8		6		4		2	
		P	a	P	a	P	a	P	a	P	a
Water cloud	20	833	0.80	861	0.83	891	0.87	924	0.90	960	0.95
	10	803	0.75	834	0.79	869	0.82	906	087	951	0.93
	0	755	0.67	789	0.71	830	0.76	877	0.82	932	0.90
	−10	680	0.56	719	0.60	765	0.66	823	0.73	898	0.84
Ice cloud	0	779	0.71	812	0.75	850	0.79	891	0.85	941	0.91
	−10	702	0.59	739	0.63	786	0.69	839	0.76	908	0.85
	−20	586	0.45	628	0.49	679	0.54	747	0.62	841	0.74
	−30	451	0.30	489	0.34	540	0.38	613	0.45	728	0.58

5.9 Precipitation from layered clouds

5.9.1 Frontal and non-frontal precipitation

5.9.1.1 Definition of intensities of (non-showery) precipitation (UK Met. Office)

Table 5.6. Definition of intensities of (non-showery) precipitation (UK Met. Office)

(a) *Rain*	
Slight	<0.5 mm h^{-1}
Moderate	0.5 to 4.0 mm h^{-1}
Heavy	>4.0 mm h^{-1}
(b) *Snow*	
Slight	<0.5 cm h^{-1}
Moderate	about 0.5 to 4.0 cm h^{-1}
Heavy	>4.0 cm h^{-1}

Note: 1.25 cm of fresh snow ≈1 mm water.
1 foot of fresh snow ≈1 inch of rain.

Observer's Handbook (1982)

5.9.1.2 Precipitation in frontal depressions (SB, Chapter 7)

Frontal precipitation often occurs in bands, usually but not always parallel to, or coincident with, one of the surface fronts. (Bands of rain ahead of a cold front may penetrate well into the warm sector or even ahead of the warm front.)

Browning (1985)
Browning et al. (1974) **Browning et al. (1975)**

5.9.1.3 Non-frontal precipitation (SB)

5.9.1.4 Quantity of precipitation (SB)

Synoptic data and radar rainfall displays are the best guide to timing the onset and cessation of precipitation and for assessing development, movement and intensity of precipitation areas.

5.9.2 Forecasting drizzle

(i) Precipitation from stratiform cloud is related more to the microphysics than broader-scale dynamics.

(ii) Drizzle is often associated with haar/sea fog (fret), affecting exposed coasts, being cleared inland by insolation and, near coasts, by advection. It thus tends to be more frequent during the latter part of the night and early morning.

(iii) For drizzle to reach the ground it must fall from stratus cloud with its base less than about 1500 ft (450 m) and a minimum depth of 2000 ft (600 m). The dew-point depression in the air below cloud should be less than 2 °C, otherwise the very small drizzle droplets (0.2–0.5 mm diameter) will evaporate.

(iv) Clouds of thickness <7500 ft (2250 m), cloud-top temperatures < -12 °C and bases colder than 0 °C rarely give rain **(Fig. 5.15)**.

(v) Satellite imagery can help to identify areas of colder cloud tops where precipitation is more likely. Heavy drizzle mostly occurs within clouds that are covering high ground but radar imagery often underestimates drizzle intensity due to the 'overshooting' of the beam (10.6).

HWF (1975), Chapter 19.7

5.9.3 Depth of cloud for precipitation

Fig. 5.15 gives a guide to the intensity of precipitation at ground level, over flat terrain, associated with different thicknesses of cloud; it thus defines criteria that distinguish precipitating from non-precipitating cloud although cloud-top temperature is not considered. It is constructed for layer clouds in which the difference in water content between the base and the top is over 1.5 g kg^{-1}. Precipitation intensity in polar air masses is likely to be enhanced by ice processes even in quite shallow clouds (about 2000 feet).

In summary:

(i) There is a high probability of precipitation from clouds with thickness >7500 feet (2250 m) with cold tops (< -10 °C).

(ii) Deep clouds with bases <3300 feet (1 km) above the 0 °C isotherm — precipitation likely, while such clouds with bases >3300 feet above the 0 °C isotherm — precipitation unlikely.

HWF (1975), Chapter 19.7

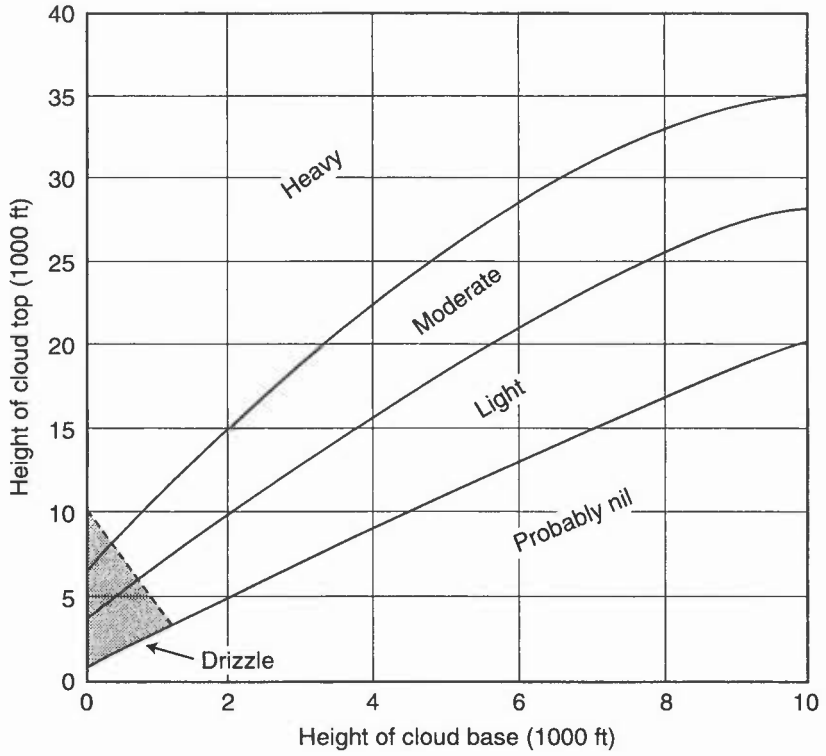

Figure 5.15. The depth of cloud related to intensity of precipitation. The stippled area indicates the conditions for the precipitation to be mainly drizzle.

Whether there is drizzle at the ground from Sc will depend on the humidity of air below cloud base and local orographic effects **(Table 5.7)**.

Table 5.7. An estimate of stratocumulus depth to produce drizzle at cloud base (taking cloud top at −5 °C)

Air mass	Minimum depth to produce drizzle at cloud base	
	(m)	(ft)
Clean maritime	500	1600
Maritime	1000	3300
Continental	2000	6600
Industrial continental	2500	8200

Bennetts et al. (1986)

5.9.4 Lowering of cloud base

(a) During continuous *rain*:
   (i) Base will be at height where temperature lapse changes from positive to less positive or to negative.
   (ii) Base will be at a height where wet bulb or dew point is a minimum.
   (iii) If rain is of sufficient duration a ceiling will occur below 2000 feet; most frequently it is a ceiling below 800 feet.
   (iv) During continuous rain a ceiling does not generally occur at the height of temperature discontinuity and/or maximum humidity until after the occurrence of a ceiling corresponding to the next higher level of temperature and/or maximum humidity.
   (v) Ceiling remains practically constant until the next lower cloud layer appears and increases in amount for its base to become the ceiling.
   Note: Ceiling is the height above ground of the base of lowest cloud layers covering more than half the sky. (Method devised for USA).

(b) In intense *showers*: the cloud base may lower rapidly by 300 m (1000 ft) or more, rising rapidly again as the shower moves on.

(c) *Falling snow*: tends to establish an isothermal lapse rate just beneath the initial 0 °C level (see 5.2.2, Fig, 5.1).

Findeisen (1940)
Goldman (1951)
HWF (1975), Chapter 19.6.2

5.9.5 Seeder and feeder clouds (SB, Fig. 5.16)

Rain, falling from upper-level cloud layers (seeder clouds), will fall through the low-level (feeder) cloud, capturing the droplets within, considerably enhancing the rainfall rate at the surface.

The degree of enhancement depends on:
(i) seeder rate >0.5 mm h^{-1};
(ii) high θ_w in low-level air;
(iii) near-saturated air upwind;
(iv) strong low level wind ahead of cold front >30 m s^{-1} at 900 m for heaviest rain;
(v) favourable topography — not too steep.

Curruthers & Choularton (1983) **Smith (1989)**
Robichaud & Austin (1988)

5.9.6 Mountain complications (SB, Fig. 5.17)

A 'bad scenario' may follow from low dew-point south-easterly air undercutting ahead of the front, giving rise to the freezing level descending to the surface, with snow at all levels.

Local Weather Manual for Scotland (1994)

5.9.7 Freezing rain from elevated layers (SB)

Ahmed et al. (1993)

5.9.8 Severe low-level icing (rain ice) (SB and Fig. 5.18)

5.10 Criteria for precipitation reaching the surface as snow or rain

5.10.1 Factors to consider (SB)

Various criteria have been derived for estimating the probability of precipitation in the United Kingdom falling as snow rather than rain. The following summary lists them in a rough order of merit; other techniques are presented.

Table 5.8.

Technique		Percentage probability of snow 90%	70%	50%	30%	10%
Adjusted value of 1000–850 hPa thickness (Boyden)	(gpm)	1281	1290	1293	1298	1303
Height of 0 °C isotherm (see Note (ii))	(hPa)	12	25	35	45	61
Surface temperature	(°C)	−0.3	1.2	1.6	2.3	3.9
1000–500 hPa thickness	(gpm)	5180	5238	5258	5292	5334

Lowndes et al. (1974)

5.10.1.1 Boyden's technique

The 1000–850 hPa thickness needs adjustment for the 1000 hPa height (H_{1000}) and the height of the ground above sea level (H_{GR}). The adjustment (m) is given by $(H_{1000} - H_{GR})/30$ and this quantity may be conveniently read off from **Fig. 5.19(a)**.

Boyden (1964)

5.10.1.2 Height of 0 °C wet-bulb temperature technique

The height of the 0 °C wet-bulb temperature additionally takes into account latent cooling effects.

Table 5.9.

Height of 0 °C wet-bulb temperature	Form of precipitation
3000 ft or over	Almost always rain; snow rare
2000–3000 ft	Mostly rain; snow unlikely
1000–2000 f	Persistent rain readily turns to snow
Below 1000 ft	Mostly snow; only light or occasional precipitation falls as rain.

Beware of cold surface air undercutting warm; Hand uses mean temperature of the lowest 100 hPa (5.10.1.3).

HWF (1975), Chapter 19.7

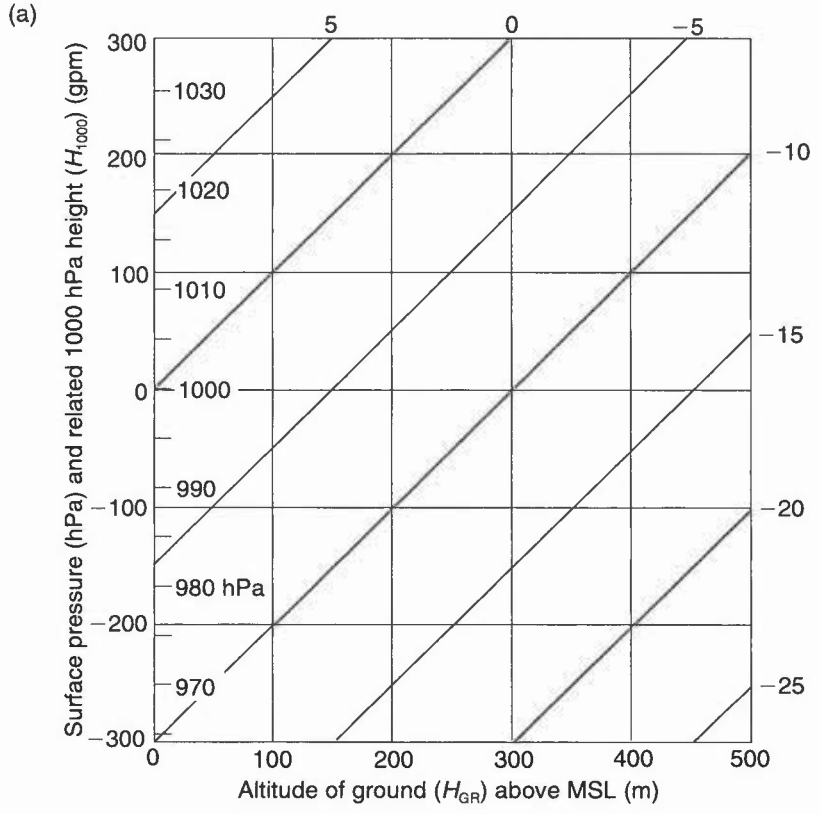

Figure 5.19(a). Forecasting the probability of precipitation as snow. This nomogram indicates the adjustment to be made to the 1000–850 hPa thickness to allow for the 1000 hPa height (or surface pressure) and altitude of ground above sea-level.

5.10.1.3 Hand's rule

Table 5.10. Use of mean temperature of lowest 100 hPa above ground to predict type of precipitation at the surface.

Mean temperature (°C) in lowest 100 hPa above surface	Precipitation type usually reaching surface
<-1.5	snow
-1.5 to 0.5	sleet
>0.5	rain

In heavy and persistent precipitation lowest layers will be further cooled by latent heat of evaporation.

Hand (1986)

5.10.1.4 Initial wet-bulb potential temperature level technique

Initial wet-bulb temperatures at which snow is likely for prolonged frontal precipitation are given in **Table 5.11**; the influence of frequent heavy showers/cold downdraughts can turn precipitation to snow with higher initial temperatures than from frontal precipitation.

Table 5.11. The relationship between downward penetration of snow beneath the 0 °C level and the initial wet-bulb temperature.

Type of precipitation	Initial wet-bulb temperature level (°C)	
	to which snow will descend	below which snow is unlikely
Prolonged frontal	+2.0 °C	+2.5 °C
Extensive moderate or heavy instability	+3.0 °C	+3.5 °C

HWF (1975), Chapter 19.7.6.1

5.10.1.5 Screen wet-bulb temperature technique (Lumb)

For an exposed station at height H (in hundreds of metres) in central and western regions of the UK under moderate easterly, or stronger, winds:

(i) for elevations up to 170 m:
Rain turns to melting snow if: $T_w<(2.1 - 0.6H)$ °C
Rain turns to lying snow if: $T_w<(0.6H)$ °C
where T_w is surface wet-bulb temperature when precipitation begins.
(ii) for elevations 170 to 350 m:
Snow probable if: $T_w<(2.1 - 0.6H)$ °C.
(iii) If $T_w>2.5$ °C rain is more likely than sleet, irrespective of elevation.

Winds should be at least moderate with a good cover of low- or medium-level cloud.

The method is summarized in **Fig. 5.20**.

Lumb (1986)

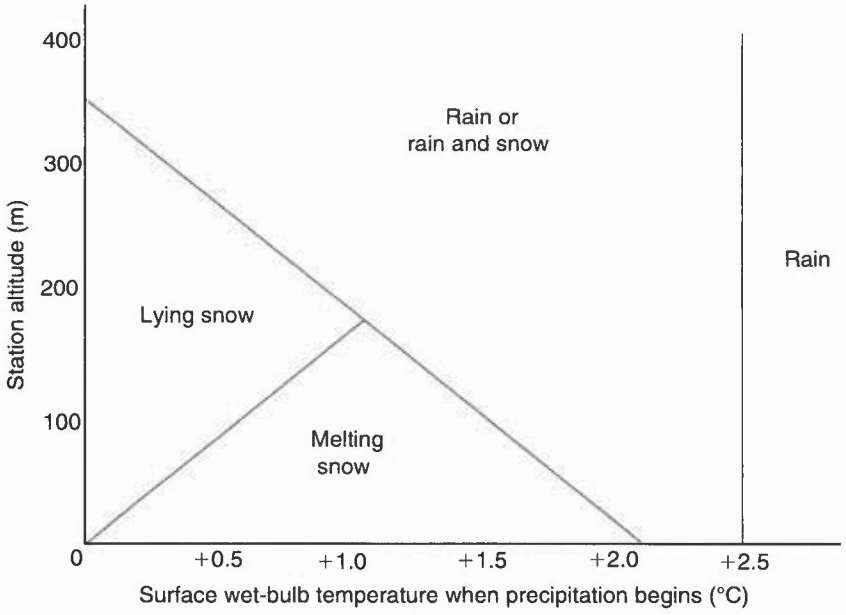

Figure 5.20. Diagrammatic form of Lumb's method for snow prediction.

5.10.1.6 Booth's snow predictor

A simple, well tried snow predictor index, I_s, is based on the relationship: $T_w \approx (T + T_d)/2$ and I_s is defined as: $T + T_d$. The predictor can be plotted on a surface chart to show the most likely areas of rain, snow or rain turning to snow according to the **Table 5.12**:

Table 5.12.

Precipitation expected			I_s
Light intensity:	(i)	probably rain if:	≥ 2
	(ii)	probably snow if:	≤ 0
If continuous moderate or heavy precipitation is expected: (if there is no warm advection at or near the surface).			≤ 7

Rain may also turn to snow over areas into which colder air with $I_s \leq 7$ is advected.

Booth (1973)

5.10.1.7 Varley snow predictor

This predictor has proven skill in forecasting the lowest level at which moderate or heavy snow (frontal or convective) will fall in the SW Midlands–South Wales area. It is used for the lowest 2000 feet (610 m) and assumes:

$T_D \approx (T + T_d)/2$ and lapse rate near the surface $\approx$ 2 °C per 1000 ft.
The height of the melting layer above the station in terms of T and T_D is:

$$250 \times (T + T_D - 4\ °C) \text{ feet} \qquad [\text{or } 76 \times (T + T_D - 4\ °C) \text{ metres}]$$

or, in terms of T and T_d: $[(T + T_d)/2 - 2]/2$ in thousands of feet
where T is the surface dry bulb, T_d the surface dew-point temperature and T_D the surface wet-bulb temperature. If, for example, $T + T_d$ in rain at a station at 20 feet is 8 °C, then at a site at 1000 feet it is likely to be snowing.

Table 5.13. An at-a-glance estimate of the melting height in terms of T and T_d

$T + T_d$ (°C)	4	5	6	7	8	9	10	11	12
Melting height (ft)	surface	250	500	750	1000	1250	1500	1750	2000

5.11 Snow

5.11.1 Synoptic situations for snow in the United Kingdom (SB, Fig. 5.20)

Fig. 5.21 illustrate the annual incidence of days with snow (a) falling, and (b) lying.

Chandler & Gregory (1976)
Wild et al. (1996)

5.11.2 Lying snow

Large amounts of lying snow will greatly distort temperature-level structure, lowering the natural condensation level, the cloud base and increasing hill fog.

Local Weather Manual — Scotland (1994)

5.11.3 Snow over high ground

The 80%, 50% and 20% snow probability lines on numerical model forecast charts are based on forecast 1000–850 hPa thickness values and refer to mean sea level. The graph **(Fig. 5.22)** has been prepared to help forecasters to adjust these values in order to estimate the probability of snow at higher levels. Thus a snow probability forecast of 20% at mean sea level from the grid-point output of a numerical model becomes 50% at 500 ft (150 m) (e.g. most of the Marlborough Downs and the Cotswolds) and over 70% at 1000 ft (300 m).

5.11.4 Drifting of snow

With the temperature below 0 °C, drifting of dry/loose snow starts when the wind speed exceeds 12 kn. Serious drifting occurs with winds above 17 kn.

A *blizzard* is defined by the UKMO as 'the simultaneous occurrence of moderate or heavy snowfall with winds of at least force 7, causing drifting snow and reduction of visibility to 200 m or less'

Met. Glossary (1991)

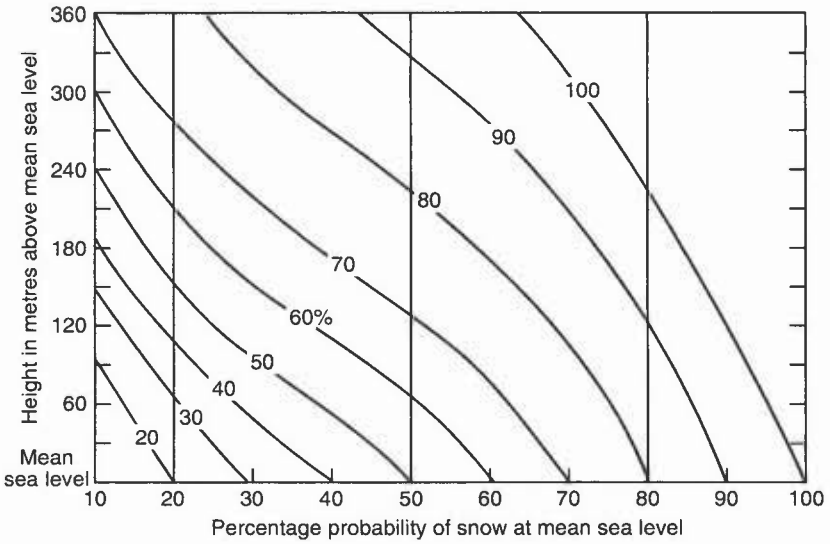

Figure 5.22. Snowfall over high ground. The increased probability of precipitation falling as snow over high ground, given its probability of occurrence at mean sea level.

5.11.5 Visibility in snow (see 3.10)

5.11.6 Thawing of snow

(i) Generally warm rain is the most effective agent for removing snow in winter since screen temperatures will not rise much above 0 °C over extensive areas of snow.

(ii) Insolation is most effective in other seasons, although it will have a negligible effect in hollows and north-facing slopes.

(iii) A depth of 150 mm (6 in) of snow requires either a continuous mild environment for several days or about 25 mm of rain to dispel it.

(iv) Since the advancing air will be cooled, thawing is less away from the windward edge of the snow cover.

(v) A screen temperature of 3 °C thaws 25 mm of snow in 24 hours, but if this warm air invasion is combined with appreciable rain, then 50 to 100 mm of snow thaws over the same period.

HWF (1975), Chapter 19.7.7

BIBLIOGRAPHY

CHAPTER 5 — LAYER CLOUDS & PRECIPITATION

Aerodrome Weather Diagrams and Characteristics (AWDC), 1960: Meteorological Office, London, HMSO (Also Airfield Weather Diagrams, Met.O.564).

Ahmed, M., Graham, R.J. and Lunnon, R.W., 1993: Creating a global climatology of freezing rain using numerical model output. *In* Proceedings of the Fifth Conference on Aviation Weather Systems. American Meteorological Society, Vienna (Virginia), USA.

Alexander, L.L., 1964: Tidal effects on the dissipation of haar. *Meteorol Mag*, **93**, 379–380.

Appleman, H.S., 1953: The formation of exhaust condensation trails by jet aircraft. *Bull Am Meteorol Soc*, **34**, 14–20.

Bennetts, D.A., McCallum, E., Nicholls, S. and Grant, J.R., 1986: Stratocumulus: an introductory account. *Meteorol Mag,* **115**, 65–76.

Booth, B.J., 1973: A simplified snow predictor. *Meteorol Mag,* **102**, 330–340.

Boyden, C.J., 1964: A comparison of snow predictors. *Meteorol Mag,* **93,** 353–365.

Browning, K.A., Hill, F.F and Pardoe, C.W., 1974: Structure and mechanism of precipitation and the effect of orography in a wintertime warm sector. *QJR Meteorol Soc,* **109**, 309–330.

Browning, K.A., Pardoe, C.W. and Hill, F.F., 1975: The nature of orographic rain at wintertime cold fronts: *QJR Meteorol Soc,* **101**, 333–352.

Browning, K.A., 1985: Conceptual models of precipitation systems. *Meteorol Mag*, **114**, 293–318.

Carruthers, D.J. and Choularton, T.W., 1983: A model of the seeder-feeder mechanism of orographic rain including stratification and wind-drift effects. *QJR Meteorol Soc,* **109**, 575–588.

Chandler, T.J. and Gregory, S., 1976: The Climate of the British Isles, Longman.

Ferris, P.D., 1996: The formation and forecasting of condensation trails behind modern aircraft. *Meteorol Appl*, **3**, (to be published).

Findeisen, W., 1940: Die Entstehung der 0 °C-Isothermie und Fraktocumulus-Bildung unter Nimbostratus. *Meteorol Z.*, **57**, p. 49.

Goldman, L, 1951: On forecasting ceiling lowering during continuous rain. *Mon Weather Rev*, **79**, 133–142.

Hand, W., communication in: Davies, T. and Hammon, O.M., 1986: Snow forecasting from the Meteorological Office fine-mesh model during the winter of 1985/86. *Meteorol Mag*, **115**, 396–404.

Handbook of Aviation Meteorology (3rd edition), 1994: London, HMSO.

James, D.G., 1957: Forecasting cirrus cloud over the British Isles. *Prof Notes*, Meteorological Office, **8**, 123.

James, D.G., 1959: Observations from aircraft of temperatures and humidities near stratocumulus clouds. *QJR Meteorol Soc*, **85**, 120–130.

Kraus, E., 1943: Some contributions to the physics of non-frontal layer clouds. *SDTM* No. 67 (Meteorological Office, London, Unpublished).

Lamb, H.H., 1945: Haars or North Sea fogs on the coast of Great Britain. Meteorological Office report (M.O.504).

Local Weather Manual — Scotland, 1994: Meteorological Office.

Lowndes, C.A.S., Beynon, A. and Hawson, C.L., 1974: An assessment of some snow predictors, *Meteorol Mag*, **103**, 341–358.

Lumb, F.E., 1986: Local snow forecasting. *Weather*, **41**, 29–30.

Mansfield, D.A., 1988: An investigation into stratus distribution over the UK. *Meteorol Mag*, **117**, 236–245.

Robichaud, A.I. and Austin, G.L., 1988: On the modelling of warm orographic rain by the seeder-feeder mechanism. *QJR Meteorol Soc*, **114**, 967–988.

Smith, R.B., 1989: Mechanisms of orographic precipitation. *Meteorol Mag*, **118**, 85–88.

Sparks, W.R., 1962: The spread of low stratus from the North Sea across East Anglia. *Meteorol Mag*, **91**, 361–365.

Warne, D.V., 1993: Stratus forecasting. *Meteorol Mag*, **122**, 113–116.

Wild, R., O'Hare, G. and Wilby, R., 1996: A historical record of blizzards/major snow events in the British Isles, 1880–1989. *Weather*, **51**, 82–91.

6.1 Turbulence in the free atmosphere

The sources are deep convection, wave motion and clear air turbulence (CAT).

6.1.1 Turbulence due to convection

This occurs at the boundaries of vertical convective currents:

(i) in cloud; cumulonimbus clouds can extend above 40,000 ft (12,200 m) in the United Kingdom, and above 60,000 ft (18,300 m) in the USA and some tropical areas;

(ii) outside cumulonimbus clouds, especially in clear air around the anvil and just above a storm top;

(iii) in dry thermals below cloud base, or in a cloudless region over any heated land mass (over deserts, dry convection may extend up to 15,000–20,000 ft (4600–6100 m)).

The magnitude of typical vertical currents in convective clouds, based on aircraft reports, are (**Table 6.1**):

Table 6.1.

Regime	Vertical velocity ($m\ s^{-1}$)	Description of turbulence
Stratocumulus		Light/moderate, occasionally severe over rugged terrain or due to instability
Altocumulus		Light/moderate, occasionally severe in unstable medium-level layers
Cumulus (humilis/mediocris)	1–3	Light
Cumulus (congestus)	3–10	Moderate
Cumulonimbus	10–25	Severe
Severe storm (USA)	>>25	Extreme
Dry thermals	1–5	Light/Moderate
Downdraughts	3–15	Moderate/Severe
Downdraughts (USA)	up to 40	Extreme

6.1.2 Wave-induced turbulence

Both *trapped* and *untrapped* waves may induce turbulence (see 1.3.2.1). Although both types are characterized by smooth, laminar flow, severe turbulence is often associated with convective instability or shearing instability of these waves. Turbulence due to mountain waves will be found:

(i) throughout middle and lower troposphere in the lee of a mountain range experiencing a severe downslope windstorm;

(ii) above the main tropospheric jet during conditions of strong mountain flow (with little change of wind vector with height);

(iii) at an elevated layer of very light winds (or flow reversal) when surface flow is strong and stably stratified;
(iv) in a layer of strong stability (or inversion) when surface flow is strong and stably stratified.

Bailey (1970) **Shutts & Broad (1993)**
Bradbury (1989) **Stull (1988)**

6.1.2.1 Inferring turbulent areas from imagery

High mountains with steep lee slopes may generate turbulence indicated on imagery by a narrow stationary clearing of jet cirrus to the lee **(SB, Fig. 6.1(a))**; this will contrast with the cloud pattern with turbulence absent (**SB**, **Fig. 6.1(b)**).

Bader et al. (1995), Chapter 8

6.1.3 Clear Air Turbulence (CAT)

Although this term can refer to any turbulence not associated with cloud, it is usually applied only to medium- and high-level disturbances.

Table 6.2(a). Typical dimensions of regions within which CAT may be encountered

Horizontally:	80–500 km (50–300 miles) along the wind direction, but only 20–100 km (12–60 miles) across the wind flow.
Vertically:	500–1000 m (1600–3300 ft), but they may be as shallow as 25 m (80 ft), or as deep as 4500 m (15,000 ft) near mountains.

Mean duration of CAT encounters experienced by jet transport aircraft in flight **(SB, Table 6.2(b)).**

Conditions for unusually prolonged, intense CAT are noted in *Empirical prediction of CAT* (6.1.3.2(iv)).

6.1.3.1 Synoptic indicators of CAT

Marked (horizontal and vertical) wind shear **(SB)**

Jet streams

About 60% of CAT reports are near jet streams. The most probable regions are those where rapid changes or development are occurring. They are illustrated in **Fig. 6.2(a)**. Not illustrated are where one jet undercuts another; where the tropopause height fluctuates.

Moderate/severe CAT is often associated with certain cirrus (Ci) boundaries and cloud patterns which identify jet streams accompanied by strong temperature gradients, shears, deformation, atmospheric waves and instability. Turbulence is usually within 3° latitude of the cloud or moisture edge. Transverse Ci bands, Ci 'scallops' and billows may indicate CAT at jet aircraft cruising level **(SB, Fig. 6.2(b))**.

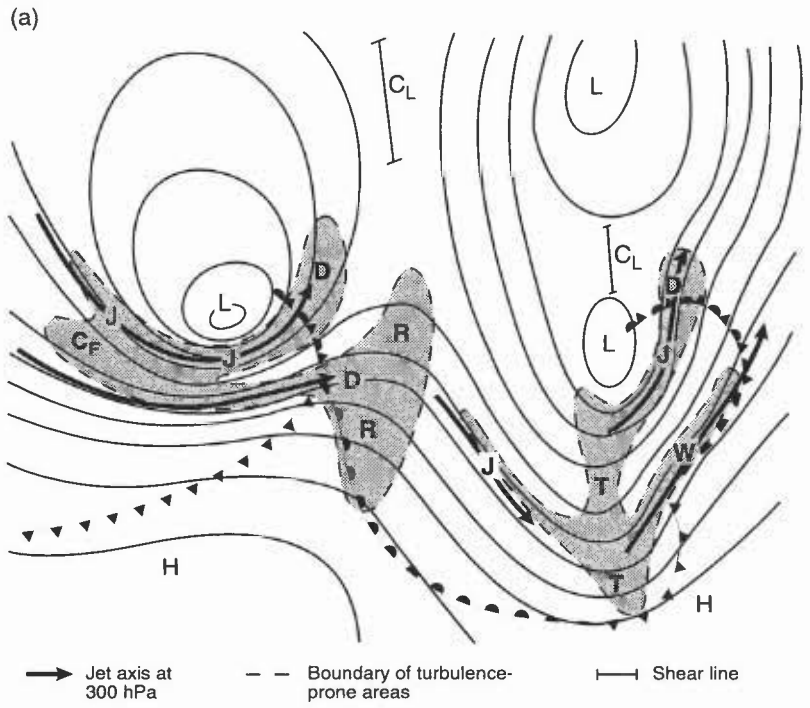

Figure 6.2(a). Main turbulence-prone areas between 500 and 200 hPa as related to features of the 300 hPa chart.

—	300 hPa contours. Fronts marked are at surface.
C_F	Region of confluence between two jet streams.
C_L	Upper-air col. Turbulence occurs in narrow bands along marked shear line.
D	Diffluent region of jet stream.
J	Jet-stream turbulence on low-pressure side.
R	Developing upper ridge.
T	Sharp upper trough.
W	Developing wave depression.

Curved flow

(i) In areas of anticyclonic curvature, where the actual wind speed approaches the critical value of twice the geostrophic wind speed.

(ii) Within 150 n mile or so of the axis of a sharp upper trough where the wind shift is over 90°.

(iii) Occasionally, across shear lines in cols where the wind direction reverses rapidly.

Turbulence in deformation zones is often associated with a transverse banding signature in Ci (**SB, Fig. 6.2(c)**); delta- and comma-shaped clouds are a reliable indicator of moderate or severe turbulence (particularly as the comma system transforms into a vortex).

Thermal gradients
Cloud edges may provide clues as to thickness gradients; near a ridge axis transverse bands (Ci streamers indicate a turbulence area **(SB, Fig. 6.2(d))**.

Topography
CAT is reported twice as often over land as over the sea, and is possibly times more frequent over mountains as over flat land.

Bader et al. (1995), Chapter 3
Ellrod, 1990
Hisscott, 1986
Sparks et al. (1976)
WMO (1977)

6.1.3.2 Empirical prediction of CAT

Useful empirical rules are:

(i) Horizontal wind shear:
If shear $\geq$20 kn deg^{-1} of latitude, forecast moderate CAT
If shear $\geq$30 kn deg^{-1} of latitude, forecast severe CAT.

(ii) Vertical wind shear:
If shear $\geq$6 kn/1000 ft, forecast moderate CAT
If shear $\geq$9 kn/1000 ft, forecast severe CAT

(iii) Jet streams:
If the core speed exceeds 100 kn, and vertical wind shear 4 kn/1000 ft, forecast moderate CAT within 150 n mile.

(iv) An unusually persistent and extensive incidence of moderate to severe CAT reported over the UK in September 1985, was associated with diffluence and anticyclonic turning below a warm-frontal zone.

(v) CAT is rare above a well-defined tropopause.

CAT probability forecasts are available from numerical prediction model output.

Hisscott, 1986
WMO, 1977

6.1.4 Intensity of turbulence and aircraft response (SB, Table 6.3)

Individual aircraft will experience different effects, depending on their track, speed, flown profile and physical characteristics.

CAA (1991, 1992)
HAM (1994), Chapter 12.3
HWF (1975), Chapter *23.3*

6.2 Turbulence near the surface

The sources will be frictional and orographic; there will also be effects due to deep convection and severe storms. Forecasts required will depend on what is at risk and the nature of the wind /gust hazard.

Hunt (1995)

6.2.1 Turbulence, gusts and squalls (SB)

(i) As a rough guide: the intensity of turbulence expected in the lowest few hundred feet in windy conditions increases as surface roughness increases.
(ii) Strong sunshine added to strong wind may increase the difficulties of controlling aircraft, especially on landing and take-off.

Violent turbulence creates a most dangerous low-level hazard to aircraft. It may occur:
(i) during or preceding the passage of an active cold front;
(ii) during or preceding a thunderstorm;
(iii) in hilly or mountainous country (1.3.2, 1.3.3);
(iv) with a steep lapse rate.

Cashmore, 1966 **HAM, 1994**
Förchtgott, 1949 **Klemp, 1978**

6.2.1.1 Criteria for forecasts of hazardous low-level wind shear/turbulence

One or more of the following to be satisfied:
(i) Mean surface wind ≥20 kn.
(ii) Magnitude of vector difference between mean surface wind and the gradient (2000 ft) wind ≥40 kn.
(iii) Thunderstorms or heavy showers within 10 km.
(iv) Significant wind shear has already been reported by aircraft in the vicinity.

MO, Heathrow(198?)

6.2.1.2 Effect of turbulence, lapse rate and wind shear

Criteria for forecasting low-level wind shears likely to hazard aircraft are in 6.2.1.1.

6.2.2 Gusts

Empirical and theoretical procedures have produced estimates for 'gust ratios' and gusts which are defined both in terms of the mean hourly wind, and relative to the gradient wind.

Table 6.4(a). Ratio of maximum (3-second) gust to mean hourly speed (for strong, steady 10 m winds)

Surface type	Range of ratios	Estimated average
Open sea	1.3	1.3
Isolated hill tops	1.4–1.5	1.4
Flat open country	1.4–1.8	1.6
*Rolling country (few wind-breaks)	1.5–2.0	1.7
Rolling country (numerous wind-breaks), forest areas, towns, outskirts of large cities	1.7–2.1	1.9
Centres of large cities	1.9–2.3	2.1

*Local variations, using this commonly used category, often give gusts varying widely in space and time from the estimated values, making airfield forecasting difficult, especially under isallobaric surging.

Table 6.4(b). Maximum wind speeds relative to the gradient wind, V_{grad}, in neutral conditions

	V_{grad}		
	units: m s^{-1} (kn)		
Surface type	10 (19)	20 (39)	30 (58)
Open sea	8.8 (17.0)	17.0 (33.1)	24.9 (48.1)
Flat open country	7.8 (14.8)	15.0 (27.3)	21.6 (41.8)
Rolling country (few wind-breaks)	7.1 (13.5)	13.4 (26.1)	19.5 (37.7)
Rolling country (numerous wind-breaks) forest areas, towns, outskirts of large cities	6.8 (12.9)	12.8 (25.0)	18.3 (35.4)
Centres of large cities	6.4 (12.1)	12.0 (23.4)	17.4 (33.6)

Maximum wind speed V_{max} is here defined statistically as: the mean wind speed V_{mean}, plus the fluctuating component in the direction of the mean wind speed (3 times the standard deviation).

These tables may be combined to give an estimate of the mean wind and the ratio of max/mean wind over different surfaces in neutral conditions in terms of the gradient wind **(Table 6.4(c))**.

Table 6.4(c). Estimate of the mean wind and the ratio max/mean wind over different surfaces in neutral conditions in terms of the gradient wind

	V_{grad}			
	units: m s^{-1} (kn)			
Surface type	10 (19)	20 (39)	30 (58)	V_{max}/V_{mean}
Open sea	6.8 (13.2)	13.1 (25.4)	19.2 (37.2)	1.3
Flat open country	4.9 (9.5)	9.4 (18.2)	13.5 (26.2)	1.6
Rolling country (few wind-breaks)	4.2 (8.1)	7.9 (15.3)	11.5 (22.3)	1.7
Rolling country (numerous wind-breaks) forest areas, towns, outskirts of large cities	3.6 (7.0)	6.7 (13.0)	9.6 (18.6)	1.9
Centres of large cities	3.0 (5.8)	5.7 (11.1)	8.3 (16.1)	2.1

Bradbury et al. (1994)
HWF (1975), Chapter 16.7.1

6.2.2.1 Gusts over hills

Limited UK observations suggest that the structure of the flow over hills associated with strong, steady winds is similar to that over flat terrain, the difference between hilly and flat terrain being the magnitude of the roughness length. The gust factor appears almost independent of hill height for hills greater than 100 m. Assuming a wavelength of hills to be 1.5 km (e.g. gust ratios representative of the Welsh hills), the geostrophic gust ratio at hill height is estimated as about 0.75.

6.2.2.2 Rotor streaming

Associated with large amplitude *trapped lee waves* and *severe downslope winds* (1.3.3.4):

(i) Surface winds often fluctuate between low and high values. The effect is considered not to extend more than 15 n mile downwind (**Fig. 6.3**).

(ii) The vertical wind/temperature profiles associated with rotor streaming are of the form:
strong winds (over 25 kn) near the ground;
a sharp decrease in wind speed, which may be accompanied by a large change in direction, at a height of 1.5 to 2 times the height of the hills;
an inversion within 1000–3000 feet of the hill tops.

Some severe cases of turbulence affecting airfields (e.g. in NW Wales) may be due to 'rotor streaming'. Initially there is a marked upwind acceleration over the hill/ridge top to 1.5 to 2 times gradient speed; speeds of some 70 kn have been encountered by helicopters. Dark lee areas in water vapour imagery can indicate the presence of hazardous, downslope surface winds.

Bader et al. (1995) Chapter 8
Bradbury (1989)
Förchtgott (1949)
Stull (1988)

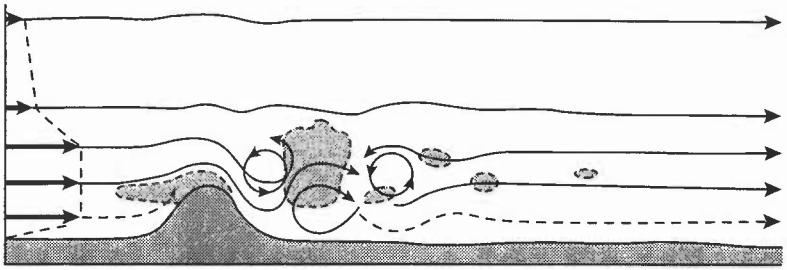

Figure 6.3. Rotor streaming (after Förchtgott). The vertical profile of the wind is shown by the bold arrows on the left.

6.2.2.3 Gust forecasting in strong wind situations

The gales that disrupted the 1979 Fastnet Yacht Race, and the Burns' Day storm of 1990 are examples of convection occurring in the presence of strong geostrophic winds in a mid-latitude depression. Damaging winds also occur in association with thunderstorms in such depressions. Convectively generated gusts in both cases are produced by two mechanisms:

(a) the production of horizontal momentum by pressure gradient forces as convective downdraughts are blocked by the surface and spread out horizontally,

(b) the downward transport of horizontal momentum by convective downdraughts in the presence of vertical shear.

The relative importance depends on the strengths of the vertical wind shear and the intensity of the downdraughts.

An effective approach to forecasting strong gusts is:
Are showers likely?

(i) *No*: use **Table 6.4(b)**

(ii) *Yes*: use gradient wind speed at 900 hPa as first guess of likely maximum gusts at exposed locations.
If showers are expected to be moderate or heavy, squalls (expected in association with a trough or front) or gusts might significantly exceed the gradient wind.

As a rule of thumb: $V^2_{gust} = V^2_{convection} + V^2_{gradient}$

where $V_{convection}$ is estimated using Fawbush and Miller (**Fig. 6.4**), or $V_{convection} = (gh\,\Delta T/T)^{0.5}$ and, ΔT is the surface temperature deficit in the downdraught, T the average absolute temperature and h the depth of the downdraught in metres.

A more explicit expression for the gust is given in **SB**.

Bradbury et al. (1994)
Nakamura et al. (1996)

6.2.2.4 Forecasting peak gusts in thunderstorms

The peak gust can be estimated using Fawbush and Miller, which relates gust strength to the negative buoyancy force in a downdraught. It is thus based mainly on the first mechanism ((a) in 6.2.2.3) (although, by its empirical nature, Fawbush and Miller may encompass elements of the second process).

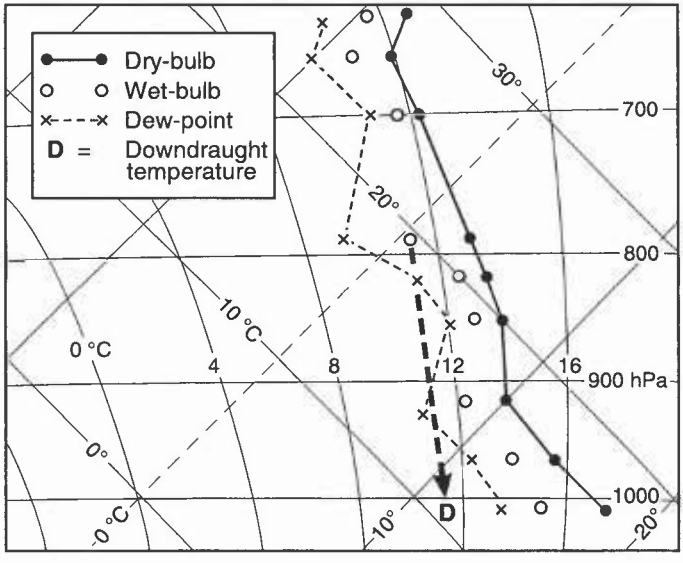

Figure 6.4. Example of a tephigram, illustrating the computation of the downdraught temperature in non-frontal thunderstorms in the USA (after Fawbush and Miller).

Procedure, in particular for summer thunderstorms when the downdraught originates near the wet-bulb freezing level (i.e. melting point for precipitation), is as follows:

(i) Peak wind speeds depend largely on the temperature difference between this cooler downdraught air and the surrounding warmer air at the surface.

(ii) Downdraught temperature may be estimated from an upper-air sounding by drawing a saturated adiabat from the level where the wet-bulb curve cuts the 0 °C isotherm to the surface pressure. **Fig. 6.4** illustrates the construction on a tephigram. **Fig. 6.5** shows the relationship between the temperature difference and the peak wind speed. A correlation coefficient of 0.86 was found in the USA (for non-frontal thunderstorms).

In wintry conditions the downdraught may originate well above the freezing level, being driven by the evaporation of snow or graupel. Such thunderstorms are usually associated with a front or trough in a depression, in which case the gust forecasting technique in the previous section is recommended.

Nakamura et al. (1996)
Fawbush & Miller (1954)

6.2.2.5 Wind-direction changes associated with gusts

Although there is widespread belief among, for example, yachtsmen that during a surface gust the wind may veer (in the northern hemisphere) by up to 20° to 30°, studies at Cardington and elsewhere have failed to show any significant tendency for this happening at low wind speeds likely to be encountered by yachts. However, there may be a conceptual difference here; for the yachtsman a gust has to last several minutes rather than a few seconds to be of interest.

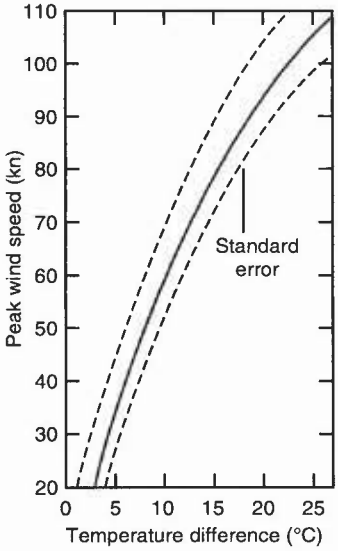

Figure 6.5. Peak wind speed at the surface related to the temperature difference between cold downdraught air and the warm surface air, during non-frontal thunderstorms in the USA.

However, severe *convective gusts* (>65 kn) occasionally occur from a substantially different direction; veers of 60° have been recorded. In high gusts of convective origin at Manston between 1980 and 1990, the mean and standard deviation veers were 40° and 65°, respectively.

Bradbury et al. (1994)
Brettle (1994, 1996)
Houghton (1984)
Singleton (1981)

6.2.3 Squalls

See 6.2.2.3; also 4.7.6.

HWF (1975), Chapter 16.7.2
Ludlam (1980)

6.2.4 Tornadoes and microbursts

6.2.4.1 Tornadoes (SB)

Tornadoes normally require:

considerable depth of convective instability;
high values of θ_w (18–23 °C) in lowest layers;
marked potential instability (θ_w falling 5 °C or more up to 500 hPa);
marked vertical wind shear with winds increasing and veering with height.

HAM (1980)
Ludlam (1980)

6.2.4.2 Microbursts (downbursts) (SB)

Strong flows associated with thunderstorm downdraughts (4.7, 6.2.2.4) pose severe risks to aircraft at take-off and landing (see 6.2.2.4, Forecasting peak gusts in thunderstorms).

Summary of indicators for thunderstorm microbursts:

Large positive CAPE.
Little or no capping inversion.
At least 1500 m of unsaturated air beneath the convective cloud base.
A moist mid-tropospheric layer between 1500 m and 4500 m above the ground.
An elevated dry layer above an altitude of 4500 m.

Bader et al. (1995), Chapter 6.5.6.5
CAA (1991)
Caracena et al. (1989)
HAM (1994)
McCarthy & Serafin, 1984
Naylor (1995)
Waters & Collier (1995)

BIBLIOGRAPHY

CHAPTER 6 — TURBULENCE AND GUSTS

Bader, M.J., Forbes, G.S., Grant, J.R., Lilley, R.B.E. and Waters, J., 1995: Images in weather forecasting. Cambridge University Press.

Bailey, M., 1970: Mountain lee-wave incidents in Scotland. *Meteorol Mag*, **99**, 110–118.

Barry, R.G., 1981: Mountain weather and climate. Methuen.

Bradbury,T., 1989: Meteorology and flight, A & C Black.

Bradbury, W.M.S., Deaves, D.M., Hunt, J.C.R., Kershaw, R., Nakamura, K. and Hardman, M.E., 1994: The importance of convective gusts. *Meteorol Appl,* **1,** 365–378.

Brettle. M.J., 1994: An investigation of possible systematic wind-direction changes associated with sudden increases in wind speed. *Meteorol Appl*, **1**, 179–183.

Brettle, M.J., 1996: Veering winds and yachting (with reply by F. Singleton). *Weather*, **51**, 320–322.

CAA, 1991: The effect of thunderstorms and associated turbulence on aircraft operations. London, Civil Aviation Authority. Aeronautical Information Circular No. 117/1991.

CAA, 1992: Low altitude wind shear, London, Civil Aviation Authority. Aeronautical Information Circular No. 48/1992.

Caracena, F., Holle, R. and Dodswell, C.A., 1989: Microbursts, a handbook for visual identification. US Dept of Commerce.

Cashmore, R.A., 1966: Severe turbulence at low levels over the United Kingdom. *Meteorol Mag*, **95**, 17–18.

Ellrod, G.P., 1990: Use of water vapour imagery to identify CAT. NOAA/NESDIS, Satellite applications information note 90/8. Washington, Dept of Commerce.

Fawbush, E.J. and Miller, R.C., 1954: A basis for forecasting peak wind gusts in non-frontal thunderstorms. *Bull Am Meteorol Soc*, **35**, 14–19.

Förchtgott, J., 1949: Wave currents on the leeward side of mountain crests. *Bull met tchecoal, Prague*, **3,** 49–51.

Handbook of Aviation Meteorology (HAM), 1994: London, HMSO.

Handbook of Weather Forecasting (HWF), 1975: Meteorological Office, Met.O.875.

Hisscott, L.A., 1986: Prolonged CAT over the British Isles on 4 September 1985. *Meteorol Mag*, **115**, 329–331.

Houghton, D., 1992: Wind strategy. Fernhurst Books.
Hunt, J.C.R., 1995: The contribution of meteorological science to wind hazard mitigation. *In* T. Wyatt (Ed), Proceedings of the Wind Engineering Society meeting on wind hazard, May 1995.

Klemp, J.B., 1978: A severe downslope windstorm and aircraft event induced by a mountain wave. *J Atmos Sci*, **35**, 59–77.

Ludlam, F.H., 1980: Clouds and storms, Pennsylvania State University Press.

McCarthy, J. and Serafin, R., 1984: The microburst: hazard to aircraft. *Weatherwise*, **37**, 120–127.

Meteorological Glossary (MG) (6th Edition), 1991: London, HMSO.

Nakamura, K., Kershaw, R. and Gait, N., 1996: Generation of near-surface gusts by deep convection. *Meteorol Appl*, **3**, (to be published).

Naylor, D.J., 1995: A probable microburst at Weston-on-the-Green on 24 July 1994. *Weather*, **50**, 278–282.

Shutts, G.J. and Broad, A., 1993: A case study of lee waves over the Lake District in northern England. *QJR Meteorol Soc*, **119**, 377–408.

Singleton, F., 1981: Weather forecasting for sailors. Hodder and Stoughton.

Sparks, W.R., Cornford, S.G. and Gibson, J.K., 1976: Bumpiness in clear air and its relation to some synoptic-scale indices. *Geophys Mem* No. 121, Meteorological Office.

Stull, R.B., 1988: An introduction to boundary layer meteorology. Kluwer Academic Publishers.

Waters, A.J. and Collier, C.G., 1995: The Farnborough storm — evidence of a microburst. *Meteorol Appl*, **2**, 221–230.

WMO, 1977: Forecasting techniques of CAT, including that associated with mountain waves. Geneva, World Meteorological Organization, Technical Note 155.

CHAPTER 11 — PROBABILITY FORECASTS

11.1 Basic concepts

Most forecasts give a categorical estimate of what various weather elements will be for a particular place/region and time/period. In reality uncertainty is inherent because:
(i) Observations do not provide a complete description of the state of the atmosphere.
(ii) Numerical models do not completely represent atmospheric processes (9.1).
(iii) Various assumptions are made in deriving expected weather from model forecasts.

The uncertainty can be implied by using such words as 'perhaps' (with the wide variations in meaning which can be attached to them) or expressed either qualitatively or quantitatively.

Probability forecasts are becoming more widely used because:
(i) They provide quantitative information for customers in uncertain situations.
(ii) They express inherent uncertainty in a precise and unambiguous manner.

11.1.1 Interpretation of probabilities

Probabilities can be interpreted in two ways:
(i) Relative frequency interpretation.
(ii) Subjective interpretation.

Thus consider a 'probability of precipitation (PoP) forecast of 30%':
(i) Relative interpretation: the present meteorological situation, observed on a large number of occasions, would give rise to precipitation on 30% of the time.
(ii) Subjective interpretation: the forecaster's judgement is that the odds against precipitation are 7 to 3 (odds against no precipitation being 3 to 7). Generally, if p is the probability, the odds against the event are:
$$(1/p - 1) \text{ to } 1.$$
(iii) The subjective interpretation gives a practical way of thinking about probabilities.

11.2 Types of probability measure

Three types of probability are in use:
(i) *Point probability*: probability that an event will occur at a particular point within a specified period of time.
(ii) *Average point probability*: the average point probability over a defined area.
(iii) *Area probability*: probability that the event will occur somewhere in the defined area within a specified period.

Point probability is easiest for interpretation and verification; average point probabilities, sometimes used for large areas by the media, can be misleading if there is a wide variation of point probability across the area.

The *area probability*, P_a, and *average point probability*, P_p, are related:
$$P_p = P_a \, a_c$$
where a_c is the proportion of the areal coverage if precipitation does occur.

(i) Note: $P_a \geq P_p$; and when precipitation is certain ($P_a = 1$), then $P_p = a_c$, i.e. the expected areal coverage of precipitation.

(ii) This area probability concept, P_a, can be very helpful when deriving P_p. Thus, if there is a 20% chance of precipitation reaching an area, $P_a = 0.2$, but if it does reach the area there will be precipitation everywhere (so that $a_c = 1$), then the average point probability, P_p, is 20%.

(iii) Similarly, if showers are certain in an area, $P_a = 1$, but if they do occur they will be scattered ($a_c = 0.2$ say), then again $P_p = 20\%$.

Conditional probabilities must be correctly identified and used.

(i) For example, if P(precip) is the probability of precipitation and P(precip|snow) is the conditional probability of snow (the probability of snow if precipitation occurs), then the probability of snow is given by:

$$P(\text{snow}) = P(\text{precip})\, P(\text{precip|snow}).$$

(ii) The difference between P(snow) and P(precip|snow) is important; it is essential that the user knows which figure is being given.

11.3 Practical considerations

11.3.1 Determination of probabilities

Successful determination of probabilities depends upon the skill and experience of the forecaster. A few general points worth considering are given:

(i) Discussion between forecasters about probabilities is likely to be beneficial.

(ii) It may be useful to assess area probability of precipitation and conditional areal coverage separately before combining them to give the average point probability.

(iii) Although forecasters are likely to start with central guidance, in principle it is beneficial to make an independent assessment and then try to reconcile this with the guidance. In practice, there may not be sufficient time available to do this.

(iv) Most effort should be put into improving on the guidance for the early forecast period; later the value of local knowledge decreases rapidly.

11.3.2 Time period

A probability forecast must refer to a particular period. However, there are some pitfalls that must be avoided, as illustrated with the PoP forecasts:

(i) PoP can change discontinuously between periods so a continuous change should not be implied. Thus '80% chance of rain this evening *but only* a 30% chance tonight' is preferable to '80% chance of rain this evening *decreasing to* a 30% chance tonight'.

(ii) Periods should not be combined. Thus, '30% chance of rain today and tonight' is ambiguous. Does the 30% refer to each period separately or to them combined?

(iii) Do not use terms that leave the time period unclear, e.g. '20% chance of rain *by* this evening'.

(iv) Avoid using a period unhelpful or ambiguous to the user, e,g. 'late this evening'.

11.3.3 Incorporating probabilities into forecasts

The following are general guidelines for probability forecasts, especially PoP forecasts, to the general public (although not necessarily applicable to specialized services):

(i) Use 'chance' rather than 'probability' and avoid reference to 'threat of' or 'risk of'.

(ii) Give only one probability for each location. Thus '10% chance of showers this morning and a 60% chance of rain this evening' is to be avoided.
(iii) Do not combine probabilities about extent and duration. Thus, '30% of scattered showers' or '40% chance of occasional rain' should be avoided.
(iv) It is important that it is clear about the type of 'precipitation' to be expected.
(v) PoP should separate different types of precipitation, e.g. 'occasional rain with the possibility of an afternoon thunderstorm. 70% chance of rain'.
(vi) When a change of precipitation type is forecast, the PoP should refer to the chance of precipitation not the chance of the type changing, e.g. 'rain, possibly turning to snow this afternoon. 70% chance of precipitation'. Statements such as: '70% chance of rain turning to snow' should *not* be used.

11.3.4 Improving probability forecasts

Effective and timely feedback from a verification scheme can increase the reliability of probability forecasts. Common problems that arise when making probability forecasts are:
(i) Over-confidence, excessive use being made of very high/low probabilities.
(ii) Probabilities are not changed when a forecast is updated or even when developing as expected.
(iii) Range of probabilities available for a fixed period decreases with the length of the forecast. 100% PoP might be reasonable for day 1 of a forecast, but not for day 5.
(iv) Some probabilities are over- or under-used.
(v) There is a tendency to over-forecast probabilities for relatively infrequent events.

Reliability of forecasts (11.4.2.1) can be improved by identifying and remedying these problems. However, accuracy must not be compromised by artificially using 'under used' probabilities.

11.3.4.1 Characteristics of a reliable probability forecast

A reliable probability forecast is characterized by the following:
(i) When an event is infrequent at a particular location the probabilities tend to be lower than at locations where the event is frequent.
(ii) Probabilities tend to be lower the shorter the length of the period.
(iii) Probabilities tend to be less extreme as the lead time to the forecast period increases. For large lead times the range of probabilities reduces to the climatological frequency.

11.4 Verification and display (SB)

11.4.1 Characteristics

The three characteristics of the verification process that are useful to assess are:
(i) Reliability.
(ii) Accuracy.
(iii) Skill.

(Another useful characteristic is 'factorization', discussed in 11.6).

In considering any summary measures from the verification scheme, it is important that the basic data are examined and displayed **(SB)**.

11.5 Making comparisons (SB)

11.6 Factorization (SB)

11.7 Ensemble forecasting and predictability (SB)

Molteni, et al. (1996)

BIBLIOGRAPHY

CHAPTER 11 — PROBABILITY FORECASTS

Gordon, N., 1993: Verification of terminal forecasts. Am Meteorol Soc, Conference on Aviation Meteorology, Vienna (Virginia), USA.

Halsey, N.G.J., 1995: Setting verification targets for minimum road temperature forecasts. *Meteorol Appl*, **2**, 193–197.

Molteni, F., Buizza, R, Palmer, T.N. and Petroliagis, T., 1996: *QJR Meteorol Soc*, **122**, 73–119.

Murphy, A.H. and Katz, R.H., 1985: Probability, statistics and decision making in the atmospheric sciences. Westview Press (Boulder, Colorado).

Stanski, H.R., Wilson, L.J. and Burrows, W.R., 1989: Survey of Common Verification Methods in Meteorology. WMO. World Weather Watch Technical Report No. 8.

Wilks, D.S., 1995: Statistical methods in the atmospheric sciences. San Diego, Academic Press.

CHAPTER 13 — SEA WAVES AND SURGES

13.1 Sea waves and swell

See **SB** Annex for Terminology.

13.1.1 Forecasting wind-wave heights and periods (SB)

13.1.1.1 Waves in deep water (WMO nomogram)

(i) For given values of wind speed and fetch, **Fig. 13.1(a)** may be used to forecast the Significant Wave Height and **Fig. 13.1(b)** the corresponding Wave Period.

(ii) The dashed lines indicate the duration in hours after which the waves will attain the computed state. If the duration is limited, the waves will not develop beyond the point given by the intersection of the wind speed and the duration on the graph.

Golding (1983) **Holt (1994)**

13.1.1.2 Waves in shallow waters (Darbyshire–Draper graphs)

Fig. 13.2 is suitable for forecasting waves in shallow coastal waters and in the southern North Sea. The layout and use of the graphs are the same as **Fig. 13.1**.

Darbyshire & Draper (1963)

13.1.2 Wave conditions at the shoreline; refraction (SB)

(a) As a wave approaches a beach its height increases and the wave breaks, how and when depending on the beach steepness, wind and other factors **(SB, Fig. 13.3)**.

(b) Wave period is similar to that in the open sea, but can be significantly altered on passing through a zone of breaking waves (e.g. over an offshore sand-bar). Longer-period waves, which may seem insignificant off shore, may become the most prominent waves on breaking.

(c) Waves may be refracted by variations in water depth and by current gradients

There are PC-based techniques for transferring near-shore model forecasts to the beach zone. Details of forecasting the effects of tides and currents and surf etc. are in the DNOM Memorandum referenced.

DNOM (1984)
Sanderson (1982)
Shore Protection Manual (1984)

13.1.3 Forecasting swell heights and periods

(a) The difficult task of forecasting in detail the range of wave heights and periods spreading out from a distant storm (which is both moving and developing in strength) is reduced by the practical limitations of the known data. These normally comprise little more than the distance of the storm, the maximum wave period generated in the storm area and the duration of wave generation in the direction from the storm to the forecast location.

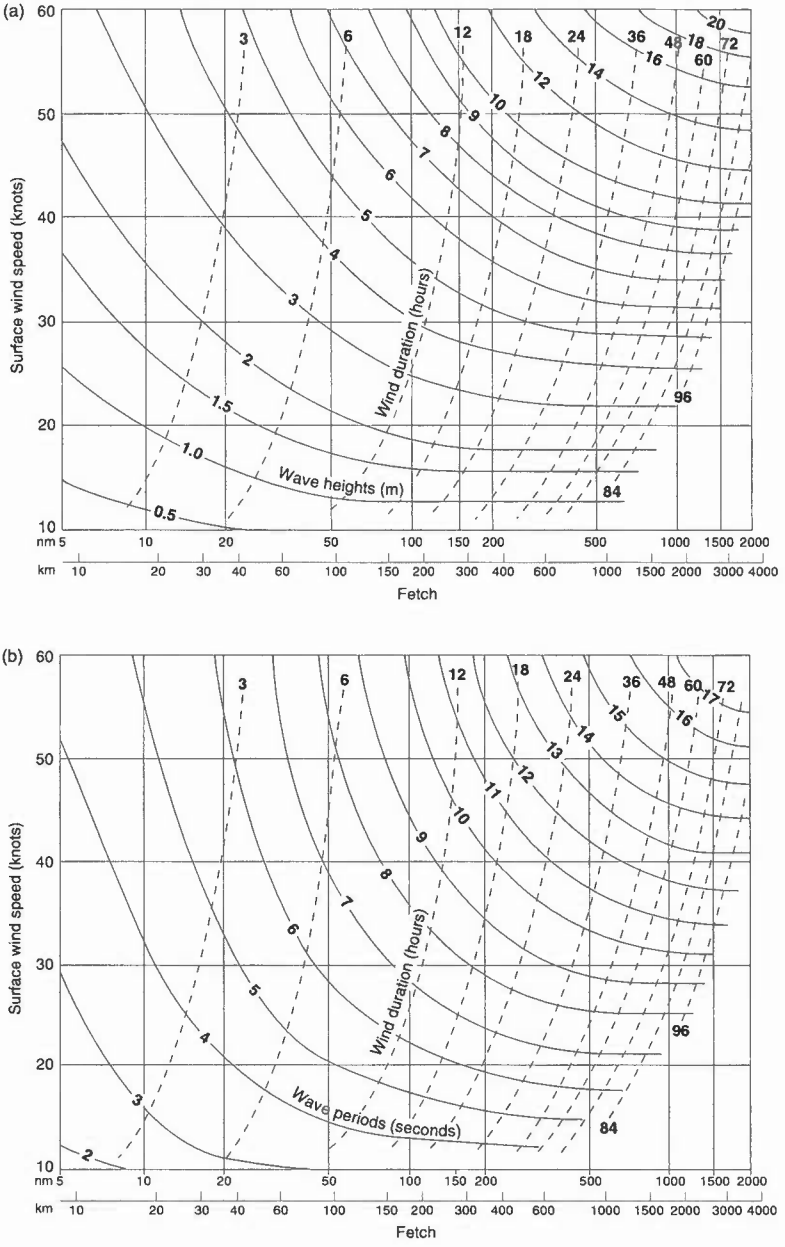

Figure 13.1. (a) Significant heights, and (b) periods, of deep-water waves (adapted from WMO nomograms).

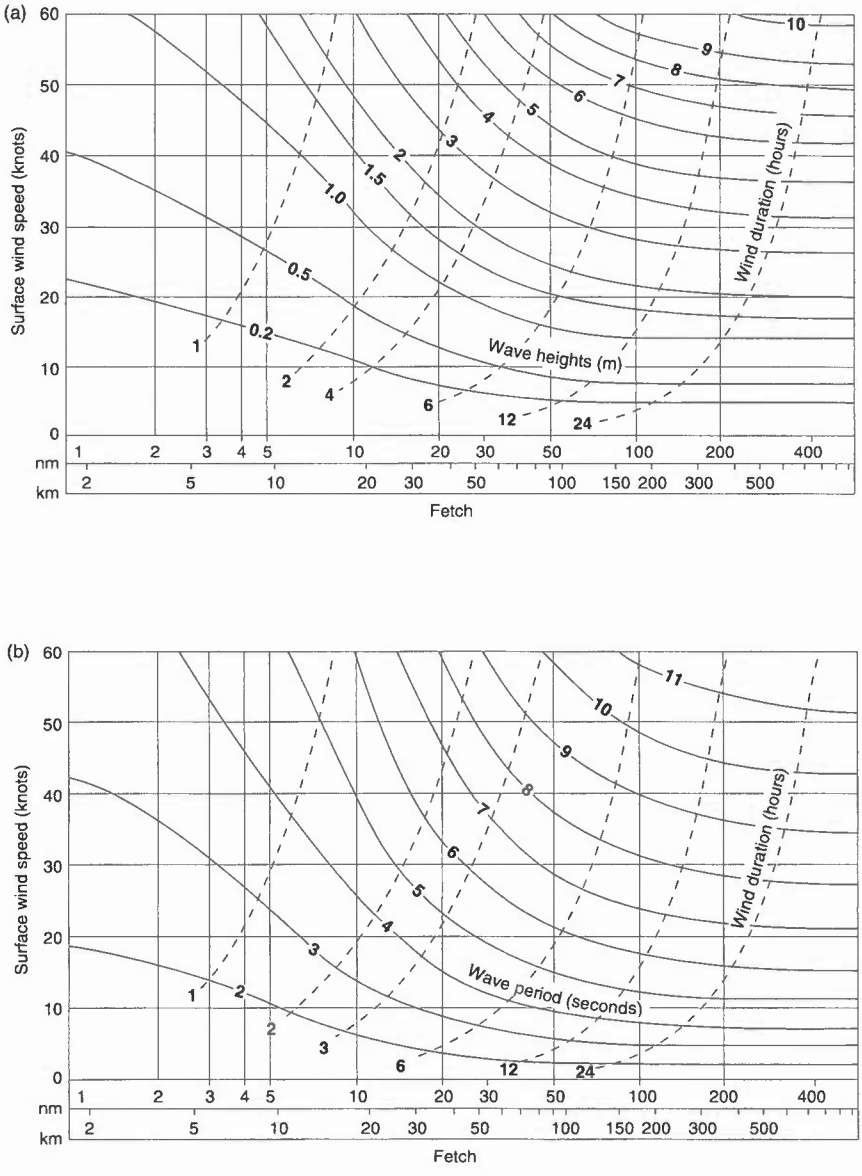

Figure 13.2. (a) Significant heights, and (b) periods, of shallow-water waves.

(b) The information that is required includes:
  (i) the arrival time of the first swell from the direction of the storm;
  (ii) the height of the swell
  (iii) the range of wave periods and wavelengths at any given time.

(c) **Fig. 13.4** may be used for estimating some of the properties of the swell from a distant storm. The initial data are entered on the horizontal and vertical axes, and from their point of intersection estimates of the swell travel time, the ratio of the swell height to the initial wave-height, and the swell period can be read off.

The height of the total sea generated by a combination of wind waves and swell is:

$$= \sqrt{[(\text{significant wave height})^2 + (\text{swell height})^2]}$$

Bretschneider (1973)

13.1.4 Forecasting maximum waves

13.1.4.1 Wind waves

The most likely maximum wave height is 1.67 × the significant wave height. **Fig. 13.5** gives the maximum wave height corresponding to a given value of the significant wave height.

13.1.4.2 Swell waves

Swell height only varies a little, and for practical forecasting it may be considered as constant.

13.1.4.3 Wind waves and swell waves combined

The maximum wave in a combined sea with wind waves and swell is:

$$\sqrt{[(\text{maximum wind wave})^2 + (\text{swell})^2]}$$

13.1.4.4 Extreme waves

When gales persist for long periods and the fetch is long, the 'maximum' wave height may be exceeded. **Fig. 13.5** gives an estimate of the 'extreme' waves which may be generated under these conditions.

DNOM (1984)
Open University (1991)

13.1.5 Tidal currents and waves

It is basic knowledge to mariners that waves become steeper and more of a hazard to shipping when the tide sets against the wind. Waves, generated in the sea before the tide has changed, have to reduce wavelength in order to conserve energy and must therefore increase amplitude.

Suthows (1945)

13.2 Storm surges (SB)

Storm surges are caused by particular combinations of wind, atmospheric pressure, waves and tides; the wind stress effects associated with a mobile low-pressure system dominate the

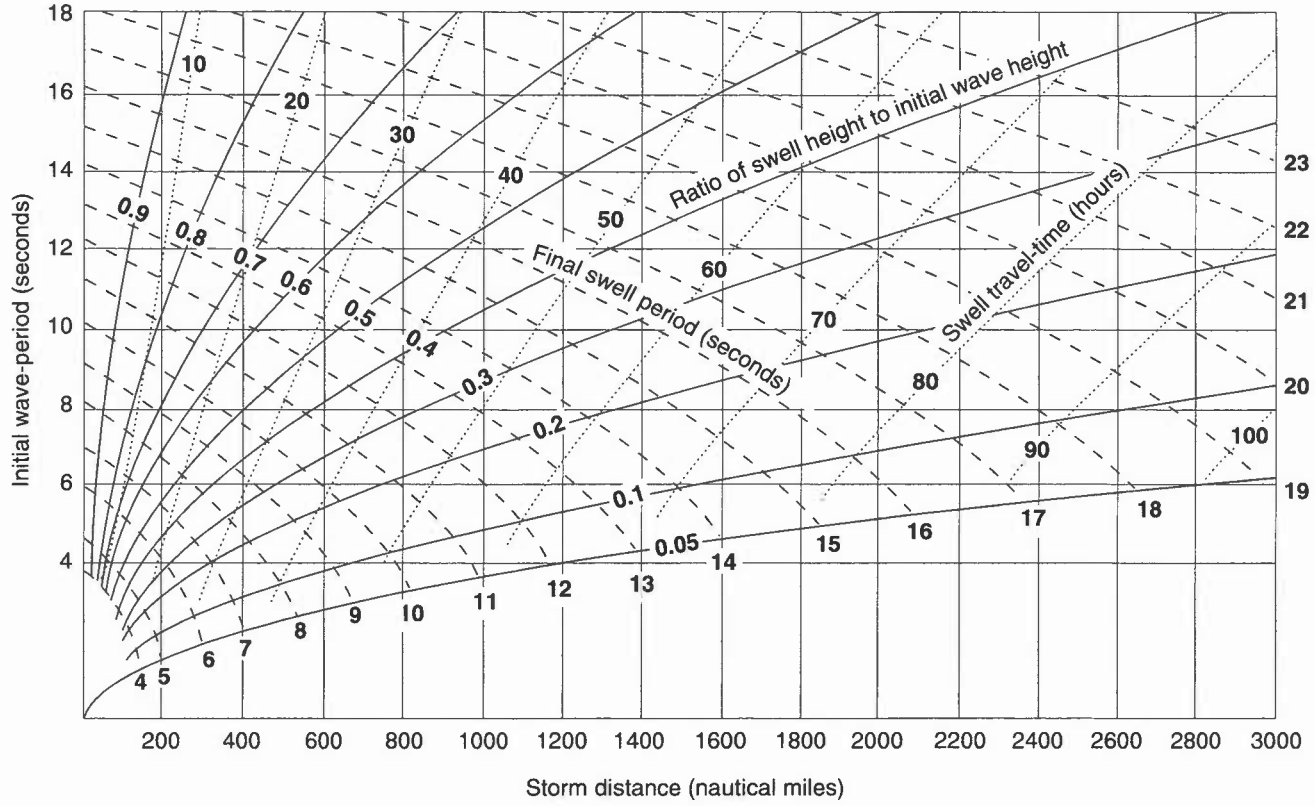

Figure 13.4. Forecasting swell height.

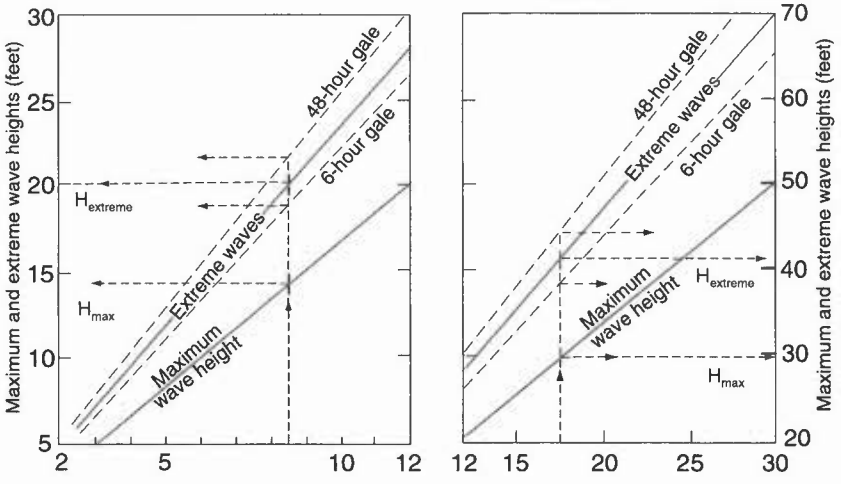

Figure 13.5. Forecasting maximum wave heights and extreme waves.

surge effect due to any change in sea level due to the pressure system alone. This effect can be important along the south coast during prolonged periods of low pressure. Large anticyclones may depress tidal levels by up to 0.3 m.

13.2.1 Causes and effects of storm surges (SB)

13.2.1.1 Atmospheric pressure

A change in atmospheric pressure of 1 hPa has the potential to cause a change in sea level of 1 cm.

13.2.1.2 Wind stress

The drag on the sea surface is assumed to be a function of the (10 m) wind speed and air density.

13.2.1.3 Wind set-up

The effect of the wind on the slope of the sea surface in a narrow channel of constant depth is dependent on the water depth and density.

13.2.1.4 Coriolis effect

The currents resulting from wind stress increase with depth as the current speed decreases so that the current profile describes an Ekman spiral.

Pugh (1987) **WMO (1988)**

13.2.2 Types and effects

13.2.2.1 North Sea surges

In a typical surge a 'positive' phase is preceded by a lowering of tidal levels at the southern end of the North Sea, due to the influence of southerly winds and to the Strait of Dover restricting flow into and out of this area. The strongest surges often result from depression on a south-easterly track crossing northern England or Scotland; the surge then can be wholly generated in the North Sea. Such surges will affect the eastern end of the English Channel.

13.2.2.2 'Negative' surges

Strong southerly winds in the North Sea may result in tidal levels much lower than tidal table predictions in the southern end of the North Sea, the Strait of Dover and the Thames Estuary (levels of over 2 m below predictions have been recorded). Such reductions in tidal levels pose a risk of grounding to deep-draught shipping with low under-keel clearance approaching port.

13.2.2.3 Frequency and extremes

(i) On east and west coasts there are about 20 events each winter with surge levels exceeding 0.6 m; negative surges in the Thames Estuary number about 15.

(ii) The 50-year return period surge is 1 m in the Hebrides, 3 m in the Thames Estuary, 1 m at Land's End.

(iii) Surge peaks only infrequently coincide with high water.

13.2.2.4 Areas at risk

(i) Low-lying southern and eastern areas are at greatest risk from tidal flooding. The east coast experiences an average of 19 surges with amplitudes exceeding 0.6 m each winter.

(ii) Flooding of susceptible areas of western Britain are generally associated with strong south-westerly winds ahead of depressions approaching from the west of Ireland. The surges may also affect the western end of the Channel.

(iii) Storm surges around the Scottish coast are usually <1 metre and will generally only cause concern when combined with periods of extreme river flow. Local conditions in areas such as the Clyde may result in larger surges and associated flooding.

Pugh (1987)

13.2.3 Forecasting surge levels

(i) The Meteorological Office's Storm Tide Warning Service monitors the National Tide Gauge Network, comprising over 40 gauges around the coasts of the British Isles. It makes use of data from the European Wave Model and uses NWP data to force surge models that are routinely run twice-daily.

(ii) Empirical techniques are available for key locations on the east coast (no similar methods are available for the west coast, although the 'Lennon' criteria give an indication of a major event in the Bristol Channel or Liverpool areas).

(iii) 2-D modelling of the shelf area surrounding the UK on a 12 km mesh gives output in the form of port tables of surge residuals (effects due to meteorological influences) for 36 hours ahead.

(iv) Data can be provided for offshore locations, together with wind-induced currents and *tidal stream velocities* (periodic, generally horizontal, movements due to periodic forces).

(v) Customer demand has resulted in fine-mesh local-area models: a model of the Bristol Channel uses a 4 km grid and runs in concert with a Severn Estuary model with a 1.3 km grid.

BIBLIOGRAPHY

CHAPTER 13 — SEA WAVES AND SURGES

Bretschneider, C.L., 1973: Prediction of waves and currents. *Look Laboratory, Hawaii*, **3**, 1–17.

Darbyshire, M. and Draper, L., 1963: Forecasting wind-generated sea waves. *Engineering*, **195**, 482–484.

DNOM: Forecasting sea swell and surf: Directorate of Naval Oceanography and Meteorology, Memorandum No 2/84.

Golding, B., 1983: A wave prediction system for real time sea state forecasting. *QJR Meteorol Soc*, **109**, 393–416.

Holt, M.W., 1994: Improvements to the UKMO wave model swell dissipation and performance in light winds. Meteorological Office FR Tech. Report No. 119.

Open University, 1991: Waves, tides and shallow-water processes. Pergamon Press/Open University.

Pugh, D.T., 1987: Tides, surges and mean sea level. Wiley and Sons.

Sanderson, R., 1982: Meteorology at sea. London, Stanford Marine.

Shore Protection Manual (4th edition), 1984: Coastal Engineering Research Center, Dept. of the Army, Mississippi, USA.

Suthows, Commander, 1945: The forecasting of sea and swell waves. Met. Branch Memo 135/45, p. 72.

WMO, 1988: Guide to wave analysis and forecasting. Geneva, World Meteorological Organization, Pub No. WMO-702.

APPENDIX I — UNITS

1. S I units

Quantity	Name (symbol)	Definition
Basic units:		
Length	metre (m)	
Mass	kilogram (kg)	
Time	second (s)	
Temperature	Kelvin (K)	
Derived units:		
Force	newton (N)	$kg\ m\ s^{-2}$
Pressure	pascal (Pa)	$N\ m^{-2}$
Energy	joule (J)	N m
Power	watt (W)	$J\ s^{-1}$
Frequency	hertz (Hz)	s^{-1}

2. Multiples of units

Multiple	Prefix	(symbol)	Multiple	Prefix	(symbol)
10^{-1}	deci	(d)	10	deca	(da)
10^{-2}	centi	(c)	10^{2}	hecto	(h)
10^{-3}	milli	(m)	10^{3}	kilo	(k)
10^{-6}	micro	(μ)	10^{6}	mega	(M)
10^{-9}	nano	(n)	10^{9}	giga	(G)
10^{-12}	pico	(p)	10^{12}	tera	(T)

APPENDIX II — CONVERSION TABLES

1. Temperature

Table A1. Celsius to Fahrenheit

°C	−40	−35	−30	−25	−20	−15	−10	−5	0	5	10	15	20	25	30	35	40	45	50
°F	−40	−31	−22	−13	−4	5	14	23	32	41	50	59	68	77	86	95	104	113	122

differences

°C	1	2	3	4	5
°F	2	4	5	7	9

Table A2. Fahrenheit to Celsius

°F	−40	−30	−20	−10	0	10	20	30	40	50	60	70	80	90	100	110	120	130	140
°C	−40	−34	−29	−23	−18	−12	−7	−1	4	10	15	21	27	32	38	43	49	54	60

differences

°F	1	2	3	4	5	6	7	8	9
°C	1	1	2	2	3	3	4	4	5

2. Distance

1 inch	=	25.4 mm	1 cm = 0.39 inch
1 foot	=	30.48 cm	1 m = 3.28 feet
1 mile	=	1.61 km	1 km = 0.62 mile
1 n.mile	=	1.85 km	1 km = 0.54 n mile

Table A3. Nautical miles to kilometres

n mile	10	20	30	40	50	60	70	80	90	100
km	18	37	56	74	93	111	130	148	167	185

Table A4. Kilometres to nautical miles

km	10	20	30	40	50	60	70	80	90	100
n mile	5	11	16	22	27	32	38	43	49	54

3. Area

1 hectare = $(100\ m)^2$ = 2.47 acres

$(1\ km)^2$ = 100 hectares = 247 acres

4. Speed

Table A5. Knots to metres/second and kilometres/hour

knots	1	2	3	4	5	10	20	30	40	50	60	70	80	90	100
m s^{-1}	0.5	1	1.5	2	2.5	5	10	15	21	26	31	36	41	46	51
km h^{-1}	1.8	3.7	5.6	7.4	9.3	19	37	56	74	93	111	130	148	167	185

1 knot = 0.515 m s^{-1} = 1.85 km h^{-1}

Table A6. Miles/hour to knots and kilometres/hour

m.p.h.	1	2	3	4	5	10	20	30	40	50	60	70	80	90	100
knots	0.9	1.7	2.6	3.5	4.4	9	17	26	35	44	52	61	70	78	87
km h^{-1}	1.6	3.2	4.8	6.4	8.1	16	32	48	64	81	97	113	129	145	161

1 m.p.h. = 0.87 knot = 1.61 km h^{-1}

Table A7. Metres/second to kilometres/hour and knots

m s^{-1}	1	2	3	4	5	10	20	30	40	50	60	70	80	90	100
km h^{-1}	3.6	7.2	10.8	14.4	18.0	36	72	108	144	180	216	252	288	324	360
knots	1.9	3.9	5.8	7.8	9.7	19	39	58	78	97	117	136	155	175	194

1 m s^{-1} = 3.60 km h^{-1} = 1.94 knots

Table A8. Kilometres/hour to knots and metres/second

km h^{-1}	1	2	3	4	5	10	20	30	40	50	60	70	80	90	100
knots	0.5	1.1	1.6	2.2	2.7	5	11	16	22	27	32	38	43	49	54
m s^{-1}	0.3	0.6	0.8	1.1	1.4	3	5	8	11	14	17	19	22	25	28

1 km h^{-1} = 0.54 knots = 0.28 m s^{-1}

Table A9. Feet/minute to knots and metres/second

ft min^{-1}	10	25	50	75	100	200	300	400	500	1000
knots	0.10	0.25	0.49	0.74	1.0	2.0	3.0	3.9	4.9	9.9
m s^{-1}	0.05	0.13	0.25	0.38	0.5	1.0	1.5	2.0	2.5	5.1

1000 ft min^{-1} = 9.87 knots = 5.08 m s^{-1}

Table A10. Runway cross-wind components

		Angle between wind direction and runway heading (deg. true)								
		10	20	30	40	50	60	70	80	90
	5	1	2	2	3	4	4	4	5	5
	10	2	3	5	6	7	8	9	9	10
	15	3	5	7	9	11	13	14	14	15
	20	3	7	10	13	15	17	18	19	20
	25	4	8	12	16	19	22	23	24	25
Wind	30	5	10	15	19	23	26	28	29	30
	35	6	12	17	22	26	30	32	34	35
speed	40	7	14	20	25	30	35	37	39	40
in	45	8	15	22	29	34	39	42	44	45
	50	9	17	25	32	38	43	47	49	50
knots	55	10	19	27	35	42	48	52	54	55
	60	10	20	30	38	46	52	56		
	65	11	22	32	42	50	56			
	70	12	24	35	45	54				
	75	13	26	37	48					
	80	14	27	40						

APPENDIX III — PHYSICAL TABLES AND CONSTANTS

1. The Earth

Dimensions

Equatorial radius	6378 km (3963 miles	
Polar radius	6357 km (3950 miles)	
Rate of rotation (Ω)	7.29×10^{-5} s^{-1}	
Total surface area	510×10^6 km^2	
Land surface area	150×10^6 km^2	(29.2% of total area)
Ocean surface area	360×10^6 km^2	(70.8% of total area)

Table A11. Gravity at mean sea level

Latitude (deg)	0	50	60	90
g (m s^{-2})	9.78	9.81	9.82	9.83

Table A12. Distance of sea horizon from viewpoint at given heights

Height (ft)	6	10	20	30	50	100	200	400	600	800
Distance (n mile)	2.8	3.6	5.1	6.3	8.1	11	16	23	28	32

Table A13. Distance corresponding to 1 degree of longitude at given latitudes

Latitude (deg)	0	15	30	45	50	55	60	75	85	90
Distance (n mile)	60.4	58.3	52.2	42.6	38.7	34.5	30.1	15.5	5.2	0

Table A14. Value of Coriolis Parameter ($f = 2\Omega\sin\varphi$)

	Latitude (φ) degrees								
	0	15	30	45	50	55	60	75	90
f (10^{-4} s^{-1})	0.00	0.38	0.73	1.03	1.12	1.19	1.26	1.41	1.46
f (h^{-1})	0.00	0.14	0.26	0.37	0.40	0.43	0.45	0.51	0.52
$\partial f/\partial y$ (10^{-11} m^{-1} s^{-1})	2.29	2.12	1.98	1.62	1.47	1.31	1.14	0.59	0.00

2. The atmosphere

(a) Some physical properties

Mass of atmosphere = 5.27×10^{18} kg

Surface pressure:
1 'atmosphere' = 1.03 kg cm^{-2} = 14.7 lb in^{-2} = 29.9 in Hg
1 millibar = 100 dynes cm^{-2} = 100 N m^{-2} = 1 hPa

Speed of light = 2.998×10^{8} m s^{-1}

Speed of sound in dry air

Temperature (°C)	−40	−20	0	20	40
Speed (m s^{-1})	306	318	331	343	354

(b) Specific heats (J deg^{-1} kg^{-1}) of atmospheric constituents:

Dry air (c_p)	1004
Dry air (c_v)	717
Water vapour (c_p)	1952
Water vapour (c_v)	1463
Liquid water (0°C)	4218
Ice (0°)	2106

(c) Latent heats (J kg^{-1}) of water substances

Vapour/Liquid	2 500 000
Liquid/Solid	334 000
Solid/Vapour	2 834 000

Table A15. ICAO Standard atmosphere (dry air)

Pressure	Temperature	Density	Height		Thickness of 1 hPa layer	
hPa	°C	g m^{-3}	m	ft	m	ft
1013.2	15.0	1225	0	0	8.3	27
1000	14.3	1212	111	364	8.4	28
950	11.5	1163	540	1773	8.8	29
900	8.6	1113	988	3243	9.2	30
850	5.5	1063	1457	4781	9.6	31
800	2.3	1012	1949	6394	10.1	33
750	−1.0	960	2466	8091	10.6	35
700	−4.6	908	3012	9882	11.2	37
650	−8.3	855	3591	11780	11.9	39
600	−12.3	802	4206	13801	12.7	42
550	−16.6	747	4865	15962	13.7	45
500	−21.2	692	5574	18289	14.7	48
450	−26.2	635	6344	20812	16.1	53
400	−31.7	577	7185	23574	17.7	58
350	−37.7	518	8117	26631	19.7	65
300	−44.5	457	9164	30065	22.3	75
250	−52.3	395	10363	33999	25.8	85
200	−56.5	322	11784	38662	31.7	104
150	−56.5	241	13608	44647	42.3	139
100	−56.5	161	16180	53083	63.4	208
90	−56.5	145	16848	55275	70.5	231
80	−56.5	128	17595	57726	79.3	260
70	−56.5	112	18442	60504	90.6	297
60	−56.5	96	19419	63711	105.7	347
50	−55.9	80	20576	67507	127.0	417
40	−54.5	64	22000	72177	160	525
30	−52.7	47	23849	78244	215	706
20	−50.0	31	26481	86881	326	1072
10	−45.4	15	31055	101885	669	2195

Table A16. The Sun

Date	Noon sun overhead (lat.)	Noon solar altitude 50° N (deg.)	Noon solar altitude 60° N	Sunrise/sunset times (UTC) London	Manchester	Glasgow	Lerwick
Jan. 1	23° S	17	7	0805/1600	0825/1600	0850/1555	0925/1440
Jan. 16	21° S	19	9	0800/1620	0815/1620	0835/1615	0905/1500
Feb. 1	17° S	23	13	0740/1650	0755/1650	0810/1650	0830/1540
Feb. 16	13° S	27	17	0715/1715	0725/1720	0740/1720	0745/1625
Mar. 1	8° S	32	22	0645/1740	0700/1745	0710/1750	0700/1705
Mar. 16	2° S	38	28	0615/1805	0625/1815	0630/1820	0620/1745
Apr. 1	4° N	44	34	0535/1835	0545/1845	0550/1855	0535/1825
Apr. 16	10° N	50	40	0505/1855	0510/1910	0510/1925	0450/1910
May 1	15° N	55	45	0435/1925	0435/1935	0435/1955	0410/1945
May 16	19° N	59	49	0405/1945	0405/2005	0405/2025	0340/2010
June 1	22° N	62	52	0350/2005	0345/2025	0340/2050	0310/2030
June 16	23° N	63	53	0340/2020	0340/2040	0330/2105	0255/2105
July 1	23° N	63	53	0345/2020	0345/2040	0335/2105	0310/2100
July 16	21° N	61	51	0400/2010	0400/2030	0355/2050	0325/2045
Aug. 1	18° N	58	48	0420/1950	0425/2005	0420/2025	0345/2010
Aug. 16	14° N	54	44	0445/1920	0450/1935	0450/1950	0420/1930
Sept. 1	8° N	48	38	0510/1850	0515/1900	0520/1915	0500/1850
Sept. 16	3° N	43	33	0535/1815	0545/1825	0550/1835	0545/1810
Oct. 1	3° S	37	27	0600/1740	0610/1745	0620/1755	0630/1730
Oct. 16	8° S	32	22	0625/1705	0635/1710	0650/1715	0710/1645
Nov. 1	14° S	26	16	0655/1635	0705/1640	0720/1640	0755/1600
Nov. 16	18° S	22	12	0720/1610	0735/1610	0755/1610	0835/1525
Dec. 1	22° S	18	8	0745/1555	0800/1555	0820/1550	0910/1500
Dec. 16	23° S	17	7	0800/1550	0820/1550	0840/1545	0930/1440

Table A17. Rossby Long Waves — wavelength of stationary waves

Latitude (deg.)	Mean zonal wind speed (knots) 10	20	30	40	50	10	20	30	40	50
	wavelength									
	kilometres					degrees of longitude				
70	5100	7200	8800	10200	11400	134	190	232	268	300
60	4200	6000	7300	8400	9400	76	108	132	152	170
50	3700	5300	6400	7400	8300	52	74	90	104	116
40	3400	4800	5900	6800	7600	40	57	69	80	90
30	3200	4500	5600	6400	7200	33	47	57	66	74

APPENDIX IV — FORECASTING WEATHER BELOW 15,000 FT

In order to prepare a low-level forecast of weather for a short period ahead (e.g.6–12 hours) for a specific region, the following elements must be considered:

- visibility (Chapter 3)
- cloud (4.3; 4.6; 5.1; 5.2; 5.4–5.6; 5.8)
- weather, including fog/hill fog (3.3; 3.4; 3.5.2; 3.6)
- low-level turbulence (6.2)
- lee-wave activity (1.3.2)
- icing and turbulence in cloud (2.9; 6.1.1)
- variations in freezing level, with possible sub-zero layers, across the area (2.9.7; 2.9.8; 2.9.9; 2.9.10)

A brief ten-point summary of the main aspects of preparing a low-level aviation chart is as follows:

- Must know weather and cloud distribution now
- How does model represent weather at data time?
- Make necessary adjustments throughout forecast period.
- Check upper-air pattern — as above, is model correct?
- Allow for possible changes in development/decay, e.g. of large rain or shower areas; use trajectories.
- Consider effects of clearing skies — fog formation.
- Check gradient wind forecasts — consider turbulence.
- Run/modify lee-wave program results according to wind direction and vertical shear in relation to topography.
- Always examine actual and forecast ascents or profiles.
- Consider sub-zero layer(s) when calculating freezing levels.

Reference

Hall, B.A. 1996: Forecasting weather below 15,000 feet. 4th Joint UK Met. Office/WMO Aeronautical Forecasting Seminar, Meteorological Office College, July 1996.

FORECASTERS' REFERENCE BOOK — INDEX

T